Slovenian Veterinary Research

Slovenski veterinarski zbornik

THE SCIENTIFIC JOURNAL OF THE VETERINARY FACULTY UNIVERSITY OF LJUBLJANA

ISSN 1580-4003

Volume 61, Number 1, Pages 1–72

Slovenian Veterinary Research

Slovenski veterinarski zbornik

THE SCIENTIFIC JOURNAL OF THE VETERINARY FACULTY UNIVERSITY OF LJUBLJANA

Volume 61, Number 1, Pages 1–72

The Scientific Journal of the Veterinary Faculty University of Ljubljana

Slovenian Veterinary Research

Slovenski veterinarski zbornik

Previously: RESEARCH REPORTS OF THE VETERINARY FACULTY UNIVERSITY OF LJUBLJANA
Prej: ZBORNIK VETERINARSKE FAKULTETE UNIVERZA V LJUBLJANI

4 issues per year / Izhaja štirikrat letno
Volume 61, Number 1 / Letnik 61, Številka 1

Published by / Založila	University of Ljubljana Press / Založba Univerze v Ljubljani
For the Publisher / Za založbo	Gregor Majdič, Rector of the University of Ljubljana / Rektor Univerze v Ljubljani
Issued by / Izdala	Veterinary Faculty University of Ljubljana / Veterinarska fakulteta Univerze v Ljubljani
For the Issuer / Za izdajatelja	Breda Jakovac Strajn, Dean of the Veterinary Faculty / Dekanja Veterinarske fakultete
Address	Veterinary Faculty, Gerbičeva 60, 1000 Ljubljana, Slovenia
Naslov	Veterinarska fakulteta, Gerbičeva 60, 1000 Ljubljana, Slovenija
Phone / Telefon	+386 (0)1 4779 100
E-mail	slovetres@vf.uni-lj.si
Sponsored by / Sofinancira	The Slovenian Research Agency / Javna agencija za raziskovalno dejavnost Republike Slovenije
Printed by / Tisk	DZS, d.d., Ljubljana, Marec 2024
Number of copies printed / Naklada	220
Indexed in / Indeksirano v	Agris, Biomedicina Slovenica, CAB Abstracts, IVSI Urlich's International Periodicals Directory, Science Citation Index Expanded, Journal Citation Reports – Science Edition
	https://www.slovetres.si/
	ISSN 1580-4003 2385 - 8761 (on-line)

Cover illustration by Pšenica Kovačič is inspired by the Review manuscript - From nature's pharmacy to swine health: harnessing natural compounds against PRRSV infection by Fredmoore Orosco.

Table of Content

Slovenian Veterinary Research
DOI 10.26873/SVR-1957-2024
UDC 616:621.384.633:615.849.4:636.09
Pages: 5–8

Editorial

Interdisciplinary Approaches for Oncological Treatments: Proton Therapy at the Intersection of Physics and Medicine

Interdisciplinarni pristopi k onkološkim zdravljenjem: Protonska terapija na presečišču fizike in medicine

Key words

proton;
therapy;
physics;
cancer

Accepted: 22 February 2024

Maša Čater

Department of Animal Science, Biotechnical Faculty, University of Ljubljana, Groblje 3, 1230 Domžale, Slovenia

masa.cater@bf.uni-lj.si

The inspiration for writing this editorial came from a recent visit to the European Organization for Nuclear Research (CERN, Conseil Européen pour la Recherche Nucléaire) in Geneva. There I had the opportunity to take a closer look at the technology of proton production and acceleration in cyclotrons. I was impressed by this direct insight into physical findings that have an impact on many other scientific fields. I learned how these scientific discoveries are used in medicine, especially in oncology, and how this interdisciplinary approach can improve patients' lives. This experience gave me a new perspective and encouraged me to research and write about this important and innovative field. In the following, we will explore how proton therapy has changed the way and success of treatments in oncology and how the interdisciplinary collaboration between physics and medicine has contributed to this progress. In addition, I have focused on the relevance of this technology to veterinary medicine and the potential it offers for improving cancer treatment in our pets.

The technology for accelerating protons was developed at the beginning of the 20th century. Protons were discovered in 1919 (1). The first large proton synchrotron was the

Navdih za pisanje tega uredniškega članka je nastal z nedavnim obiskom Evropske organizacije za jedrske raziskave (CERN, Conseil Européen pour la Recherche Nucléaire) v Ženevi. Tam sem imela priložnost pobliže spoznati tehnologijo pridobivanja protonov in njihovega pospeševanja v ciklotronih. Ta neposreden vpogled v fizikalno znanje, ki seva v mnoga druga znanstvena področja, me je navdušil. Spoznala sem, kako se ta znanstvena odkritja uporabljajo v medicini, zlasti v onkologiji, in kako lahko ta interdisciplinarni pristop izboljša življenja bolnikov. Ta izkušnja mi je dala novo perspektivo in me spodbudila k raziskovanju in pisanju o tem pomembnem in inovativnem področju. V nadaljevanju bomo raziskali, kako je protonska terapija preoblikovala način in uspešnost zdravljenj v onkologiji in kako je interdisciplinarno sodelovanje med fiziko in medicino prispevalo k temu napredku. Pri tem sem se osredotočila o pomenu te tehnologije za veterinarsko medicino in kakšen potencial predstavlja pri izboljšanju zdravljenja raka pri naših ljubljenčkih.

Tehnologija pospeševanja protonov se je začela razvijati v zgodnjem 20. stoletju. Protoni so bili odkriti leta 1919

Cosmotron at Brookhaven National Laboratory, which accelerated protons to about 3 GeV (2). CERN played an important role in the development of proton acceleration technology. Their Proton Synchrotron (PS) there accelerated protons for the first time in 1959 and was briefly the most powerful particle accelerator in the world (3). The PS was CERN's first synchrotron and was initially CERN's main accelerator. When the laboratory built new accelerators in the 1970s, the main task of the PS became to supply these accelerators with particles. The Super Proton Synchrotron (SPS) was built after the PS and served as the main accelerator for several years until the Large Hadron Collider (LHC) was built. The Large Electron-Positron Collider (LEP) was built in the same tunnel that now houses the LHC and was the largest electron-positron collider in the world. The LHC is currently the largest and most powerful particle accelerator in the world (4). In accelerators, protons are accelerated to speeds of up to 60% of the speed of light (5) with the help of powerful magnets. This allows protons to reach enormous amounts of energy, up to 230 million electron volts (6).

The idea of using protons for medical treatment was first proposed in 1946 by the physicist Robert R. Wilson (7). Wilson suggested that protons could be used to deliver a precise dose of radiation to tumors while protecting the surrounding healthy tissue. Proton therapy is therefore a form of radiotherapy in which charged particles, protons, are used to irradiate cancerous tissue. With a speed of up to 60 % of the speed of light, protons gain so much energy that they can penetrate about 32 g/cm², which enables the treatment of tumors located deep in the body (8). The unique physical properties of protons allow precise control of the irradiation depth and intensity, making proton therapy ideal for treating brain tumors located near important neuronal structures, for example (9).

The first attempts to treat patients with proton beams began as early as 1954 at the Lawrence Berkeley National Laboratory in California, USA (10). In the same year and in the same laboratory, proton therapy was also used for the first time to treat animals, namely a dog with breast cancer (10). The dog's pituitary gland was removed by radiosurgery using proton beams, and the dog lived for at least two years after the treatment. However, it was not until the late 1970s, when advanced imaging technologies, sophisticated computers and improved accelerator technology were developed, that proton therapy could be used for routine medical and veterinary applications. Today, proton therapy is used in human medicine to treat various types of cancer, and there are proton therapy centers around the world that offer this advanced form of radiation therapy. Unfortunately, medical facilities in Slovenia do not yet offer proton therapy (11, 12). The closest center for irradiating cancer patients with protons is MedAustron near Vienna (13). Proton therapy has also become an important part of veterinary oncology. There are not as many documented examples of its use in veterinary medicine in the literature as there is an extensive database for human medicine. However, the data shows that it is most commonly used or researched for the treatment of cancer

(1). Prvi veliki protonski sinhrotron je bil Cosmotron v Brookhaven National Laboratory, ki je pospešil protone do približno 3 GeV (2). CERN je imel pomembno vlogo pri razvoju tehnologije pospeševanja protonov. Njihov Proton Synchrotron (PS) je prvič pospešil protone leta 1959 in za kratek čas postal najmočnejši delcev pospeševalnik na svetu (3). PS je bil prvi sinhrotron CERN-a in je bil sprva glavni pospeševalnik CERN-a. Ko je laboratorij v 70-ih letih prejšnjega stoletja zgradil nove pospeševalnike, je glavna vloga PS postala dobava delcev le-tem. Super Proton Sinhrotron (SPS) je bil zgrajen po PS in je služil kot glavni pospeševalnik več let, dokler ni bil zgrajen Veliki hadronski trkalnik (LHC). Large Electron-Positron Collider (LEP) je bil zgrajen v istem tunelu, kjer se danes nahaja LHC in je bil največji elektron-pozitronski trkalnik na svetu. LHC pa je trenutno največji in najmočnejši pospeševalnik delcev na svetu (4). V teh pospeševalnikih se protone s pomočjo mogočnih magnetov pospeši do hitrosti, ki dosežejo do 60% hitrosti svetlobe (5). To omogoča, da protoni dosežejo ogromne količine energije, do 230 milijonov elektron voltov (6).

Ideja o uporabi protonov za medicinsko zdravljenje je prvič vzniknila leta 1946 s strani fizika Roberta R. Wilsona (7). Wilson je predlagal, da bi se protoni lahko uporabljali za natančno doziranje sevanja na tumorje, pri čemer bi varovali okoliško zdravo tkivo. Protonska terapija je tako oblika radioterapije, ki uporablja nabite delce, protone, za usmerjeno oddajanje sevanja na rakavo tkivo. Pri hitrosti do 60 % svetlobne hitrosti protoni dobijo tako veliko energije, da lahko prodrejo približno 32 g/cm² globoko v telo, kar omogoča zdravljenje tumorjev, ki so globoko v telesu (8). Edinstvene fizikalne lastnosti protonov omogočajo natančen nadzor nad globino in intenzivnostjo sevanja, zaradi česar je protonska terapija idealna na primer za zdravljenje možganskih tumorjev, ki so blizu ključnih nevralnih struktur (9).

Prvi poskusi uporabe protonskih žarkov za zdravljenje bolnikov so se začeli že leta 1954 v Nacionalnem laboratoriju Lawrence Berkeley v Kaliforniji, ZDA (10). V istem letu in v istem laboratoriju se je protonska terapija prvič uporabila tudi za zdravljenje živali in sicer pri psu z rakom dojk (10). Pri psu so z radiokirurgijo odstranili hipofizo z uporabo protonskih žarkov, in pes je po zdravljenju živel vsaj še 2 leti. Vendar pa je bilo šele v poznih 70. letih, ko so se razvile napredne tehnologije slikanja, sofisticirani računalniki in izboljšana tehnologija pospeševalnikov in je bilo protonsko terapijo mogoče uporabljati za rutinske medicinske in veterinarske aplikacije. Danes se v humani medicini protonska terapija uporablja za zdravljenje različnih vrst rakov, in po vsem svetu obstajajo centri za protonske terapije, ki ponujajo to napredno obliko radioterapije. Žal v Sloveniji medicinske ustanove protonske terapije še ne ponujajo (11, 12). Nam najbližji center za obsevanje bolnikov z rakom s protoni je MedAustron pri Dunaju (13). Tudi v veterinarski onkologiji je protonska terapija postala pomemben del. V literaturi sicer ni toliko dokumentiranih del uporabe v veterinarski medicini, kakor je baza obširna za humano medicino. Podatki pa kažejo, da se najpogosteje uporablja oziroma raziskuje za

in dogs. With normal radiation, dogs survive on average 2 to 4 months. With proton therapy, survival time is extended because less damage is done to healthy tissue and the tumor is irradiated with more energy than with conventional radiation. It is also believed that proton therapy improves the dog's immune response to the tumor (14). Although proton therapy is still considered a new therapy in veterinary medicine, it is spreading rapidly and the technology is constantly being developed and improved.

Crucial to the development of proton therapy are preclinical studies that contribute to the understanding and improvement of this advanced method of cancer treatment. These studies include research on laboratory animals and cell models to better understand the effects of proton beams on tumor cells and surrounding healthy tissue. Preclinical studies are also helping to develop more precise and effective methods for using proton beams that can improve treatment outcomes (15). In the preclinical phase, there are also studies investigating combined radiation. In the study by Rozanova et al. (2022), they investigated the effects of combined proton and neutron irradiation on the solid form of ascitic Ehrlich carcinoma on tumor response and skin reactions in mice bearing the tumor (16). They found that irradiation of mice with neutrons both before and after irradiation with protons effectively inhibited the growth of the carcinoma one month after exposure. Based on the frequency and severity of skin lesions observed in mice 15–40 days after therapy, neutron irradiation after proton irradiation significantly improved these indicators compared to exposure to proton beams alone; however, neutron irradiation before proton irradiation showed more damage than the other variants. They also showed that the incidence of tumor recurrence was significantly higher and overall survival lower in the groups of animals with combined irradiation than in the group of mice irradiated with protons alone. In addition, preclinical studies are key to exploring and resolving some unresolved issues in proton therapy, such as the relative biological effectiveness (RBE) of protons. All preclinical research thus forms the basis for clinical studies and the further development of proton therapy.

In oncology, innovative therapeutic options are constantly being sought to improve the precision of tumor treatment. Proton therapy, which emerged from cutting-edge physics research, has established itself as a revolutionary medical procedure that offers unprecedented precision in the irradiation of tumors. In addition to its use in human medicine, proton therapy is also of great importance in veterinary medicine. Thanks to the precision it offers, veterinarians can treat tumors in animals in a more targeted way, reducing side effects and improving the quality of life of our pets. This interdisciplinary approach, which combines physics and medicine, therefore promises major advances in the treatment of cancer in humans and animals.

zdravljenje raka pri psih. Pri prejemanju običajnega obsevanja, psi v povprečju preživijo 2 – 4 mesece. S protonsko terapijo pa se dobo preživetja podaljša, saj nastane manj poškodb zdravega tkiva, tumor pa je obsevan z večjo energijo kot pri običajnem obsevanju. Poleg tega naj bi protonska terapija izboljšala imunske odzive psa proti tumorju (14). Čeprav še vedno velja za novo terapijo, se uporaba protonske terapije v veterinarski medicini hitro širi, tehnologija pa se neprestano razvija in izboljšuje.

Za sam razvoj protonske terapije so ključne predklinične raziskave protonske terapije, ki doprinašajo k razumevanju in izboljšanju te napredne metode zdravljenja raka. Te raziskave vključujejo študije na laboratorijskih živalih in celičnih modelih, da bi bolje razumeli učinke protonskih žarkov na tumorske celice in okoliško zdravo tkivo. Predklinične raziskave prav tako pomagajo pri razvoju natančnejših in učinkovitejših načinov dostave protonskih žarkov, kar lahko izboljša rezultate zdravljenja (15). V predklinični fazi so tudi študije, ki raziskujejo kombinirano obsevanje. V študiji Rozanova in sod. (2022) so raziskovali učinke kombiniranega obsevanja s protoni in nevtroni na trdni obliki ascitskega Ehrlichovega karcinoma na odziv tumorja in reakcije kože pri miših (16). Ugotovili so, da je obsevanje miši z nevtroni tako pred kot po obsevanju s protoni učinkovito zaviralo rast karcinoma v enem mesecu po izpostavljenosti. Glede na pogostost in resnost poškodb kože, opaženih pri miših 15–40 dni po terapiji, je obsevanje z nevtroni po obsevanju s protoni privedlo do pomembnega izboljšanja teh kazalnikov v primerjavi z delovanjem samo protonskih žarkov; vendar pa je obsevanje z nevtroni pred protoni izkazalo večjo škodo kot v drugih variantah. Prav tako so pokazali, da je bila pogostost ponovitve tumorja v skupinah živali z kombiniranim obsevanjem bistveno višja, skupna življenjska doba pa nižja v primerjavi s skupino miši, ki so bile obsevane samo s protoni. Predklinične raziskave so ključne tudi za raziskovanje in reševanje nekaterih nerešenih vprašanj v protonski terapiji, kot je relativna biološka učinkovitost (RBE) protonov. Raziskave na predkliničnem nivoju so tako temelj za klinične študije in nadaljnji razvoj protonske terapije.

V onkologiji se nenehno iščejo inovativne terapevtske možnosti, ki bi izboljšale natančnost ciljanja tumorjev. Protonska terapija, ki izhaja iz naprednih fizikalnih raziskav, se je uveljavila kot revolucionarna medicinska metoda z neprekosljivo natančnostjo pri obsevanju tumorjev. Poleg uporabe v humani medicini, ima protonska terapija pomemben pomen tudi v veterinarski medicini. Z natančnostjo, ki jo omogoča, lahko veterinarji bolje ciljajo na tumorje pri živalih, kar zmanjšuje stranske učinke in izboljšuje kakovost življenja naših ljubljenčkov. Ta interdisciplinarni pristop, ki združuje fiziko in medicino, tako obeta velik napredek v zdravljenju raka tako pri ljudeh kot pri živalih.

References

1. CERN. The proton synchrotron. Geneve: CERN, 2024. https://home.cern/science/accelerators/proton-synchrotron (13. 2. 2024)
2. Wikipedia. Particle accelerator. San Francisco: Wikimedia Foundation, 2024. https://en.wikipedia.org/wiki/Particle_accelerator (13. 2. 2024)
3. CERN. AWAKE. Geneve: CERN, 2024. https://home.cern/science/accelerators/awake (13. 2. 2024)
4. CERN. Accelerators. Geneve: CERN, 2024. https://home.cern/science/accelerators (13. 2. 2024)
5. Maughan R. Proton therapy: behind the scenes. Philadelphia: OncoLink, 2022. available online: https://www.oncolink.org/cancer-treatment/radiation/types-of-radiation-therapy/pr oton-therapy/overviews-of-proton-therapy/proton-therapy-behind-the-scenes (13. 2. 2024)
6. Pearson E, et al. Development of cyclotrons for proton and particle therapy. In: Rath AK, eds. Particle radiotherapy: emerging technology for treatment of cancer. New Delhi: Springer, 2016: 21-35.
7. Wilson RR. Radiological use of fast protons. Radiology 1946; 47(5): 487–91. doi: 10.1148/47.5.487
8. Schippers JM. Cyclotrons for particle therapy. CERN YelloW Reports 2017; 1: 165–75. doi: 10.23730/CYRSP-2017-001
9. Lomax AJ. Intensity modulated proton therapy and its sensitivity to treatment uncertainties 2: the potential effects of inter-fraction and inter-field motions. Phys Med Biol 2008; 53(4): 1043–56. doi: 10.1088/0031-9155/53/4/015
10. Tsuboi K. Early history of biology and clinical application of proton beam therapy. In: Tsuboi K., (eds) Proton beam radiotherapy. Singapore: Springer, 2020: 9–21.
11. Bošnjak D. S protoni nad tumorje. Ljubana: Delo, 2019. https://www.delo.si/novice/znanoteh/s-protoni-nad-tumorje/ (13. 2. 2024)
12. Ferlič Žgajnar B. Ni znano, kdaj bo Slovenija dobila protonski center. Ljubljana: Delo, 2022. https://www.delo.si/novice/slovenija/ni-znano-kdaj-bo-slovenijadobila-protonski-center/ (13. 2. 2024)
13. Prešeren P. V centru za protonsko in ionsko terapijo MedAustron: novi načini zdravljenja dajejo upanje bolnikom. Ljubljana: MMC RTV SLO, 2022. https://www.rtvslo.si/znanost-in-tehnologija/v-centru-za-protonsko-in-ionsko-terapijomedaustron-novi-nacini-zdravljenja-dajejo-upanje-bolnikom/651115 (13. 2. 2024)
14. Evaluation of flash proton RT in dogs with bone cancer of the leg. Lancaster: Penn Veterinary Supply, 2019. https://www.vet.upenn.edu/research/clinical-trials-vcic/all-clinical-trials/clinicaltrial/osteosarcoma-evaluation-of-flash-proton-rt-in-dogs-with-bone-cancer-of-the-leg (13. 2. 2024)
15. Schneider M, Bodenstein E, Bock J, et al. Combined proton radiography and irradiation for high-precision preclinical studies in small animals. Front Oncol 2022; 12: 982417. doi: 10.3389/fonc.2022.982417
16. Rozanova OM, Smirnova EN, Belyakova TA, Strelnikova NS, Shemyakov AE, Smirnov AV. The effect of irradiation with a sequence of neutrons and protons on the tumor response of solid ehrlich carcinoma and skin reactions in mice in the early and long terms. Biophysics 2022; 67(5): 802–10. doi: 10.1134/S0006350922050153

Slovenian Veterinary Research
DOI 10.26873/SVR-1789-2023
UDC 636.4:578.76:616.2:615.2
Pages: 9–28

Review Article

From Nature's Pharmacy to Swine Health: Harnessing Natural Compounds against PRRSV Infection

Key words

antiviral agents;
natural compounds;
PRRSV;
swine industry

Fredmoore L. Orosco[1,2,3]

[1]Virology and Vaccine Institute of the Philippines Program, Industrial Technology Development Institute, [2]S&T Fellows Program, Department of Science and Technology, Bicutan, Taguig City, 1634, [3]Department of Biology, College of Arts and Sciences, University of the Philippines Manila, Ermita, Manila, 1000, Philippines

***Corresponding author:** orosco.fredmoore@gmail.com

Abstract: Porcine reproductive and respiratory syndrome virus (PRRSV) is a significant viral pathogen that causes substantial economic losses to the swine industry worldwide. The limited efficacy of current therapeutic approaches and emergence of new PRRSV strains highlight the urgent need for novel antiviral strategies. Natural compounds derived from plants, animals, bacteria, and fungi have attracted increasing attention as potential antiviral agents. This comprehensive review focuses on natural compounds with antiviral activity against PRRSV and explores their mechanisms of action, efficacy, and potential applications. These compounds exhibit diverse antiviral mechanisms such as viral attachment and entry inhibition, replication suppression, and modulation of host immune responses. This review also highlights challenges and future directions in this field. Research gaps include the need for further elucidation of the precise mechanisms of action, comprehensive evaluation of safety profiles, and exploration of combination therapies to enhance efficacy. Further research and translational studies are warranted to harness the full potential of these natural compounds and pave the way for the effective control and management of PRRSV infections in the swine industry.

Received: 11 June 2023
Accepted: 22 December 2023

Introduction

Porcine reproductive and respiratory syndrome virus (PRRSV) is the etiological agent responsible for the pathological condition observed in swine, which was initially documented within the borders of the United States (U.S.) in 1987 and subsequently in Europe in 1990 (1). These outbreaks were characterized by detrimental effects on reproduction, post-weaning pneumonia, and elevated mortality rates in growing swine. In the early stages, attempts to identify the causative agent responsible for this novel syndrome proved to be futile, leading to its provisional designation as a mystery swine disease (MSD) in North America. However, in 1991, Koch's postulates for MSD were eventually satisfied through the discovery of a hitherto unidentified RNA virus in Europe, which was subsequently named the Lelystad virus (LV) (2). Shortly after this significant finding, the virus was successfully isolated in North America and was initially referred to as swine infertility and respiratory syndrome virus (SIRSV) (3).

PRRSV has emerged as a pervasive pathogen in most swine-producing nations, posing substantial economic repercussions to the swine industry. PRRSV can infect pigs across all age groups; however, its clinical manifestations are particularly pronounced in pregnant sows and young pigs (4). In pregnant sows, PRRSV infection during the final trimester of gestation may lead to adverse outcomes, such as abortion, characterized by the delivery of stillborn, partially autolyzed, and mummified fetuses. Conversely, young pigs infected with PRRSV commonly display clinical signs, including elevated body temperature, severe dyspnea, diminished appetite, lethargy, eyelid edema, and ear discoloration, appearing either blue or red (5).

The term PRRSV encompasses two distinct genotypes: PRRSV-1, comprising genotypes initially isolated in Europe, and PRRSV-2, which consists of genotypes first identified in North America (6). Presently, both virus types have

achieved global distribution, with PRRSV-1 primarily prevalent in Europe, whereas PRRSV-2 exhibits a wider geographic range, including North America, Asia, and South America (7). Recent investigations into multiple arteriviral nucleotide sequences in nonhuman primates have prompted the reclassification of PRRSV into two separate entities: PRRSV-1 and PRRSV-2 (8). This classification was substantiated by the recognition of remarkable genetic variability within both PRRSV-1 and PRRSV-2, as evidenced by phylogenetic analysis based on ORF5 (9). The extensive genetic diversity exhibited by PRRSV poses a significant challenge for the development of effective antiviral therapeutics. This review aims to discuss the molecular biology, clinical characteristics, transmission, and different natural compounds with antiviral activity against PRRSV, and their respective molecular mechanisms.

Molecular Biology of PRRSV

Taxonomy and Structure

PRRSV is an enveloped RNA virus characterized by a single positive strand (Figure 1) (10). Taxonomically, it belongs to the order *Nidovirales* and family *Arteriviridae*, which also encompasses other viruses such as the lactate dehydrogenase-elevating virus of mice, equine arteritis virus, and simian hemorrhagic fever virus (11). The arterivirus genome is enclosed within a lipid envelope and associated with a singular N protein comprising 110-128 amino acids, forming a core structure. Furthermore, the viral particles exhibited an approximately spherical or oval shape with diameters ranging from 50 to 60 nm. The reported buoyant densities of PRRSV virions in sucrose range from 1.13 to 1.17 g/cm^3 (12). The enveloped surface of the virions appears relatively smooth, which can be attributed to the limited size of the ectodomains of the two major envelope proteins, GP5 and M.

Genome Organization

The complete genome of PRRSV spans approximately 15 kb, featuring a cap structure at the 5' end during mRNA processing and a poly A tail structure at the 3' end (Figure 2) (13). PRRSV isolates can be categorized into two distinct genotypes based on their genomic and antigenic variations: North American (NA), PRRSV-2, and European (EU), or PRRSV-1. These genotypes exhibit an approximate sequence identity of 65% (14).

The PRRSV genome comprises 12 open reading frames (ORFs) designated as ORF1a, ORF1a', TF, ORF1b, ORF2a, ORF2b, ORF3, ORF4, ORF5a, and ORF5–ORF7 (15). Among these, ORF1a and ORF1b encode polyproteins pp1a and pp1ab, which undergo processing to yield 17 nonstructural proteins (NSPs) (NSP1α, NSP1β, NSP2, NSP2N, NSP2TF, and NSP3-14), which play a pivotal role in virus replication (16). Recently, a novel ORF known as the ORF trans-frame (TF) was discovered within the nsp2 region (17). This ORF, expressed through both −1 and −2 ribosomal frameshifting, gives rise to two additional nsps: nsp2N, a truncated version of nsp2; and nsp2TF, a fusion protein formed by the N-terminal two-thirds of nsp2 and a C-terminal region encoded by the TF ORF spanning 169 amino acids (18). The major envelope proteins GP5 and M are encoded by ORF5 and ORF6, respectively. These proteins interact with each

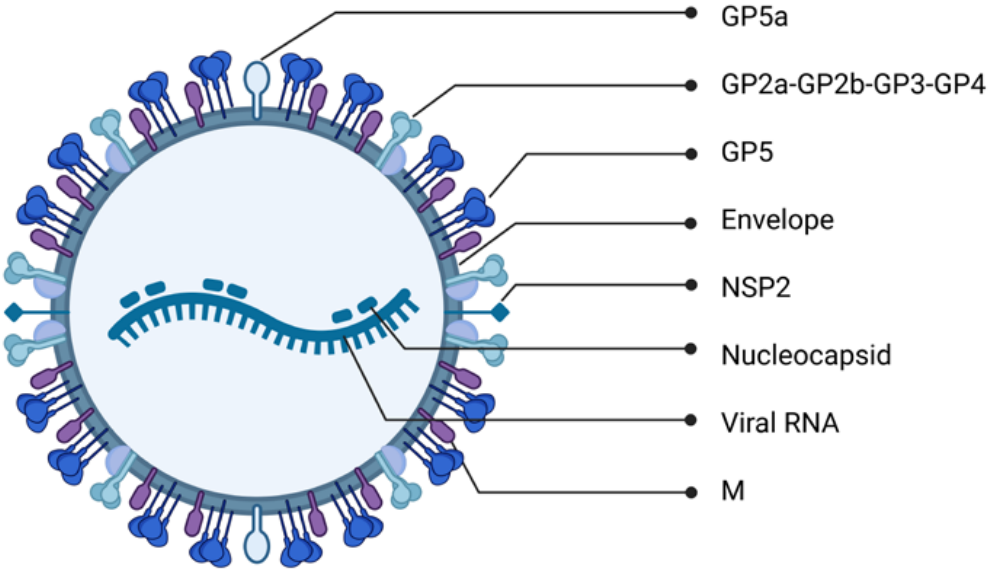

Figure 1: Schematic representation of PRRSV structure

PRRSV mature viral particle, composed of a lipid bilayer envelope with viral receptor glycoproteins involved in infection and cell internalization. Single-stranded positive RNA is associated with nucleocapsid protein in the internal layer of the virus.

other to form heterodimers on the surface of viral particles. Notably, GP5 exhibits substantial variability among structural proteins in the PRRSV genome, making it a commonly employed target for phylogenetic analyses (19). ORF2, ORF3, and ORF4 encode the minor envelope proteins GP2a, GP3, and GP4, respectively, forming noncovalent heterodimers. In addition, two small non-glycosylated proteins, E and GP5a, are encoded by ORF2b and ORF5a, respectively. The highly conserved nucleocapsid protein (N protein) is encoded by ORF7 (20).

Clinical Characteristics

PRRSV infections are characterized by several distinctive clinical features, including elevated body temperature, pronounced contagiousness, and substantial morbidity and fatality rates. Following infection, pigs often experience a rapid increase in body temperature, reaching 41-42°C within a span–1-2 days (21). This heightened contagiousness results in infection spreading throughout the entire pig population within 3-5 days, with a disease duration typically lasting 1-3 weeks. Notably, the highly pathogenic PRRSV (HP-PRRSV) demonstrated a particularly high fatality rate in suckling pigs (100%) and nursery pigs (approximately 70%). Furthermore, adult pigs exhibit an increased mortality rate, with finishing pigs experiencing a mortality rate of 20% and pregnant sows experiencing a minimum of 10% mortality (22). Additionally, PRRSV infections are frequently associated with an elevated incidence of abortions, ranging from 40% to 100%. Furthermore, affected pigs often display signs, such as skin erythema and severe respiratory symptoms, including coughing, dyspnea, and tachypnea. Some pigs may also exhibit neurological signs, such as limping, and gastrointestinal manifestations, such as constipation or diarrhea (21).

PRRSV infection induces a wide array of pathological changes in affected pigs. Among the prominent gross lesions, multifocal hemorrhages are particularly notable, affecting various tissues and organs, such as the skin, lungs, lymph nodes, kidneys, and heart (22). Another significant observation was the presence of lymphadenopathy accompanied by pronounced interstitial pneumonia, characterized by severe pulmonary edema and consolidation. In certain instances, edema and congestion can be observed within the brain. Additionally, severe thymus atrophy is frequently encountered, especially in piglets infected with HP-PRRSV (21).

Secondary bacterial infections are a significant and frequently encountered issue in the context of HP-PRRSV infections. Among the commonly detected bacterial pathogens, *Escherichia coli*, *Streptococcus suis*, *Haemophilus parasuis*, and *Mycoplasma hyopneumoniae* are frequently implicated (22). Furthermore, PRRSV-infected pig populations often exhibit the presence of various viral pathogens, including classical swine fever virus (CSFV), pseudorabies virus (PRV), and porcine circovirus type 2 (PCV2). The potential synergistic effects of these coinfections on PRRSV pathogenesis have garnered substantial attention within the PRRSV research community, prompting intensive investigation (21).

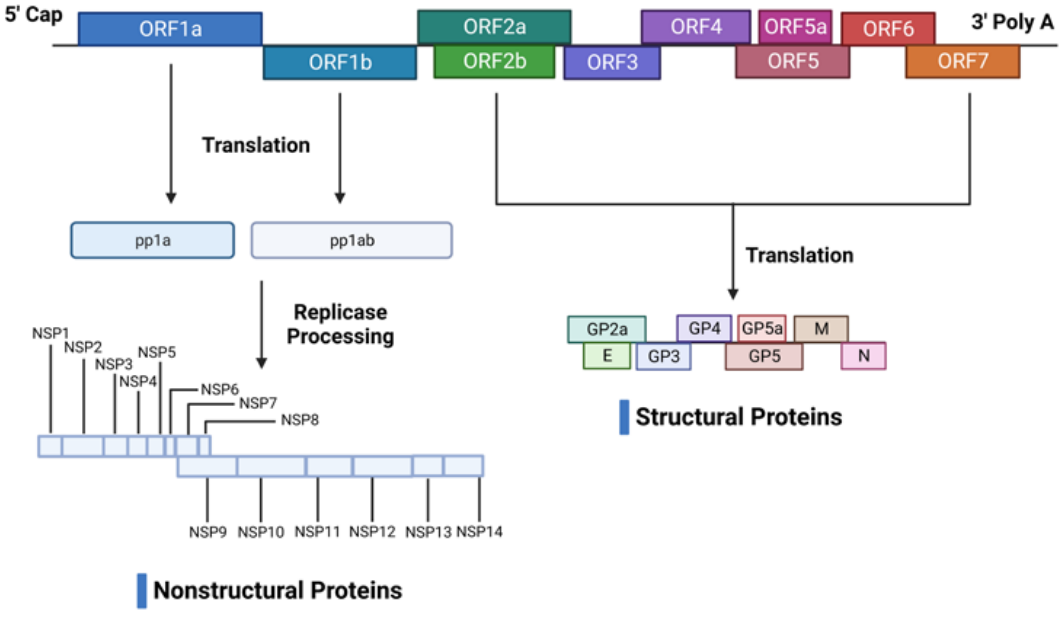

Figure 2: Genome organization of PRRSV virus

Non-structural proteins are located in the 5' end of the genome, coding for two different polyproteins pp1a and pp1ab that is cleaved into at least 14 nsps. Structural proteins near the 3' end are associated with the viral envelope and RNA packaging.

Transmission of PRRSV

Transmission Routes

PRRSV transmission in pigs can occur through various routes, including direct contact and indirect transmission via fomites. Exposure to PRRSV primarily occurs through respiratory and oral routes as well as through mucosal or percutaneous routes. The modes of transmission encompass aerial transmission, either over short or longer distances, as well as transmission through coitus or insemination, ingestion, contact, and occasionally through inoculation, often arising from iatrogenic factors. Vertical transmission during the later stages of gestation is particularly noteworthy. The minimum infectious dose (MID) of PRRSV depends on the specific route of exposure. For instance, infectious dose 50 (ID_{50}) through oral and nasal exposure has been previously evaluated. Notably, variations in infectivity have been observed among different PRRSV isolates via various transmission routes (23). In terms of sexual transmission, the ID_{50} for exposure via artificial insemination is 103.3 $TCID_{50}$ (24).

Based on available data, percutaneous exposure is associated with the lowest MID. Within the farm environment, parenteral exposure is likely to occur frequently, involving routine practices, such as ear notching, tail docking, teeth clipping, and the administration of drugs and vaccines. During the peak viremia stage, infected animals typically exhibit a viral load of at least 103–104 $TCID_{50}$/mL (25). Regular pig behavior can also contribute to parenteral exposure, such as bites, cuts, scrapes, and abrasions, during instances of inter-pig fighting. Aggressive interactions between infected sows and susceptible contacts may play a significant role in PRRSV transmission (26).

PRRSV is notably susceptible to inactivation by various means, including lipid solvents, heat, desiccation, and extreme pH conditions (27). Notably, LV was shown to undergo inactivation after 6 min at 56°C or 3 h at 37°C. However, it displays stability for up to 140 hours at 4°C and remains viable for several months when maintained in a cell culture medium at pH 7.5 and temperatures ranging from -70°C to -20°C (28). In terms of disinfection, iodine (0.0075%) and quaternary ammonium compounds (0.0063%) achieve complete inactivation of the virus within 1 min (29). Chlorine can also completely inactivate PRRSV, although higher disinfectant concentrations (0.03%) and longer exposure times (10 min) are required. Additionally, a 10-minute exposure to ultraviolet light effectively leads to the complete inactivation of the virus on commonly encountered farm surfaces and materials (30).

Development of Viremia and Viral Persistence

Following exposure to PRRSV, viral replication initially occurs within permissive macrophages located in lymphoid tissues at the entry portal. Subsequently, the virus rapidly disseminates throughout the body via the lympho-haematic route. In a genotype 2 model, detectable viremia was observed as early as 12 hours post-infection (hpi) (31). The viral load in the serum peak around 7-10 days post-infection (dpi). The duration of viremia can vary depending on factors such as the specific PRRSV strain and age of the infected animal (32). Various studies have indicated that the viremic period ranges from a few weeks, typically less than four weeks, in adult or grower-finisher pigs, to as long as three months in very young piglets (33). In the case of adult sows infected with genotype 1 PRRSV, viremia may be limited to just one week (34).

During the initial phase of infection, the lungs and various lymphoid organs, including tonsils, Peyer's patches, thymus, and spleen, exhibit the highest viral loads (35). In the lungs, viral detection can typically be observed from 1 to 28 dpi (36). Notably, in young pigs, the virus has been reported to persist in the lungs for up to 49 dpi (37).

Subsequent to the viraemic phase, viral infection enters a stage characterized by the sequestration of the virus within secondary lymphoid tissues, leading to a decline in viral replication. Over time, contagiousness diminishes, although transmission remains feasible for up to three months in horizontally infected pigs. However, in congenitally infected animals, the period of contagiousness may extend beyond this time frame (38). Several situations inducing stress, such as farrowing or regrouping, can trigger reactivation of viral replication and shedding (39).

Viral Shedding

The presence of viremia and the distribution of susceptible macrophages within the body contribute to PRRSV shedding through various routes. In particular, nasal shedding appears to exhibit strain-dependent characteristics, particularly in genotype 1 PRRSV. For instance, nasal shedding of genotype 1 was limited, with only four out of eight pigs showing isolation of the virus at 3 dpi and one out of eight pigs at 7 dpi, always at low titers (25). In the case of genotype 2, nasal secretion was reported in only 1.9% (2/105) of nasal swabs collected from experimentally inoculated pigs during a 28-day observation period (40). Additionally, no virus has been isolated from the nasal secretions of experimentally infected pigs (31).

The shedding of PRRSV in oral fluids appears to be relatively consistent, although most of the available data focus on genotype 2 viruses. The presence of the virus in oral fluids and the steady nature of its shedding over time have important implications for PRRSV transmission. With regard to viral shedding in the semen of infected boars, the detection of the viral genome using RT-PCR has been reported as early as 3 dpi and persisted up to 92 dpi in 1 out of 4 boars inoculated with the VR-2332 isolate (41). PRRSV has also been found in the urine (40) and mammary gland secretions (42). In experimentally infected sows, genotype

2 PRRSV was detected using RT-PCR on the first day of lactation (42). Lastly, infected pigs have been observed to generate aerosols contaminated with the virus during respiratory activities, such as breathing, sneezing, or coughing, although the extent of aerosol transmission can vary depending on the strain (43).

Anti-PRRSV Agents

Natural compounds derived from plants, animals, fungi, and bacteria have received significant research attention because of their potent antiviral activities *in vitro* and *in vivo*. These compounds possess different molecular mechanisms, such as activation of TLR signaling, activation of interferon signaling, downregulation of receptors, and blocking of virus attachment, fusion, replication, translation, assembly, maturation, and release (Figure 3). The compounds are discussed in detail in this section.

Plant-derived Compounds

Tea polyphenols

Tea polyphenol (TPP) refers to the collective group of polyphenols found in tea leaves, with catechins and their derivatives being the primary constituents (44). TPP exhibits a wide range of physiological activities, including antioxidant, anti-radiation, anti-aging, blood lipid-lowering, blood sugar-lowering, and inhibition of bacteria and enzymes (45). Structurally, TPP possesses polyphenolic characteristics such as catechins and anthocyanins (46). Green tea, which serves as a primary source of TPP, exerts notable antiviral and antifungal effects (47). Notably, epigallocatechin gallate (EGCG) has demonstrated antiviral properties against

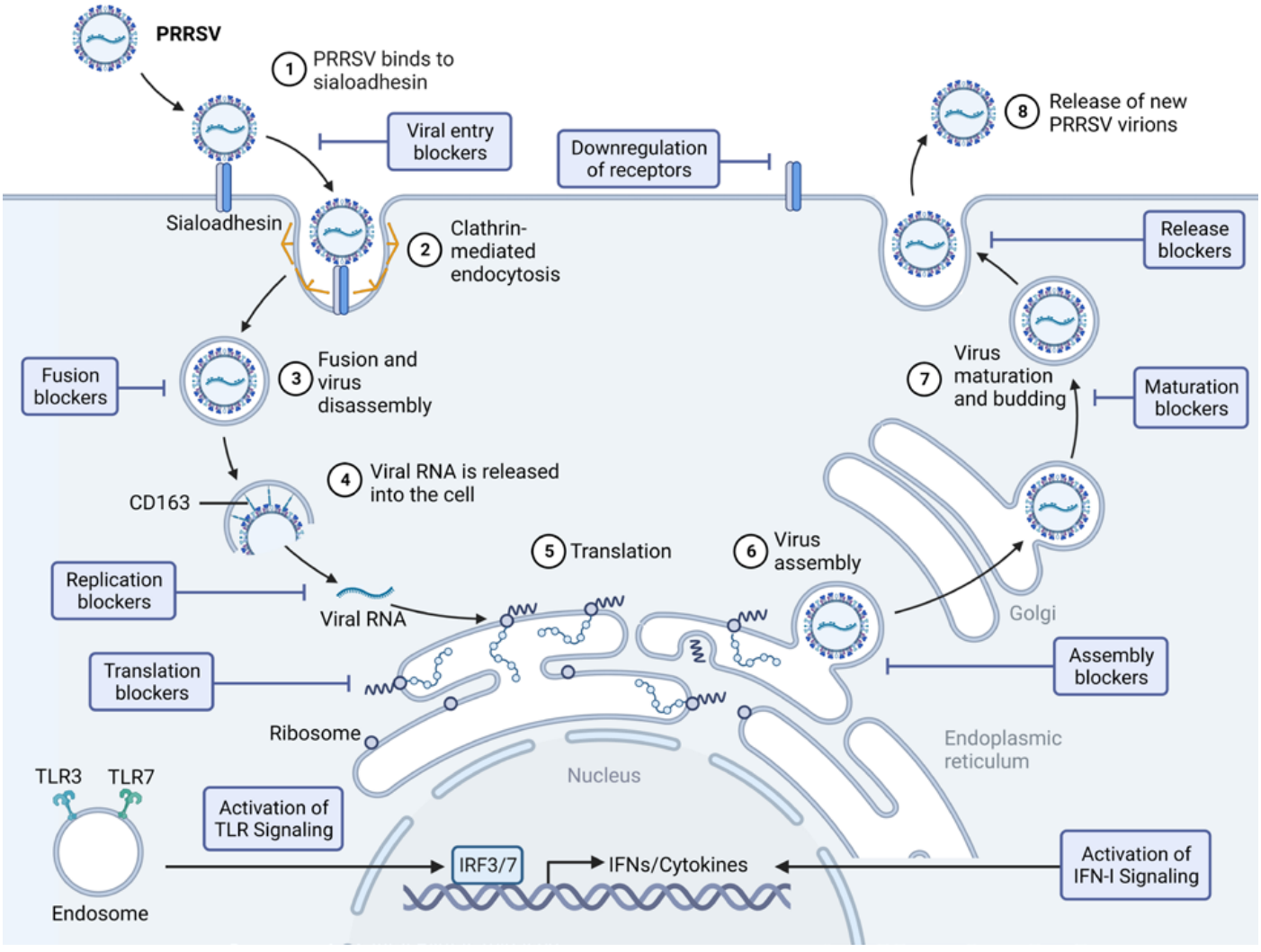

Figure 3: Life cycle and molecular targets of antiviral compound

The life cycle of PRSSV begins with binding of PRRSV with sialoadhesin (1) that will trigger clathrin-mediated endocytosis (2) to fuse with an endosome (3). The virus is then disassembled and the viral RNA is released (4) for translation in the endoplasmic reticulum (5). Translated viral proteins are assembled into new progeny virions (6) followed by maturation and budding in the Golgi body (7). This new progeny virions are released outside of the cell via exocytosis (8).

various viruses, including hepatitis C (HCV), chikungunya (CHIKV), hepatitis B (HBV), and Zika (ZIKV) viruses (48).

TPP potently inhibited PRRSV infection in Marc-145 cells in a dose-dependent manner. TPP exerts its inhibitory effects across multiple stages of the PRRSV life cycle, including attachment, internalization, replication, and release. Mechanistically, TPP impeded the transport of p65 into the nucleus, thereby suppressing the activation of the NF-κB signaling pathway, which ultimately resulted in the downregulation of inflammatory cytokine expression induced by PRRSV infection. Additionally, TPP can interfere with the synthesis of viral nsp2, a crucial component of replication transcription complexes (RTC), leading to inhibition of viral protein translation and assembly (49).

Matrine

Matrine, a prominent quinolizidine alkaloid derived from the dried roots of *Sophora flavescens* Ait, as described in the Chinese Pharmacopeia 2005, exhibits a range of pharmacological effects, including antiviral, anti-inflammatory, and immunoregulatory properties (50). Previous studies have revealed the inhibitory effects of matrine on PRRSV infection in Marc-145 cells, suggesting that matrine can directly inactivate PRRSV and disrupt viral replication within host cells. Furthermore, an indirect immunofluorescence assay and western blot analysis demonstrated that matrine is capable of inhibiting the expression of N protein in Marc-145 cells. Additionally, matrine impedes PRRSV-induced apoptosis by inhibiting the activation of caspase-3 (51).

Moreover, matrine exhibits antiviral activity against both PRRSV and PCV2 (51). The antiviral mechanisms underlying the effects of matrine are thought to involve partial regulation of the TLR3/TLR4/NF-κB/TNF-α pathway (50). Notably, matrine treatment has been shown to improve pneumonia symptoms in PRRSV/PCV2 co-infected mice and has shown efficacy in attenuating inflammation in mice with LPS-induced acute lung injury. Furthermore, matrine directly hindered PRRSV replication by inhibiting the activity of Nsp9. Recent studies have also revealed that matrine can inhibit IL-1β secretion in primary porcine alveolar macrophages (PAMs) by acting on the MyD88/NF-κB pathway and the NLRP3 inflammasome. This inhibition is associated with downregulated expression of MyD88, NLRP3, and caspase-1 as well as suppression of ASC speck formation, IκBα phosphorylation, and hindered translocation of NF-κB from the cytoplasm to the nucleus (52).

Rottlerin

Rottlerin, a polyphenolic ketone compound derived from the Indian Kamala tree (*Mallotus philippensis* Muell. Arg), has gained prominence as a selective PKCδ inhibitor (53). Historically, rottlerin has been used in traditional Indian medicine to treat tapeworm, scabies, and herpetic ringworm infections, implying its long-standing safety record. Notably, several prior studies have documented the antiviral properties of rottlerin against various viruses, including rabies, influenza, human immunodeficiency virus, and PRRSV (54).

Earlier investigations have highlighted the significant impact of rottlerin pretreatment on diminishing both viral RNA synthesis and titer. More recently, it has been demonstrated that the administration of rottlerin during the early stages of PRRSV infection effectively impedes viral replication. PRRSV infection is known to induce phosphorylation of protein kinase C-δ, a process that is specifically counteracted by rottlerin (55). Treatment with rottlerin disrupts the entry pathway of PRRSV by impeding endocytosis of virions. Moreover, *in vivo* studies involving the administration of rottlerin-liposomes to PRRSV-infected pigs, specifically those infected with LMY or FL12 strains, revealed a notable dose-dependent reduction in blood viral load, interstitial pneumonia, and clinical scores when compared to untreated pigs (55).

Sanguinarine

Sanguinarine, a quaternary benzo[c]phenanthridine alkaloid found in various plants such as *Macleaya cordata* (Wild.) R.Br., *Bocconia frutescens* L., *Chelidonium majus* L., *Fumaria officinalis* L., and *Sanguinaria canadensis* L., has been extensively studied for its anti-inflammatory, anti-tumor, and antimicrobial properties (56). While its antiviral activity has rarely been reported, there have been observations of moderate antiviral effects of sanguinarine against tobacco mosaic virus (57). Furthermore, a derivative of sanguinarine, 8-hydroxydihydrosanguinarine, has recently emerged as a potential drug candidate for combating COVID-19 (58).

Regarding its effects on PRRSV, sanguinarine demonstrates potent antiviral activity by targeting multiple stages of the virus life cycle, including internalization, replication, and release (59). Network pharmacology and molecular docking studies identified potential anti-PRRSV targets of sanguinarine, including ALB, AR, MAPK8, MAPK14, IGF1, GSK3B, PTGS2, and NOS2. Additionally, the combination of sanguinarine and chelerythrine, another bioactive alkaloid derived from *Macleaya cordata*, has shown improved antiviral effects (59).

Platycodin D

Platycodon grandiflorum A. DC is a widely recognized Chinese herb that is used to treat pulmonary and respiratory diseases. Notably, saponins have been identified as the primary bioactive constituents of P. grandiflorum roots (60). Among these saponins, platycodin D (PD), an oleanane-type triterpenoid saponin with sugar chains attached at the C-3 and C-28 positions of the aglycone, is the most potent in terms of biological activity (61). Previous investigations have demonstrated the diverse pharmacological effects of PD, including its antitumor properties (62), anti-inflammatory effects (63), and immunological adjuvant activities (60). Moreover, PD has been shown to possess hepatoprotective properties and anti-hepatitis C virus (HCV) activity (64).

PD demonstrated remarkable efficacy against PRRSV infection in both Marc-145 cells and primary PAMs (65). Its inhibitory effects extend across various strains of PRRSV, including the highly pathogenic type 2 strains GD-HD and GD-XH, as well as the classical strains CH-1a and VR2332. Notably, PD displayed dose-dependent inhibition of PRRSV RNA synthesis, viral protein expression, and production of progeny viruses, with significant effects observed at concentrations ranging from 1 to 4 μM. The EC_{50} values of PD against the four tested PRRSV strains in Marc-145 cells ranged from 0.74 to 1.76 μM (65).

The antiviral mechanism of PD involves direct interaction with PRRSV virions, thereby affecting multiple stages of the viral life cycle, including viral entry and release of progeny virus. Furthermore, PD exhibited the ability decreases the production of cytokines (IFN-α, IFN-β, IL-1α, IL-6, IL-8, and TNF-α) induced by both PRRSV and LPS in PAMs (65).

Cryptotanshinone

Cryptotanshinone (CPT) is a natural compound derived from the roots of *Salvia miltiorrhiza* Bunge (Danshen). The roots of *S. miltiorrhiza* have long been used in traditional oriental medicine to treat various circulatory disorders, liver diseases, coronary heart disease, hepatitis, and chronic renal failure (66). Notably, CPT exhibited remarkable antibacterial activity, surpassing the effectiveness of the other tested tanshinones. Furthermore, its anti-inflammatory properties have been attributed to the inhibition of cyclooxygenase II activity and endothelin-1 expression (67).

CPT has demonstrated notable efficacy in impeding the infection of diverse PRRSV strains in PAMs, which serve as primary targets of PRRSV *in vivo*. The underlying mechanism involves the inhibition of signal transducer and activator of transcription 3 (STAT3) activation, the blockade of interleukin 10 (IL-10)-stimulated CD163 expression, and the basal level of CD163 expression in PAMs (68). Remarkably, CPT was effective in both pre- and post-PRRSV infection treatment, with the combined application resulting in substantial dose-dependent inhibition of PRRSV infection. Moreover, CPT displays inhibitory effects against both type I and type II PRRSV infections in PAMs (68).

Allicin

Garlic (*Allium sativum* L.) and its organosulfur compounds (OSC) have been extensively studied for their pharmacological properties, including antibacterial, antiviral, anti-inflammatory, anticancer, and antioxidant effects (69). Allicin, an OSC present in garlic, onion, and other Allium plants, has been recognized for its significant antiviral activity against herpes simplex virus-1 and 2, parainfluenza-3, vaccinia virus, vesicular stomatitis virus, and human rhinovirus-2 (70). Previous investigations have also demonstrated the antiviral potential of allicin against respiratory viruses, such as influenza, SARS-CoV, and rhinovirus (71). In a recent study, allicin was found to alleviate SARS-CoV-2 infection *in vitro* and restore host cellular pathways disrupted by viral infections (72). Furthermore, allicin has shown efficacy as an antiviral agent against the reticuloendotheliosis virus by reducing inflammation and oxidative damage, primarily through inhibition of the ERK/MAPK pathway (73). Additionally, allicin exhibits anti-inflammatory properties by inhibiting the P38 and JNK pathways as well as the TLR4/NF-κB signaling pathway (74).

Supplementation of garlic botanicals in the nursery basal diet has been shown to have beneficial effects on PRRSV-infected pigs, including reduction of viral loads and improvement of immune responses (75). Allicin demonstrated a dose-dependent inhibitory effect on both HP-PRRSV and NADC30-like PRRSV. It exerts its antiviral activity by interfering with various stages of the viral life cycle, including entry, replication, and assembly. Additionally, allicin alleviates the expression of pro-inflammatory cytokines (such as IFN-β, IL-6, and TNFα) induced by PRRSV infection. Treatment with allicin effectively restores dysregulated pro-inflammatory signaling pathways, including the TNF and MAPK signaling pathways, which are upregulated during PRRSV infection (76).

Curcumin

Curcumin, a natural polyphenolic compound isolated from *Curcuma longa* L. rhizomes, has been extensively studied for its various biological and pharmacological effects. It is the major component of *C. longa* and accounts for its immunomodulatory, antitumor, anti-inflammatory, antioxidant, antimutagenic, antibacterial, antifungal, and antiviral activities associated with this plant (77). Among its antiviral properties, curcumin has been shown to inhibit the entry of several viruses into cells, including HCV, CHIKV, and vesicular stomatitis virus (VSV) (78). In the context of PRRSV infection, curcumin has been found to effectively inhibited the infection of both Marc-145 cells and PAMs by four different genotype 2 PRRSV strains. Interestingly, curcumin did not affect the levels of major PRRSV receptor proteins on the cell surface or PRRSV binding to cells. Instead, it specifically targets two crucial steps in the PRRSV infection process: virus internalization and virus-mediated cell fusion (79).

Aloe vera extracts

Aloe vera is known for its remarkable inhibitory effect on a wide range of viruses, including herpes simplex virus type 1, influenza virus, and pigeon paramyxovirus type 1 (80). Notably, this antiviral property has been attributed not only to the whole extract of Aloe vera but also to its isolated compounds. Emodin (1, 3, 8-trihydroxy-6-methylanthraquinone), an anthraquinone compound found in the roots and bark of pharmaceutical plants, such as Chinese rhubar (*Rheum palmatum* L.) and *Aloe vera* L. (81), has demonstrated significant inhibitory effects against various viruses. These include Cyprinid herpesvirus 3 (CHV3) (82), coxsackieviruses (CV) (83), ZIKV (84), enterovirus 71 (EV71) (85), Epstein-Barr virus (EBV) (86), HCoV-OC43 (87), herpes simplex virus (HSV) (88), HBV (89), and SARS-CoV

(90). Emodin exerts its antiviral activity through multiple mechanisms, including blockade of virus-receptor interactions, inhibition of viral protein translation, suppression of viral maturation, and inhibition of viral release (90).

Aloe extract (Ae) has been found to exhibit potent inhibitory effects against PRRSV *in vitro*, specifically in Marc-145 cells and PAMs (91). Emodin demonstrated an inhibitory effect by targeting various stages of the PRRSV infection cycle. Emodin was able to directly inactivate PRRSV particles. Additionally, emodin treatment significantly upregulated the expression of Toll-like receptor 3 (TLR3) ($p < 0.01$), IFN-α ($p < 0.05$), and IFN-β in iPAMs. This suggested that the anti-PRRSV effect of emodin may be attributed to the induction of antiviral agents through TLR3 activation (91).

Cepharanthine

Cepharanthine (CEP) is an alkaloid derived from *Stephania cepharantha* Hayata, which has a long history of use in Japanese medicine for various conditions, including radiation-induced leukopenia and certain skin and ear disorders (92). The therapeutic potential of CEP extends beyond its traditional applications, as it possesses diverse properties such as anti-inflammatory, antioxidant, immunomodulatory, and antiparasitic effects, making it an attractive candidate for treating viral diseases such as COVID-19 (93).

Notably, CEP has demonstrated antiviral activity against HCoV-OC43, a mildly pathogenic human coronavirus (94), and severe acute respiratory syndrome coronavirus (SARS-CoV) (95). Moreover, in a comprehensive drug screening study involving 2406 clinically approved drugs, CEP emerged as the most effective compound against pangolin coronavirus closely related to SARS-CoV-2, the virus responsible for the COVID-19 pandemic (96). This discovery is particularly significant considering the high genomic similarity between SARS-CoV and SARS-CoV-2 (97). Given these promising findings, CEP has garnered significant attention as a potential therapeutic option for the treatment of COVID-19 by exploiting its established antiviral properties and favorable activity against related coronaviruses (96).

In recent investigations, CEP has demonstrated superior inhibitory effects on PRRSV infection compared to tilmicosin, as evidenced by reductions in both RNA and protein levels. Notably, CEP treatment led to a 5.6-fold decrease in $TCID_{50}$, providing substantial protection against PRRSV infection in Marc-145 cells (98). Mechanistically, detailed analyses involving western blot assessments of Marc-145 cells and PAMs subjected to CEP treatment and PRRSV infection at various time points revealed the ability of CEP to suppress the expression of integrins β1 and β3, integrin-linked kinase (ILK), RACK1, and PKCα. These effects culminated in the suppression of NF-κB signaling, ultimately alleviating PRRSV infection. These findings underscore the potential of CEP as a valuable intervention strategy against PRRSV infection, offering new insights into its antiviral mechanisms and therapeutic implications (98).

Glycyrrhizin

Glycyrrhizin, a triterpene saponin found in licorice root (*Glycyrrhiza glabra* L.), possesses a diverse range of biological activities, including antibacterial, antiviral, anti-inflammatory, anticancer, antioxidant, liver protection, neuroprotection, skin whitening, hypoglycemic, and memory-enhancing properties (99). These characteristics highlight the promising potential of licorice in cosmetic production and therapeutic applications for various conditions such as liver disease, diabetes, ischemia-reperfusion injury, Alzheimer's disease, Parkinson's disease, epilepsy, depression, and cancer (100).

Numerous studies have documented the potent antiviral effects of glycyrrhizin against a range of viruses, including the hepatitis B virus (HBV) (101), HCV (102), herpes simplex virus (HSV) (103), SARS coronavirus (104), and influenza viruses (105). Recent studies have revealed dose-dependent inhibitory effects of glycyrrhizin on the proliferation of PRRSV. Treatment with glycyrrhizin effectively reduced PRRSV proliferation and PRRSV-encoded protein expression, which primarily targeted the penetration stage of the PRRSV life cycle, exerting minimal influence on the processes of viral adsorption or release (105).

Flavaspidic acid AB

Flavaspidic acid AB (FA-AB) is a naturally occurring compound derived from *Dryopteris crassirhizoma* Nakai, a semi-evergreen fern with a rich history in traditional Chinese medicine (106). The rhizome of *D. crassirhizoma* has traditionally been employed as an anti-infection agent, particularly for respiratory ailments such as the common cold and flu. Notably, it has been utilized in combination with other Chinese herbal medicines, including Astragalus, Atractylodes, Red Atractylodes, Pogostemon, Adenophora, and Lonicera, in a prescription formula to prevent SARS (106).

FA-AB belongs to the phloroglucinol derivative family (107). Extensive investigations have demonstrated the antibacterial, antitumor, and antioxidant properties of phloroglucinol derivatives (107). Additionally, dimeric phloroglucinols have shown inhibitory effects against HIV-1 reverse transcriptase, highlighting their potential for antiviral intervention (108).

FA-AB inhibits the internalization and intercellular transmission of PRRSV, although it does not interfere with the initial binding of PRRSV to host cells (109). Remarkably, when FA-AB treatment was initiated 24 hours after viral infection, it effectively suppressed PRRSV replication, as evidenced by kinetic analysis of viral replication. Moreover, FA-AB can induce the expression of important antiviral cytokines, including IFN-α, IFN-β, and IL1-β, in PAMs (109).

***Caesalpinia sappan* (CS) heartwood**

Caesalpinia sappan L. 1753 (CS), derived from the *Leguminosae* family, is a renowned medicinal plant that is

widely distributed and cultivated in various tropical Asian regions such as Southern China, India, Myanmar, Vietnam, Sri Lanka, and Thailand (110). CS dried heartwood has been utilized in traditional medicine practices, including Indian Ayurveda and Traditional Chinese Medicine (111). CS heartwood exhibits a diverse range of biological activities, including antioxidant (112), antibacterial (113), anti-inflammatory (114), hypoglycemic (115), and hepatoprotective (116) properties, as reported in previous studies. Moreover, CS extract constituents have demonstrated significant activity against the H3N2 strain of influenza virus (117). Additionally, CS showed promising antiviral activity against PRRSV replication in MARC-145 cells, with a significant reduction in the viral titer observed at 72 hpi. Notably, this antiviral effect was attributed to the presence of specific compounds such as byakangelicin, brazilin, naringenin, and brazilein (118).

Saponin Components

Saikosaponin A (SSA), Saikosaponin D (SSD), Panax notoginseng saponins (PNS), Notoginsenoside R1 (SR1), and Anemoside B4 (AB4) have gained significant attention in recent research because of their diverse bioactivity (119). Specifically, its antiviral potential against PRRSV was investigated. In a study involving 132 healthy piglets, saponin components were evaluated for their effects on PRRSV-induced immunopathological damages (120). Piglets were divided into 22 groups, with each group consisting of six animals. The control group received an intramuscular injection of PRRSV solution, while the low-, middle-, and high-dose treatment groups were administered PRRSV solution followed by intraperitoneal injections of AB4, PNS, SR1, SSA, or SSD at varying doses. The results demonstrated that all five saponin components reduced the incidence and severity of PRRSV-induced immunopathological damage, including symptoms, such as elevated body temperature, weight loss, anemia, and internal inflammation. Furthermore, these saponin components exhibited the ability to enhance protein absorption and immune responses (120).

Isobavachalcone

Isobavachalcone (IBC) is a prenylated chalcone compound belonging to the flavonoid subclass that was originally derived from *Psoralea corylifolia* L. (121). Extensive research has revealed that IBC exhibits a broad range of biological activities, including antibacterial, antifungal, anticancer, antireverse transcriptase, antitubercular, and antioxidant properties (121). Notably, IBC demonstrated inhibitory effects on PRRSV replication at the post-entry stage of infection. This suggests that IBC may serve as a promising therapeutic candidate for the treatment of PRRSV infection in swine (122).

Ursolic acid derivatives

Ursolic acid (UA) and its derivatives are widely recognized as prominent examples of pentacyclic triterpenoids (PTs), which possess diverse biological activities, including antiviral and antibacterial properties. UA has exceptional anti-HIV activity, which is attributed to its ability to inhibit HIV-1 proteases (123). Both oleanolic acid (OA) and UA possess anti-HCV activity by suppressing the enzymatic activity of HCV NS5B RNA-dependent RNA polymerase, acting as non-competitive inhibitors (124).

Recent investigations have revealed that the amidation of the 17-carboxylic acid group of UA yields notable improvements in both anti-PRRSV efficacy and cytotoxicity attenuation in MARC-145 cells. This modified derivative potently inhibited PRRSV infection not only in MARC-145 cells but also in PAMs and PRRSV-infected cells *in vivo* (125). Moreover, it displayed broad-spectrum inhibitory activities against various PRRSV strains, including the highly pathogenic NADC30-like and GD-XH strains, as well as the classical CH-1a and VR2332 strains *in vitro*. Mechanistically, the compound exerted its antiviral effects by directly inactivating PRRSV virions, thereby disrupting multiple stages of the viral life cycle, including viral entry, replication, and release, while leaving cellular susceptibility to PRRSV unaffected (125).

Xanthohumol

Xanthohumol (Xn), a prenylated flavonoid originating from the hop plant *Humulus lupulus* L., emerges as a natural compound with diverse bioactive properties, (126). Notably, Xn has garnered attention for its anti-inflammatory potential, as demonstrated by its ability to counteract lipopolysaccharide (LPS)-induced acute lung injury and ischemia reperfusion-induced liver injury in murine models (127). Additionally, Xn exhibits anti-proliferative effects in various cancer cell lines, including breast, colon, and ovarian cancers (128). The antiviral activity of Xn has also been documented against human immunodeficiency virus (HIV), bovine viral diarrhea virus (BVDV), and HSV-1 and -2 (129).

Xn, a prenylated flavonoid compound, displays potent inhibitory effects against various sub-genotype strains of PRRSV when tested on PAMs (130). Notably, Xn exhibited a low half-maximal inhibitory concentration (IC_{50}), emphasizing its efficacy in combating PRRSV infections *in vitro*. Furthermore, Xn treatment led to a reduction in the expression levels of pro-inflammatory cytokines, including IL-1β, IL-6, IL-8, and TNF-α, in PAMs infected with PRRSV and those treated with LPS. Animal challenge experiments using highly pathogenic PRRSV infections have shown that Xn effectively mitigates clinical signs, lung pathology, and inflammatory responses in the lung tissues of infected pigs (130).

Toosendanin

Toosendanin (TSN) is a tetracyclic triterpene derived from the bark and fruit of *Melia toosendans* Sieb. et Zucc. Traditionally, it has been used as an agricultural insecticide and digestive tract parasiticide in China (131). Notably, TSN has demonstrated significant efficacy in combating botulism, as evidenced by *in vivo* and *in vitro* studies (132). Subsequent studies have highlighted its potential as an anticancer agent with the ability to induce apoptosis in diverse

cancer cell types (133). Recently, TSN has garnered attention for its antiviral properties, exhibiting activity against influenza A virus (IAV) (134), HCV (135), severe fever with thrombocytopenia syndrome virus (SFTSV), and SARS-CoV-2 (136).

TSN exhibited robust inhibitory effects on the replication of type 2 PRRSV both *in vitro*, using Marc-145 cells, and ex vivo, using PAMs, even at sub-micromolar concentrations (137). Transcriptomic analyses further elucidated that TSN treatment upregulated IFI16 expression in Marc-145 cells. Additionally, we demonstrated that TSN induces the activation of caspase-1 and maturation of IL-1β through an IFI16-dependent pathway (137).

Iota-Carrageenan

Carrageenan (CG), a sulfated galactan derived from marine red algae (*Rhodophyta*), has garnered significant attention because of its various biological activities (138). It is widely recognized as a safe compound by regulatory authorities and has extensive applications in the food, cosmetic, and pharmaceutical industries as a stabilizer, emulsifier, or thickener (139). Previous studies have demonstrated the anticoagulant, antitumor, and immunomodulatory properties of carrageenan (140). Notably, carrageenan exhibits potent inhibitory effects against a range of viruses including IAV, dengue virus-2 (DENV-2), human rhinovirus (HRV), and HSV-1 (141).

Recent investigations have revealed the effectiveness of CG in inhibiting replication of the CH-1a strain of PRRSV at both the mRNA and protein levels in Marc-145 cells and PAMs (142). The antiviral mechanism of CG primarily occurs during viral attachment and entry into the viral life cycle. Moreover, CG hampered viral release in Marc-145 cells and mitigated CH-1a-induced apoptosis during the late stages of infection. Furthermore, CG inhibits CH-1a-induced NF-κB activation, thereby interfering with cytokine production in both Marc-145 cells and PAMs (142).

Griffithsin

Griffithsin, a lectin derived from marine red algae of *Griffithsia* spp., is a small protein consisting of 121 amino acids (143). Griffithsin effectively inhibits viral infectivity through its interaction with glycan moieties associated with the glycoproteins of various enveloped viruses (144). Extensive studies have demonstrated the remarkable antiviral activity of Griffithsin against several human enveloped viruses, including HIV (143), Middle East respiratory syndrome coronavirus (MERS-CoV) (145),SARS-CoV (146), HCV (147), HSV-2 (148), and Japanese encephalitis virus (JEV) (149).

An exceptional characteristic of Griffithsin is its impressive thermostability, as it remains stable even at temperatures as high as 80°C (150). Griffithsin displays resistance to organic solvents (143) and protease degradation (151), further emphasizing its potential as a therapeutic agent. Moreover, extensive cytotoxicity studies have revealed the superior safety profile of Griffithsin (152). No cytotoxic effects were observed against various cell types, and it demonstrated minimal impact on peripheral blood mononuclear cell activation as well as cytokine and chemokine production (152).

Griffithsin demonstrated potent antiviral activity against PRRSV, which was likely mediated by its specific interactions with glycans present on the surface of the virus, thereby impeding viral entry. Notably, Griffithsin effectively blocked viral adsorption while leaving viral penetration unaffected. Additionally, Griffithsin exhibited the ability to hinder cell-to-cell spread, thereby interrupting virus transmission (153).

Proanthocyanidin A2

Proanthocyanidins, a class of naturally occurring polyphenolic bioflavonoids abundant in various plant sources, such as fruits, vegetables, nuts, seeds, and bark, including grape seeds, have garnered attention for their diverse array of bioactive properties, including antioxidant, cardioprotective, anticancer, antibacterial, antiviral, and anti-inflammatory activities (154). Notably, grape seed-derived proanthocyanidins have demonstrated significant bioactivity *in vitro* (155).

Of particular interest is Proanthocyanidin A2 (PA2), a dimeric form of proanthocyanidin that results from the condensation of catechins (156). The antiviral potential of PA2 and its analogs has been highlighted against various viruses, including HSV, Coxsackie B virus (CBV), and canine distemper virus (CDV) (157).

PA2 showed remarkable antiviral activity against PRRSV infection both *in vitro* (158). Notably, PA2 exhibited broad-spectrum inhibitory effects against traditional genotype II PRRSV strains, such as CH-1a, GD-XH, and GD-HD strains, with comparable potency and EC_{50} values ranging from 2.2 to 3.2 μg/ml. Treatment with PA2 results in a dose-dependent reduction in viral RNA synthesis, viral protein expression, and progeny virus production in PRRSV-infected Marc-145 cells (158).

Furthermore, PA2 exerted immunomodulatory effects by suppressing the expression of key cytokines (TNF-α, IFN-α, IL-1β, and IL-6) induced by PRRSV infection in PAMs. This highlights the potential of PA2 in mitigating the inflammatory response associated with PRRSV infection. Mechanistically, PA2 exhibits multifaceted antiviral mechanisms by targeting various pathways, including inhibition of viral entry and blocking progeny virus release (158).

Bacterial Compounds

Tilmicosin

Tilmicosin, a chemically modified macrolide antibiotic derived from tylosin, is an essential veterinary antimicrobial agent used to treat bacterial infections in animals. Originally synthesized in *Streptomyces fradiae*, tilmicosin

has specifically been formulated for veterinary use in cattle, sheep, and swine. It is available in injectable form for cattle and sheep, whereas a premix feed formulation is utilized for swine (159). The antimicrobial activity of tilmicosin is effective against a wide range of gram-positive and gram-negative bacteria. Additionally, tilmicosin demonstrates efficacy against intracellular bacteria such as *Rhodococcus* sp. and *Mycoplasma* sp., making it a valuable therapeutic option in veterinary medicine (160).

Limited research has explored the antiviral properties of tilmicosin against PRRSV; however, promising findings have emerged. Previous investigations have demonstrated the dose-dependent inhibitory effects of tilmicosin on PRRSV replication in cultured PAMs (160). Additionally, tylvalosin, a macrolide derivative, exhibits inhibitory activity against both European and North American strains of PRRSV in cultured cells (161). In an experimental setting using PRRSV-infected pigs, the administration of tilmicosin as a feed additive resulted in noticeable reductions in lymph node hypertrophy, lung lesions, and viremia compared with non-medicated infected controls (162).

Tilmicosin has demonstrated significant potential for mitigating the severity of PRRSV infections in various experimental settings. In a study involving experimentally PRRSV-infected nursery pigs, tilmicosin treatment yielded notable improvements in disease outcomes, as evidenced by reduced clinical signs, improved feed consumption, and enhanced weight gain, compared to non-medicated challenged pigs. Furthermore, there was a tendency towards lower virus titers in the lungs and serum of tilmicosin-treated pigs (163).

Field evaluations of tilmicosin in sows have yielded promising results (164). In one study, the administration of an aqueous form of tilmicosin to nursery pigs in a controlled environment resulted in a 50% reduction in mortality, lower body temperature, a significant increase in average daily gain, and reduced lung lesions in the medicated group compared to the non-treated group (165,166). These findings highlight the potential of tilmicosin in improving both clinical outcomes and performance indicators in PRRSV-infected pigs. The accumulation of tilmicosin in macrophages, the primary target cells for PRRSV replication, may provide a mechanistic explanation for the observed reduction in clinical severity (167).

Tulathromycin

Tulathromycin (TUL), a triamide compound, possesses unique structural features characterized by a lactone ring containing three polar amine groups. This antimicrobial agent is commonly employed for the treatment and prevention of swine respiratory diseases associated with *Actinobacillus pleuropneumoniae* (App), a gram-negative bacterium frequently found in PRRSV-infected pigs (168).

Recent investigations have revealed additional properties of tulathromycin beyond its antimicrobial effects. Studies have demonstrated its ability to inhibit the production of CXCL-8 and LTB4, the key mediators of inflammation, in stimulated neutrophils and macrophages (169). Moreover, tulathromycin promotes apoptotic death of neutrophils and facilitates their phagocytic clearance by macrophages, a crucial process known as efferocytosis, which contributes to the resolution of inflammation (170). TUL also exhibited potent immunomodulatory properties in the absence of any direct antiviral effects against PRRSV. TUL has exhibited an additive effect with PRRSV in inducing macrophage apoptosis and effectively inhibiting virus-induced necrosis (171).

Actinobacillus pleuropneumoniae

Porcine pleuropneumonia, a significant disease affecting the swine industry worldwide, is caused by *Actinobacillus pleuropneumoniae* (App). In recent years, *in vitro* models using St. Jude Porcine Lung (SJPL) cell line, an immortalized epithelial cell line, have been developed to investigate host-pathogen interactions (172). These models have been instrumental in studying co-infections involving App and porcine viral pathogens. Interestingly, during App-PRRSV coinfection of SJPL cells, it was unexpectedly observed that App culture supernatants exhibited robust antiviral activity against PRRSV (173). This finding was further supported by another study that confirmed the antiviral effect of App culture supernatant (174). Antiviral activity of App against PRRSV has also been observed in PAMs (174). Moreover, App inhibits PRRSV replication by inducing cell cycle arrest in the G2/M phase of SJPL cells (175).

Fungal Compounds

Cryptoporus volvatus

The utilization of mushrooms in medical applications has a rich history in Asian countries, and its usage has slightly increased in the Western hemisphere over the past few decades (176). Antiviral properties have been attributed not only to whole mushroom extracts but also to isolated compounds (177). *C. volvatus*, a member of the Order *Aphyllophorales* and genus *Cryptoporus* (178), is found in specific regions of China. The fruiting body of this mushroom has been traditionally employed in the treatment of asthma and bronchitis, with references dating back to the 15th century in the "Materia Medica of Yunnan" (178).

Extracts of *C. volvatus* obtained from various separation processes exhibit differing degrees of inhibitory activity against PRRSV (179). A specific anti-PRRSV component, CM-H-L-5, was isolated from a water-soluble fraction of *C. volvatus*. The inhibitory effect of CM-H-L-5 against PRRSV was dose-dependent. Chemical analysis revealed that CM-H-L-5 is a low-molecular-weight polyol fragment containing amide and carboxylic acid groups (179).

Deoxynivalenol (DON) Mycotoxin

Deoxynivalenol (DON), a trichothecene mycotoxin, is produced by various *Fusarium* spp. molds that are commonly found in feed and other organic substrates. Cereal grains such as wheat, barley, and corn are major sources of DON contamination (180). Pigs, owing to their high grain-based diets, are particularly susceptible to DON toxicity, making them frequently exposed to this mycotoxin (181).

In the context of PRRSV infection, it has been observed that DON concentrations ranging from 140 to 280 exert a significant impact on cell survival (182). Specifically, these DON concentrations remarkably increased the survival rate of PRRSV-infected cells. Furthermore, DON at these concentrations led to a substantial reduction in PRRSV replication. This inhibitory effect is attributed to the induction of pro-inflammatory cytokines and the early activation of apoptosis. These mechanisms appear to interrupt the viral replication cycle and impede PRRSV propagation within the host (182).

Animal-Derived Compounds

Honeybee Venom

Honeybee (*Apis mellifera* Linnaeus 1758) venom (HBV) is recognized as an alternative medicine owing to its therapeutic properties, particularly in the management of pain, inflammation, and immune-related conditions such as rheumatoid arthritis and multiple sclerosis (183). Notably, HBV has demonstrated immunomodulatory effects on the Th1 immune response. Administration of HBV leads to the differentiation of CD4+ T lymphocytes into Th1 cells, thereby enhancing the production of interferon-gamma (IFN-γ) in mouse models (184). Furthermore, HBV phospholipase plays an important role in the maturation of dendritic cells and subsequent activation of dendritic cell-associated immune responses (185,186).

Investigations have been conducted to explore the potential antiviral activity of HBV against PRRSV. In a recent study, HBV was administered to healthy pigs via nasal, neck, and rectal routes, followed by intranasal inoculation with PRRSV (187). Significantly increased levels of CD4+/CD8+ cell ratio, IFN-γ, and IL-12 were observed in HBV-administered pigs via nasal and rectal administration. In pigs experimentally challenged with PRRSV, the viral genome load in the serum, lung, bronchial lymph nodes, and tonsils was significantly reduced, accompanied by mitigation of interstitial pneumonia severity in the nasal and rectal administration groups. Moreover, HBV administration leads to a substantial elevation in the levels of Th1 cytokines (IFN-γ and IL-12) and upregulation of pro-inflammatory cytokines (TNF-α and IL-1β) (187).

Caprylic Monoglyceride

Medium-chain fatty acids (MCFAs), including caprylic monoglycerides (CMG), are a class of fatty acids with carbon chain lengths ranging from 8 to 10 carbon atoms. While MCFAs are present in small quantities in nature, they are primarily derived from milk and breast milk and can also be found in palm kernel oil and coconut oil (188). Notably, MCFAs possess antimicrobial properties and their effects on animal productivity vary depending on the dosage employed (189).

One significant application of MCFAs is their ability to mitigate the transmission of the porcine epidemic diarrhea virus (PEDV) through feed and ingredients (190). Additionally, MCFAs have been demonstrated to influence the growth performance of animals by serving as readily available energy substrates, modulating gastrointestinal morphology, and exerting antimicrobial effects (191). MCFAs as a feed additive can also suppress African swine fever virus (ASFV) infection(192).

In light of the potential antiviral and antimicrobial effects of MCFAs, we investigated their antiviral activity against PRRSV. Recently, a study evaluated the cytotoxicity of four MCFAs, namely caprylic acid, CMG, decanoic monoglyceride, and monolaurin, along with their inhibitory effects on PRRSV. The results demonstrated that CMG exhibited the lowest toxicity towards cells among the four MCFAs, while displaying the highest inhibition rate against PRRSV (193).

To further assess the impact of CMG on PRRSV infection, piglets were treated with varying concentrations of CMG, revealing a significant decrease in mortality and viral load following PRRSV infection in piglets administered higher CMG concentrations ($p < 0.05$). Additionally, the pulmonary pathology in piglets was ameliorated by CMG treatment. Notably, CMG administration resulted in a significant downregulation of pro-inflammatory cytokines, including IL-6, IL-8, IL-1β, IFN-γ, and TNF-α, while upregulating the levels of the anti-inflammatory cytokine IL-10 in comparison to the positive control group ($p < 0.05$) (193).

Protegrin-1

Antimicrobial peptides (AMPs), including protegrin-1 (PG-1), are polypeptides of less than 100 amino acids (194). AMPs are found in both plant and animal kingdoms and exhibit broad-spectrum antimicrobial activity against bacteria, fungi, and viruses involved in the innate immune response to infection (195). PG-1, originally isolated from porcine leukocytes (196), is considered to be an antibiotic agent against Gram-positive and Gram-negative bacteria and fungi *in vitro* (197). Furthermore, previous studies have shown that PG-1 inhibits dengue NS2B-NS3 serine protease and viral replication in MK2 cells (198).

PG-1 also strongly inhibits PRRSV infection and replication by suppressing viral RNA and protein synthesis, virus progeny production, and viral particle release. Furthermore, during the PRRSV life cycle, PG-1 mainly blocked viral attachment in Marc-145 cells. However, in PAMs, PG-1 neither inhibits PRRSV replication nor elevates antiviral cytokine expression (199).

Porcine Plasma Ficoline

Ficolins are proteins that activate the complement system and exhibit the ability to bind N-acetyl groups in various saccharides, particularly N-acetylglucosamine (GlcNAc) (200). This suggests that ficolins may also have the capacity to bind certain viruses that display host glycans on their surfaces (201).

Viral glycoproteins often possess complex-type oligosaccharides that are characterized by two terminal GlcNAc residues (202). Similar collagenous lectins have been shown to bind glycoproteins in IAV, HIV, HSV, and non-enveloped rotavirus (RV) (203). In a recent study, the antiviral activity of plasma-purified and recombinant ficolin α was assessed against PRRSV. The results revealed a reduction in the cytopathic effect of PRRSV-infected Marc-145 cells and inhibition of viral replication in the presence of ficolin α, which is dependent on GlcNAc recognition. Additionally, plasma ficolin α and recombinant ficolin α bind to PRRSV-coated wells in a GlcNAc-dependent manner (204).

Cecropin P1

Cecropin P1 (CP1) is a small antimicrobial peptide originally derived from the intestine of pigs, and it has demonstrated antiviral activity against various viruses, including infectious hematopoietic necrosis virus, viral hemorrhagic septicemia virus, snakehead rhabdovirus, and infectious pancreatic necrosis virus, in *in vitro* studies (205). CP1 exhibits significant antiviral effects against PRRSV, both as an extracellular virucidal agent and as an inhibitor, when administered prior to, simultaneously with, or following viral inoculation. The inhibitory mechanism of CP1 primarily targets viral attachment rather than viral entry into Marc-145 cells (206). Moreover, CP1 effectively impeded viral particle release and mitigated virus-induced apoptosis during the late stages of infection. The inhibitory action of CP1 against PRRSV was also extended to PAMs *in vivo*. Additionally, CP1 upregulates the expression of IL6 in PAMs, which could potentially contribute to its ability to inhibit PRRSV infection (206).

Cecropin D

Cecropin D (CD) is an antimicrobial peptide originally derived from Hyalophora cecropia Linnaeus 1758 pupae, and it has been previously demonstrated to possess antibacterial activity against both Gram-positive and Gram-negative bacteria, including *Escherichia coli* DH5α, K88, K99, *Streptococcus zooepidemicus* C55138, and *Staphylococcus aureus* Cowan I (207). In the context of PRRSV infection, CD exerted inhibitory effects during viral attachment and the early stages of viral entry into Marc-145 cells. Furthermore, CD effectively suppressed virus-induced apoptosis during the late phase of PRRSV infection and attenuated viral release within cells. These observations collectively contribute to the inhibition of PRRSV infection by CD. Importantly, similar inhibitory effects against PRRSV infection are evident when CD is utilized in PAMs during *in vivo* infection in pigs (208).

Conclusions

This comprehensive review highlights the potential of natural compounds derived from plants, animals, bacteria, and fungi as effective antiviral agents against PRRSV. These compounds exhibit diverse mechanisms of action targeting various stages of the PRRSV replication cycle (attachment, entry, fusion, replication, translation, maturation, and release). These compounds have shown promising broad-spectrum antiviral activities both *in vitro* and *in vivo*.

Although significant progress has been made in the field of natural compounds with antiviral activity against PRRSV, several research gaps still need to be addressed. First, further studies are needed to elucidate the precise mechanisms by which these natural compounds exert their antiviral effects. Understanding the molecular interactions between these compounds and PRRSV components will provide valuable insights for the development of more targeted interventions. Second, comprehensive investigations on the safety, pharmacokinetics, and toxicity profiles of these natural compounds are essential. These studies will help determine the optimal dosage and administration routes as well as evaluate potential side effects, ensuring their safe use in veterinary medicine. Finally, there is a need for more comprehensive studies to evaluate the efficacy of combination therapies using natural compounds. Investigating the synergistic effects of combining different compounds or combining them with existing antiviral drugs may enhance overall antiviral efficacy and reduce the emergence of drug-resistant viral strains.

Future research should explore the application of advanced technologies, such as nanotechnology and targeted delivery systems, to enhance the bioavailability and therapeutic potential of these natural compounds. These innovative approaches may improve compound stability, increase tissue specificity, and enhance the antiviral efficacy. Further research addressing the aforementioned research gaps and exploring new avenues, combined with rigorous preclinical and clinical trials, will accelerate the translation of these natural compounds into effective antiviral therapies for the control and prevention of PRRSV infections in swine.

Acknowledgments

The author would like to thank the DOST S&T Fellows Program, the Philippine Council for Agriculture, Aquatic and Natural Resources Research and Development (DOST-PCAARRD) for funding this research project, and the Industrial Technology Development Institute (DOST-ITDI) for hosting this research project.

Conflict of Interest. The author declares that there are no conflicts of interest.

Author Contributions. Fredmoore Orosco: Conception and design of the study, wrote the first draft of the manuscript, critically revised the manuscript, funding acquisition.

References

1. Wensvoort G, Terpstra C, Pol JM, et al. Mystery swine disease in The Netherlands: the isolation of Lelystad virus. Vet Q 1991; 13:121–30.
2. Terpstra C, Wensvoort G, Pol JM. Experimental reproduction of porcine epidemic abortion and respiratory syndrome (mystery swine disease) by infection with Lelystad virus: Koch's postulates fulfilled. Vet Q 1991; 13:131–6.
3. Collins JE, Benfield DA, Christianson WT, et al. Isolation of swine infertility and respiratory syndrome virus (isolate ATCC VR-2332) in North America and experimental reproduction of the disease in gnotobiotic pigs. J Vet Diagn Investig Off Publ Am Assoc Vet Lab Diagn Inc 1992; 4:117–26.
4. Rahe MC, Murtaugh MP. Mechanisms of adaptive immunity to porcine reproductive and respiratory syndrome virus. Viruses 2017; 9: 148. doi: 10.3390/v9060148
5. Chaudhari J, Vu HLX. Porcine reproductive and respiratory syndrome virus reverse genetics and the major applications. Viruses 2020; 12: 1245.
6. Allende R, Lewis TL, Lu Z, et al. North American and European porcine reproductive and respiratory syndrome viruses differ in non-structural protein coding regions. J Gen Virol 1999; 80 :307–15.
7. Zimmerman JJ, Dee SA, Holtkamp DJ, et al. Porcine reproductive and respiratory syndrome viruses (porcine arteriviruses). In: Zimmerman JJ, eds. Diseases of swine. 11th ed. St. Luis, 2019: 685–708. doi: 10.1002/9781119350927.ch41
8. Kuhn JH, Lauck M, Bailey AL, et al. Reorganization and expansion of the nidoviral family Arteriviridae. Arch Virol 2016; 161: 755–68.
9. Brar MS, Shi M, Murtaugh MP, Leung FC-C. Evolutionary diversification of type 2 porcine reproductive and respiratory syndrome virus. J Gen Virol 2015; 96:1570–80.
10. Li Y, Fang L, Zhou Y, Tao R, Wang D, Xiao S. Porcine reproductive and respiratory syndrome virus infection induces both eIF2α phosphorylation-dependent and -independent host translation shutoff. J Virol 2018; 92: e0060–18. doi: 10.1128/jvi.00600-18.
11. Dokland T. The structural biology of PRRSV. Virus Res 2010; 154: 86–97.
12. Snijder EJ, Kikkert M, Fang Y. Arterivirus molecular biology and pathogenesis. J Gen Virol 2013; 94: 2141–63.
13. Li P, Shen Y, Wang T, et al. Epidemiological survey of PRRS and genetic variation analysis of the ORF5 gene in Shandong Province, 2020–2021. Front Vet Sci 2022; 9: 987667. doi: 10.3389/fvets.2022.987667
14. Nelsen CJ, Murtaugh MP, Faaberg KS. Porcine reproductive and respiratory syndrome virus comparison: divergent evolution on two continents. J Virol 1999; 73: 270–80.
15. Wang Q, Peng J, Sun Y, et al. Unique epitopes recognized by monoclonal antibodies against HP-PRRSV: deep understanding of antigenic structure and virus-antibody interaction. PLoS One 2014; 9:e111633. doi: 10.1371/journal.pone.0111633
16. Han G, Xu H, Wang K, He F. Emergence of Two different recombinant PRRSV strains with low neutralizing antibody susceptibility in China. Sci Rep 2019; 9: 2490. doi: 10.1073/pnas.1211145109
17. Fang Y, Treffers EE, Li Y, et al. Efficient −2 frameshifting by mammalian ribosomes to synthesize an additional arterivirus protein. Proc Natl Acad Sci 2012; 109: E2920–8.
18. Orosco FL. Current progress in diagnostics, therapeutics, and vaccines for African swine fever virus. Vet Integr Sci 2023; 21: 751–81. doi:10.12982/VIS.2023.054
19. Evans AB, Loyd H, Dunkelberger JR, et al. Antigenic and biological characterization of ORF2–6 variants at early times following PRRSV nfection. Viruses 2017; 9: 113. doi: 10.3390/v9050113
20. Chen N, Li S, Tian Y, et al. Chimeric HP-PRRSV2 containing an ORF2-6 consensus sequence induces antibodies with broadly neutralizing activity and confers cross protection against virulent NADC30-like isolate. Vet Res 2021; 52: 74. doi: 10.1186/s13567-021-00944-8
21. Han J, Zhou L, Ge X, Guo X, Yang H. Pathogenesis and control of the Chinese highly pathogenic porcine reproductive and respiratory syndrome virus. Vet Microbiol 2017; 209: 30–47. doi: 10.1016/j.vetmic.2017.02.020
22. Zhou L, Yang H. Porcine reproductive and respiratory syndrome in China. Virus Res 2010; 154: 31–7. doi: 10.1016/j.virusres.2010.07.016.
23. Hermann JR, Muñoz-Zanzi CA, Roof MB, Burkhart K, Zimmerman JJ. Probability of porcine reproductive and respiratory syndrome (PRRS) virus infection as a function of exposure route and dose. Vet Microbiol 2005; 110: 7–16. doi: 10.1016/j.vetmic.2005.06.012
24. Christopher-Hennings J, Nelson EA, Nelson JK, et al. Detection of porcine reproductive and respiratory syndrome virus in boar semen by PCR. J Clin Microbiol 1995; 33: 1730–4. doi: 10.1128/jcm.33.7.1730-1734.1995
25. Duan X, Nauwynck HJ, Pensaert MB. Virus quantification and identification of cellular targets in the lungs and lymphoid tissues of pigs at different time intervals after inoculation with porcine reproductive and respiratory syndrome virus (PRRSV). Vet Microbiol 1997; 56: 9–19. doi: 10.1016/S0378-1135(96)01347-8
26. Bierk MD, Dee SA, Rossow KD, Otake S, Collins JE, Molitor TW. Transmission of porcine reproductive and respiratory syndrome virus from persistently infected sows to contact controls. Can J Vet Res 2001; 65: 261–6.
27. Benfield DA, Nelson E, Collins JE, et al. Characterization of swine infertility and respiratory syndrome (SIRS) virus (isolate ATCC VR-2332). J Vet Diagn Invest 1992; 4: 127–33.
28. Bloemraad M, de Kluijver EP, Petersen A, Burkhardt GE, Wensvoort G. Porcine reproductive and respiratory syndrome: temperature and pH stability of Lelystad virus and its survival in tissue specimens from viraemic pigs. Vet Microbiol 1994; 42: 361–71.
29. Orosco F. Advancing the frontiers: revolutionary control and prevention paradigms against Nipah virus. Open Vet J 2023; 13: 1056–70. doi: 10.5455/OVJ.2023.v13.i9.1
30. Dee S, Otake S, Deen J. An evaluation of ultraviolet light (UV254) as a means to inactivate porcine reproductive and respiratory syndrome virus on common farm surfaces and materials. Vet Microbiol 2011; 150: 96–9. doi: 10.1016/j.vetmic.2011.01.014
31. Rossow KD, Collins JE, Goyal SM, Nelson EA, Christopher-Hennings J, Benfield DA. Pathogenesis of porcine reproductive and respiratory syndrome virus infection in gnotobiotic pigs. Vet Pathol 1995; 32: 361–73.
32. Díaz I, Gimeno M, Darwich L, et al. Characterization of homologous and heterologous adaptive immune responses in porcine reproductive and respiratory syndrome virus infection. Vet Res 2012; 43: 30. doi:10.1186/1297-9716-43-30

33. Wills RW, Doster AR, Galeota JA, Sur J-H, Osorio FA. Duration of infection and proportion of pigs persistently infected with porcine reproductive and respiratory syndrome virus. J Clin Microbiol 2003; 41: 58–62.

34. Karniychuk UU, Saha D, Vanhee M, et al. Impact of a novel inactivated PRRS virus vaccine on virus replication and virus-induced pathology in fetal implantation sites and fetuses upon challenge. Theriogenology 2012; 78: 1527–37. doi: 10.1016/j.theriogenology.2012.06.015

35. Lamontagne L, Pagé C, Larochelle R, Magar R. Porcine reproductive and respiratory syndrome virus persistence in blood, spleen, lymph nodes, and tonsils of experimentally infected pigs depends on the level of CD8high T cells. Viral Immunol 2003; 16: 395–406. doi: 10.1089/088282403322396181

36. Halbur PG, Paul PS, Frey ML, et al. Comparison of the antigen distribution of two US porcine reproductive and respiratory syndrome virus isolates with that of the Lelystad virus. Vet Pathol 1996; 33: 159–70.

37. Beyer J, Fichtner D, Schirrmeier H, Polster U, Weiland E, Wege H. Porcine reproductive and respiratory syndrome virus (PRRSV): kinetics of infection in lymphatic organs and lung. J Vet Med B 2000; 47: 9–25. doi: 10.1046/j.1439-0450.2000.00305.x

38. Pileri E, Mateu E. Review on the transmission porcine reproductive and respiratory syndrome virus between pigs and farms and impact on vaccination. Vet Res 2016; 47: 108. doi: 10.1186/s13567-016-0391-4

39. Albina E, Madec F, Cariolet R, Torrison J. Immune response and persistence of the porcine reproductive and respiratory syndrome virus in infected pigs and farm units. Vet Rec 1994; 134: 567–73.

40. Rossow KD, Bautista EM, Goyal SM, et al. Experimental porcine reproductive and respiratory syndrome virus infection in one-, four-, and 10-week-old pigs. J Vet Diagn Invest 1994; 6: 3–12.

41. Christopher-Hennings J, Nelson EA, Hines RJ, et al. Persistence of porcine reproductive and respiratory syndrome virus in serum and semen of adult boars. J Vet Diagn Invest 1995; 7: 456–64.

42. Kang I, Ha Y, Kim D, et al. Localization of porcine reproductive and respiratory syndrome virus in mammary glands of experimentally infected sows. Res Vet Sci 2010; 88: 304–6.

43. Cho JG, Dee SA, Deen J, et al. The impact of animal age, bacterial coinfection, and isolate pathogenicity on the shedding of Porcine reproductive and respiratory syndrome virus in aerosols from experimentally infected pigs. Can J Vet Res 2006; 70: 297–301.

44. Tang G-Y, Meng X, Gan R-Y, et al. Health functions and related molecular mechanisms of tea components: an update review. Int J Mol Sci 2019; 20 :6196. doi: 10.3390/ijms20246196

45. Khan N, Mukhtar H. Tea polyphenols in promotion of human health. Nutrients 2019; 11: 39. doi: 10.3390/nu11010039

46. Saeed M, Naveed M, Arif M, et al. Green tea (Camellia sinensis) and l-theanine: medicinal values and beneficial applications in humans-A comprehensive review. Biomed Pharmacother 2017; 95: 1260–75. doi: 10.1016/j.biopha.2017.09.024

47. Majidinia M, Bishayee A, Yousefi B. Polyphenols: major regulators of key components of DNA damage response in cancer. DNA Repair (Amst) 2019; 82: 102679. doi: 10.1016/j.dnarep.2019.102679

48. Ge M, Xiao Y, Chen H, Luo F, Du G, Zeng F. Multiple antiviral approaches of (-)-epigallocatechin-3-gallate (EGCG) against porcine reproductive and respiratory syndrome virus infection *in vitro*. Antiviral Res 2018; 158: 52–62. doi: 10.1016/j.antiviral.2018.07.012

49. Wang X, Dong W, Zhang X, et al. Antiviral mechanism of tea polyphenols against porcine reproductive and respiratory syndrome virus. Pathogens 2021; 10: 202. doi: 10.3390/pathogens10020202

50. Sun N, Wang Z-W, Wu C-H, et al. Antiviral activity and underlying molecular mechanisms of Matrine against porcine reproductive and respiratory syndrome virus *in vitro*. Res Vet Sci 2014; 96: 323–7. doi: 10.1016/j.rvsc.2013.12.009

51. Sun N, Sun P, Lv H, et al. Matrine displayed antiviral activity in porcine alveolar macrophages co-infected by porcine reproductive and respiratory syndrome virus and porcine circovirus type 2. Sci Rep 2016; 6: 24401. doi: 10.1038/srep24401

52. Sun P, Sun N, Yin W, et al. Matrine inhibits IL-1β secretion in primary porcine alveolar macrophages through the MyD88/NF-κB pathway and NLRP3 inflammasome. Vet Res 2019; 50: 53. doi: 10.1186/s13567-019-0671-x

53. Zhao H, Guo X, Bi Y, Zhu Y, Feng W. PKCδ is required for porcine reproductive and respiratory syndrome virus replication. Virology 2014; 468–470: 96–103. doi: 10.1016/j.virol.2014.07.040

54. Lama Z, Gaudin Y, Blondel D, Lagaudrière-Gesbert C. Kinase inhibitors tyrphostin 9 and rottlerin block early steps of rabies virus cycle. Antiviral Res 2019; 168: 51–60. doi: 10.1016/j.antiviral.2019.04.014

55. Kang Y-L, Oh C, Ahn S-H, et al. Inhibition of endocytosis of porcine reproductive and respiratory syndrome virus by rottlerin and its potential prophylactic administration in piglets. Antiviral Res 2021; 195: 105191. doi: 10.1016/j.antiviral.2021.105191

56. Singh N, Sharma B. Toxicological effects of berberine and sanguinarine. Front Mol Biosci 2018; 5: 21. doi: 10.3389/fmolb.2018.00021

57. Guo W, Lu X, Liu B, Yan H, Feng J. Anti-TMV activity and mode of action of three alkaloids isolated from Chelidonium majus. Pest Manag Sci 2021; 77: 510–7. doi: 10.1002/ps.6049

58. Jena AB, Kanungo N, Chainy GBN, Devaraji V, Das SK, Dandapat J. A computational insight on the Inhibitory Potential of 8-Hydroxydihydrosanguinarine (8-HDS), a pyridone containing analog of sanguinarine, against SARS CoV2. Chem Biodivers 2022; 19: e202200266. doi: 10.1002/cbdv.202200266

59. Ke Q, Duan K, Cheng Y, Xu S, Xiao S, Fang L. Sanguinarine exhibits antiviral activity against porcine reproductive and respiratory syndrome virus via multisite inhibition mechanisms. Viruses 2023; 15: 688. doi: 10.3390/v15030688

60. Xie Y, Ye Y-P, Sun H-X, Li D. Contribution of the glycidic moieties to the haemolytic and adjuvant activity of platycodigenin-type saponins from the root of Platycodon grandiflorum. Vaccine 2008; 26: 3452–60.

61. Xie Y, Sun H-X, Li D. Platycodin D is a potent adjuvant of specific cellular and humoral immune responses against recombinant hepatitis B antigen. Vaccine 2009; 27: 757–64.

62. Khan M, Maryam A, Zhang H, Mehmood T, Ma T. Killing cancer with platycodin D through multiple mechanisms. J Cell Mol Med 2016; 20: 389–402.

63. Fu Y, Xin Z, Liu B, et al. Platycodin D inhibits inflammatory response in LPS-stimulated primary rat microglia cells through activating LXRα-ABCA1 signaling pathway. Front Immunol 2017; 8: 1929. doi: 10.3389/fimmu.2017.01929

64. Kim T-W, Lim J-H, Song I-B, et al. Hepatoprotective and anti-hepatitis C viral activity of Platycodon grandiflorum extract on carbon tetrachloride-induced acute hepatic injury in mice. J Nutr Sci Vitaminol (Tokyo) 2012; 58: 187–94. doi: 10.3177/jnsv.58.187

65. Zhang M, Du T, Long F, et al. Platycodin D suppresses type 2 porcine reproductive and respiratory syndrome virus in primary and established cell lines. Viruses 2018; 10: 657. doi: 10.3390/v10110657

66. Nagappan A, Kim J-H, Jung DY, Jung MH. Cryptotanshinone from the Salvia miltiorrhiza Bunge Attenuates Ethanol-Induced Liver Injury by Activation of AMPK/SIRT1 and Nrf2 Signaling Pathways. Int J Mol Sci 2020; 21:265.

67. Naziri M, Ghafari A, Mehrabi H, et al. A mini-review of the anticancer properties of Cryptotanshinone: a quinoid diterpene extracted from the root of Salvia miotiorrhiza bunge. Front Drug Discov 2022; 2: 815017. doi: 10.3389/fddsv.2022.815017

68. Huang C, Zhu J, Wang L, et al. Cryptotanshinone protects porcine alveolar macrophages from infection with porcine reproductive and respiratory syndrome virus. Antiviral Res 2020; 183: 104937. doi: 10.1016/j.antiviral.2020.104937

69. Catanzaro E, Canistro D, Pellicioni V, Vivarelli F, Fimognari C. Anticancer potential of allicin: a review. Pharmacol Res 2022; 177: 106118. doi: 10.1016/j.phrs.2022.106118

70. Weber ND, Andersen DO, North JA, Murray BK, Lawson LD, Hughes BG. *In vitro* virucidal effects of Allium sativum (Garlic) extract and compounds. Planta Med 1992; 58 : 417–23.

71. Rouf R, Uddin SJ, Sarker DK, et al. Antiviral potential of garlic (Allium sativum) and its organosulfur compounds: a systematic update of pre-clinical and clinical data. Trends Food Sci Technol 2020; 104: 219–34. doi: 10.1016/j.tifs.2020.08.006

72. Mösbauer K, Fritsch VN, Adrian L, et al. The effect of allicin on the proteome of SARS-CoV-2 infected calu-3 cells. Front Microbiol 2021; 12: 746795. doi: 10.3389/fmicb.2021.746795

73. Wang L, Jiao H, Zhao J, Wang X, Sun S, Lin H. Allicin alleviates reticuloendotheliosis virus-induced immunosuppression via ERK/mitogen-activated protein kinase pathway in specific pathogen-free chickens. Front Immunol 2017; 8: 1856. doi: 10.3389/fimmu.2017.01856

74. Che H-Y, Zhou C-H, Lyu C-C, et al. Allicin alleviated LPS-induced mastitis via the TLR4/NF-κB signaling pathway in bovine mammary epithelial cells. Int J Mol Sci 2023; 24: 3805. doi: 10.3390/ijms24043805

75. Liu Y, Che TM, Song M, et al. Dietary plant extracts improve immune responses and growth efficiency of pigs experimentally infected with porcine reproductive and respiratory syndrome virus. J Anim Sci 2013; 91: 5668–79.

76. Hu J, Li C, Zhou Y, Ding J, Li X, Li Y. Allicin inhibits porcine reproductive and respiratory syndrome virus infection *in vitro* and alleviates inflammatory responses. Viruses 2023; 15: 1050. doi: 10.3390/v15051050.

77. Pulido-Moran M, Moreno-Fernandez J, Ramirez-Tortosa C, Ramirez-Tortosa M. Curcumin and health. Molecules 2016; 21: 264. doi: 10.3390/molecules21030264

78. von Rhein C, Weidner T, Henß L, et al. Curcumin and Boswellia serrata gum resin extract inhibit chikungunya and vesicular stomatitis virus infections *in vitro.* Antiviral Res 2016; 125: 51–7. doi: 10.1016/j.antiviral.2015.11.007

79. Du T, Shi Y, Xiao S, et al. Curcumin is a promising inhibitor of genotype 2 porcine reproductive and respiratory syndrome virus infection. BMC Vet Res 2017; 13: 298. doi: 10.1186/s12917-017-1218-x

80. Gansukh E, Gopal J, Paul D, et al. Ultrasound mediated accelerated Anti-influenza activity of Aloe vera. Sci Rep 2018; 8: 17782. doi: 10.1038/s41598-018-35935-x

81. Cui Y, Chen L-J, Huang T, Ying J-Q, Li J. The pharmacology, toxicology and therapeutic potential of anthraquinone derivative emodin. Chin J Nat Med 2020; 18: 425–35.

82. Wang Z, Zheng N, Liang J, et al. Emodin resists to cyprinid herpesvirus 3 replication via the pathways of Nrf2/Keap1-ARE and NF-κB in the ornamental koi carp (Cyprinus carpio haematopterus). Comp Biochem Physiol Part C Toxicol Pharmacol 2021; 246: 109023. doi: 10.1016/j.cbpc.2021.109023

83. Ding Y, Xu J, Cheng L, et al. Effect of emodin on coxsackievirus B3m-mediated encephalitis in hand, foot, and mouth disease by inhibiting toll-like receptor 3 pathway *in vitro* and *in vivo.* J Infect Dis 2020; 222: 443–55.

84. Batista MN, Braga ACS, Campos GRF, et al. Natural products isolated from oriental medicinal herbs inactivate Zika virus. Viruses 2019; 11: 49. doi: 10.3390/v11010049

85. Zhong T, Zhang L-Y, Wang Z-Y, et al. Rheum emodin inhibits enterovirus 71 viral replication and affects the host cell cycle environment. Acta Pharmacol Sin 2017; 38: 392–401.

86. Yiu C-Y, Chen S-Y, Yang T-H, et al. Inhibition of Epstein-Barr virus lytic cycle by an ethyl acetate subfraction separated from Polygonum cuspidatum root and its major component, emodin. Molecules 2014; 19: 1258–72. doi: 10.3390/molecules19011258

87. Schwarz S, Wang K, Yu W, Sun B, Schwarz W. Emodin inhibits current through SARS-associated coronavirus 3a protein. Antiviral Res 2011; 90: 64–9.

88. Xiong H-R, Luo J, Hou W, Xiao H, Yang Z-Q. The effect of emodin, an anthraquinone derivative extracted from the roots of Rheum tanguticum, against herpes simplex virus *in vitro* and *in vivo.* J Ethnopharmacol 2011; 133: 718–23.

89. Shuangsuo D, Zhengguo Z, Yunru C, et al. Inhibition of the replication of hepatitis B virus *in vitro* by emodin. Med Sci Monit 2006; 12: BR302-6.

90. Ho T-Y, Wu S-L, Chen J-C, Li C-C, Hsiang C-Y. Emodin blocks the SARS coronavirus spike protein and angiotensin-converting enzyme 2 interaction. Antiviral Res 2007; 74: 92–101.

91. Xu Z, Huang M, Xia Y, et al. Emodin from aloe nhibits porcine reproductive and respiratory syndrome virus via toll-like receptor 3 activation. Viruses 2021; 13: 1243. doi: 10.3390/v13071243

92. Rogosnitzky M, Danks R. Therapeutic potential of the biscoclaurine alkaloid, cepharanthine, for a range of clinical conditions. Pharmacol Rep PR 2011; 63:337–47.

93. Bailly C. Cepharanthine: an update of its mode of action, pharmacological properties and medical applications. Phytomedicine 2019; 62: 152956. doi: 10.1016/j.phymed.2019.152956

94. Kim DE, Min JS, Jang MS, et al. Natural bis-benzylisoquinoline alkaloids-tetrandrine, fangchinoline, and cepharanthine, inhibit human Coronavirus OC43 infection of MRC-5 human lung cells. Biomolecules 2019; 9: 696. doi: 10.3390/biom9110696

95. Zhang C, Wang Y, Liu X, et al. Antiviral activity of cepharanthine against severe acute respiratory syndrome coronavirus *in vitro.* Chin Med J (Engl) 2005; 118:493–6.

96. Fan H-H, Wang L-Q, Liu W-L, et al. Repurposing of clinically approved drugs for treatment of coronavirus disease 2019 in a 2019-novel coronavirus-related coronavirus model. Chin Med J (Engl) 2020; 133: 1051–6.

97. Zhou P, Yang X-L, Wang X-G, et al. A pneumonia outbreak associated with a new coronavirus of probable bat origin. Nature 2020; 579: 270–3.

98. Yang C, Zuo Q, Liu X, et al. Small molecule screening identified cepharanthine as an inhibitor of porcine reproductive and respiratory syndrome virus infection *in vitro* by suppressing integrins/ILK/RACK1/PKCα/NF-κB signalling axis. Vet Microbiol 2021; 255: 109016. doi: 10.1016/j.vetmic.2021.109016

99. Petramfar P, Hajari F, Yousefi G, Azadi S, Hamedi A. Efficacy of oral administration of licorice as an adjunct therapy on improving the symptoms of patients with Parkinson's disease, a randomized double blinded clinical trial. J Ethnopharmacol 2020; 247: 112226. doi: 10.1016/j.jep.2019.112226

100. Zhang Z, Yang L, Hou J, Tian S, Liu Y. Molecular mechanisms underlying the anticancer activities of licorice flavonoids. J Ethnopharmacol 2021; 267: 113635. doi: 10.1016/j.jep.2020.113635

101. Sato H, Goto W, Yamamura J, et al. Therapeutic basis of glycyrrhizin on chronic hepatitis B. Antiviral Res 1996; 30: 171–7.

102. Matsumoto Y, Matsuura T, Aoyagi H, et al. Antiviral activity of glycyrrhizin against Hepatitis C virus *In vitro*. PLoS One 2013; 8: e68992. doi: 10.1371/journal.pone.0068992

103. Huang W, Chen X, Li Q, et al. Inhibition ofIntercellular adhesion in Herpex simplex virus infection by glycyrrhizin. Cell Biochem Biophys 2012; 62: 137–40.

104. Cinatl J, Morgenstern B, Bauer G, Chandra P, Rabenau H, Doerr H. Glycyrrhizin, an active component of liquorice roots, and replication of SARS-associated coronavirus. Lancet 2003; 361: 2045–6. doi: 10.1016/s0140-6736(03)13615-x

105. Wolkerstorfer A, Kurz H, Bachhofner N, Szolar OHJ. Glycyrrhizin inhibits influenza A virus uptake into the cell. Antiviral Res 2009; 83: 171–8.

106. Lee HB, Kim JC, Lee SM. Antibacterial activity of two phloroglucinols, flavaspidic acids AB and PB, from Dryopteris crassirhizoma. Arch Pharm Res 2009; 32: 655–9.

107. Lee S-M, Na M-K, An R-B, Min B-S, Lee H-K. Antioxidant activity of two phloroglucinol derivatives from Dryopteris crassirhizoma. Biol Pharm Bull 2003; 26: 1354–6.

108. Gupta P, Kumar R, Garg P, Singh IP. Active site binding modes of dimeric phloroglucinols for HIV-1 reverse transcriptase, protease and integrase. Bioorg Med Chem Lett 2010; 20: 4427–31.

109. Yang Q, Gao L, Si J, et al. Inhibition of porcine reproductive and respiratory syndrome virus replication by flavaspidic acid AB. Antiviral Res 2013; 97: 66–73.

110. Syamsunarno MRA, Safitri R, Kamisah Y. Protective effects of Caesalpinia sappan Linn. and its bioactive compounds on cardiovascular organs. Front Pharmacol 2021; 12: 725745. doi: 10.3389/fphar.2021.725745

111. Liang C-H, Chan L-P, Chou T-H, et al. Brazilein from Caesalpinia sappan L. Antioxidant Inhibits Adipocyte Differentiation and Induces Apoptosis through Caspase-3 Activity and Anthelmintic Activities against Hymenolepis nana and Anisakis simplex. Evid Based Complement Alternat Med 2013; 2013: 864892. doi: 10.1155/2013/864892

112. Arjin C, Pringproa K, Hongsibsong S, et al. *In vitro* screening antiviral activity of Thai medicinal plants against porcine reproductive and respiratory syndrome virus. BMC Vet Res 2020; 16: 102. doi: 10.1186/s12917-020-02320-8

113. Settharaksa S, Monton C, Charoenchai L. Optimization of Caesalpinia sappan L. heartwood extraction procedure to obtain the highest content of brazilin and greatest antibacterial activity. J Integr Med 2019; 17: 351–8.

114. Hu C-M, Liu Y-H, Cheah K-P, et al. Heme oxygenase-1 mediates the inhibitory actions of brazilin in RAW264.7 macrophages stimulated with lipopolysaccharide. J Ethnopharmacol 2009; 121: 79–85.

115. Ferrari F, Moretti A, Villa RF. Incretin-based drugs as potential therapy for neurodegenerative diseases: current status and perspectives. Pharmacol Ther 2022; 239: 108277. doi: 10.1016/j.pharmthera.2022.108277

116. Moon CK, Park KS, Kim SG, Won HS, Chung JH. Brazilin protects cultured rat hepatocytes from BrCCl3-induced toxicity. Drug Chem Toxicol 1992; 15: 81–91.

117. Liu A-L, Shu S-H, Qin H-L, Lee SMY, Wang Y-T, Du G-H. *In vitro* anti-influenza viral activities of constituents from Caesalpinia sappan. Planta Med 2009; 75: 337–9.

118. Arjin C, Hongsibsong S, Pringproa K, et al. Effect of ethanolic Caesalpinia sappan fraction on *in vitro* antiviral activity against porcine reproductive and respiratory syndrome virus. Vet Sci 2021; 8: 106. doi: 10.3390/vetsci8060106

119. Na-Bangchang K, Karbwang J. Traditional herbal medicine for the control of tropical diseases. Trop Med Health 2014; 42: 3–13.

120. Hu Y, Zhang B, Wang W, Zhou J, Li B, He K. Therapeutic effects of saponin components on porcine reproductive and respiratory syndrome virus-infected piglets. J Anim Physiol Anim Nutr 2020; 104: 637–44.

121. Kuete V, Sandjo LP. Isobavachalcone: an overview. Chin J Integr Med 2012; 18: 543–7.

122. Wang H-M, Liu T-X, Wang T-Y, et al. Isobavachalcone inhibits post-entry stages of the porcine reproductive and respiratory syndrome virus life cycle. Arch Virol 2018; 163: 1263–70. doi: 10.1007/s00705-018-3755

123. Quéré L, Wenger T, Schramm HJ. Triterpenes as potential dimerization inhibitors of HIV-1 protease. Biochem Biophys Res Commun 1996; 227: 484–8.

124. Kong L, Li S, Liao Q, et al. Oleanolic acid and ursolic acid: novel hepatitis C virus antivirals that inhibit NS5B activity. Antiviral Res 2013; 98: 44–53.

125. Chen Y, Li H, Wu L, et al. Ursolic acid derivatives are potent inhibitors against porcine reproductive and respiratory syndrome virus. RSC Adv 2020; 10: 22783–96. doi: 10.1039/d0ra04070c

126. Pinto C, Duque AL, Rodríguez-Galdón B, Cestero JJ, Macías P. Xanthohumol prevents carbon tetrachloride-induced acute liver injury in rats. Food Chem Toxicol 2012; 50: 3405–12. doi: 10.1016/j.fct.2012.07.035.

127. Ge M, Yao W, Yuan D, et al. Brg1-mediated Nrf2/HO-1 pathway activation alleviates hepatic ischemia–reperfusion injury. Cell Death Dis 2017; 8:e2841. doi: 10.1038/cddis.2017.236

128. Miranda CL, Stevens JF, Helmrich A, et al. Antiproliferative and cytotoxic effects of prenylated flavonoids from hops (Humulus lupulus) in human cancer cell lines. Food Chem Toxicol 1999; 37: 271–85.

129. Cos P, Maes L, Vlietinck A, Pieters L. Plant-derived leading compounds for chemotherapy of human immunodefiency virus (HIV) infection – an update (1998 – 2007). Planta Med 2008: 1323–37.

130. Liu X, Bai J, Jiang C, et al. Therapeutic effect of Xanthohumol against highly pathogenic porcine reproductive and respiratory syndrome viruses. Vet Microbiol 2019; 238: 108431. doi: 10.1016/j.vetmic.2019.108431

131. Ma Z, Gulia-Nuss M, Zhang X, Brown MR. Effects of the botanical insecticide, toosendanin, on blood digestion and egg production by female Aedes aegypti (Diptera: Culicidae): topical application and ingestion. J Med Entomol 2013; 50: 112–21.

132. Shi Y-L, Li M-F. Biological effects of toosendanin, a triterpenoid extracted from Chinese traditional medicine. Prog Neurobiol 2007; 82: 1–10. doi: 10.1016/j.pneurobio.2007.02.002

133. Wang Q, Wang Z, Hou G, Huang P. Toosendanin suppresses glioma progression property and induces apoptosis by regulating miR-608/Notch Axis. Cancer Manag Res 2020; 12: 3419–31. doi: 10.2147/CMAR.S240268

134. Jin Y-H, Kwon S, Choi J-G, Cho W-K, Lee B, Ma JY. Toosendanin from melia fructus suppresses Influenza A virus infection by altering nuclear localization of viral polymerase PA Protein. Front Pharmacol 2019; 10: 1025. doi: 10.3389/fphar.2019.01025

135. Watanabe T, Sakamoto N, Nakagawa M, et al. Inhibitory effect of a triterpenoid compound, with or without alpha interferon, on hepatitis C virus infection. Antimicrob Agents Chemother 2011; 55: 2537–45.

136. Li S, Ye M, Chen Y, et al. Screening of a small molecule compound library identifies toosendanin as an inhibitor against bunyavirus and SARS-CoV-2. Front Pharmacol 2021; 12: 735223. doi: 10.3389/fphar.2021.735223

137. Zhang M, Lu C, Su L, et al. Toosendanin activates caspase-1 and induces maturation of IL-1β to inhibit type 2 porcine reproductive and respiratory syndrome virus replication via an IFI16-dependent pathway. Vet Res 2022; 53: 61. doi: 10.1186/s13567-022-01077-2

138. Chiu Y-H, Chan Y-L, Tsai L-W, Li T-L, Wu C-J. Prevention of human enterovirus 71 infection by kappa carrageenan. Antiviral Res 2012; 95: 128–34.

139. Leibbrandt A, Meier C, König-Schuster M, et al. Iota-carrageenan is a potent inhibitor of influenza A virus infection. PLoS One 2010; 5: e14320. doi: 10.1371/journal.pone.0014320

140. Rodríguez A, Kleinbeck K, Mizenina O, et al. *In vitro* and *in vivo* evaluation of two carrageenan-based formulations to prevent HPV acquisition. Antiviral Res 2014; 108: 88–93.

141. Shao Q, Guo Q, Xu W ping, Li Z, Zhao TT. Specific inhibitory effect of κ-Carrageenan Polysaccharide on Swine Pandemic 2009 H1N1 Influenza Virus. PloS One 2015; 10:e0126577.

142. Guo C, Zhu Z, Yu P, et al. Inhibitory effect of iota-carrageenan on porcine reproductive and respiratory syndrome virus *in vitro*. Antivir Ther 2019; 24: 261–70.

143. Mori T, O'Keefe BR, Sowder RC, et al. Isolation and Characterization of griffithsin, a novel HIV-inactivating protein, from the red Alga Griffithsia sp. *. J Biol Chem 2005; 280: 9345–53.

144. Lusvarghi S, Bewley CA. Griffithsin: an antiviral lectin with outstanding therapeutic potential. Viruses 2016; 8: 296. doi: 10.3390/v8100296

145. Millet JK, Séron K, Labitt RN, et al. Middle East respiratory syndrome coronavirus infection is inhibited by griffithsin. Antiviral Res 2016; 133:1–8.

146. O'Keefe BR, Giomarelli B, Barnard DL, et al. Broad-spectrum *in vitro* activity and *in vivo* efficacy of the antiviral protein griffithsin against emerging viruses of the family Coronaviridae. J Virol 2010; 84: 2511–21.

147. Takebe Y, Saucedo CJ, Lund G, et al. Antiviral lectins from red and blue-green algae show potent *In vitro* and *In vivo* activity against Hepatitis C virus. PLoS One 2013; 8: e64449. doi: 10.1371/journal.pone.0064449

148. Levendosky K, Mizenina O, Martinelli E, et al. Griffithsin and Carrageenan Combination To Target Herpes Simplex Virus 2 and Human Papillomavirus. Antimicrob Agents Chemother 2015; 59:7290–8.

149. Ishag HZA, Li C, Wang F, Mao X. Griffithsin binds to the glycosylated proteins (E and prM) of Japanese encephalitis virus and inhibit its infection. Virus Res 2016; 215: 50–4.

150. Fuqua JL, Wanga V, Palmer KE. Improving the large scale purification of the HIV microbicide, griffithsin. BMC Biotechnol 2015; 15: 12. doi: 10.1186/s12896-015-0120-5

151. Moncla BJ, Pryke K, Rohan LC, Graebing PW. Degradation of naturally occurring and engineered antimicrobial peptides by proteases. Adv Biosci Biotechnol 2011; 2:404–8.

152. Kouokam JC, Lasnik AB, Palmer KE. Studies in a murine model confirm the safety of griffithsin and advocate its further development as a microbicide targeting HIV-1 and other enveloped viruses. Viruses 2016; 8: 311. doi: 10.3390/v8110311

153. Li L, Tian X, Chen J, Li P, Zheng Q, Hou J. Griffithsin inhibits porcine reproductive and respiratory syndrome virus infection *in vitro*. Arch Virol 2018; 163: 3317–25.

154. Bagchi D, Sen CK, Ray SD, et al. Molecular mechanisms of cardioprotection by a novel grape seed proanthocyanidin extract. Mutat Res 2003; 523–524: 87–97.

155. Singh RP, Tyagi AK, Dhanalakshmi S, Agarwal R, Agarwal C. Grape seed extract inhibits advanced human prostate tumor growth and angiogenesis and upregulates insulin-like growth factor binding protein-3. Int J Cancer 2004; 108: 733–40.

156. Fine AM. Oligomeric proanthocyanidin complexes: history, structure, and phytopharmaceutical applications. Altern Med Rev J Clin Ther 2000; 5: 144–51.

157. Gallina L, Dal Pozzo F, Galligioni V, Bombardelli E, Scagliarini A. Inhibition of viral RNA synthesis in canine distemper virus infection by proanthocyanidin A2. Antiviral Res 2011; 92: 447–52.

158. Zhang M, Wu Q, Chen Y, et al. Inhibition of proanthocyanidin A2 on porcine reproductive and respiratory syndrome virus replication *in vitro*. PLoS One 2018; 13: e0193309. doi: 10.1371/journal.pone.0193309

159. Modric S, Webb AI, Derendorf H. Pharmacokinetics and pharmacodynamics of tilmicosin in sheep and cattle. J Vet Pharmacol Ther 1998; 21: 444–52.

160. Molitor T, Bautista E, Shin J, McGruder E, Armbruster G. Tilmicosin affects porcine reproductive and respiratory syndrome virus replication. Minnesota: Digital conservancy, 2001. http://conservancy.umn.edu/handle/11299/160605 (27. 2. 2024)

161. Tang X, Wang C, Sun W, et al. Evaluating anti-viral effect of Tylvalosin tartrate on porcine reproductive and respiratory syndrome virus and analyzing the related gene regulation by transcriptomics. Virol J 2023; 20: 79. doi: 10.1186/s12985-023-02043-w

162. Benfield D, Chase CCL, Moore G, et al.An evaluation of the effects of tilmicosin in feed on nursery pigs inoculated with porcine reproductive and respiratory syndrome virus. https://www.academia.edu/50598418/An_evaluation_of_the_effects_of_tilmicosin_in_feed_on_nursery_pigs_inoculated_with_porcine_reproductive_and_respiratory_syndrome_virus (27. 2. 2024)

163. Preliminary evaluation of clinical effects and cost-effectiveness of in-feed Pulmotil® (tilmicosin) and serum inoculation in an outbreak of PRRS. In: IPVS- Biennial international congress – Copenhagen, 2006. https://www.ivis.org/library/ipvs/ipvs-biennial-international-congress-denmark-2006/preliminary-evaluation-of-clinical (27. 2. 2024)

164. Batista L, Paradis MA, Gagnon C, et al. Evaluation of the effects of tilmicosin (Pulmotil Ac®) administered in the drinking water on nursery pigs inoculated with porcine reproductive and respiratory syndrome virus. In: IPVS – Bienal International congress – Durban, 2008. https://www.ivis.org/library/ipvs/ipvs-biennial-international-congress-south-africa-2008/evaluation-of-effects-of (27. 2. 2024)

165. Blais J, Chamberland S. Intracellular accumulation of tilmicosin in primary swine alveolar macrophages. Rome: Food and agriculture organization, 2024. https://scholar.google.com/scholar_lookup?title=Intracellular+accumulation+of+tilmicosin+in+primary+swine+alveolar+macrophages&author=Blais%2C+J.&publication_year=1994 (27. 2. 2024)

166. Du Y, Yoo D, Paradis MA, Scherba G. Antiviral activity of tilmicosin for type 1 and type 2 porcine reproductive and respiratory syndrome virus in cultured porcine alveolar macrophages. J Antivir Antiretrovir 2011; 3: 28–33.

167. Scorneaux B, Shryock TR. Intracellular accumulation, subcellular distribution and efflux of tilmicosin in swine phagocytes. J Vet Pharmacol Ther 1998; 21: 257–68.

168. Opriessnig T, Giménez-Lirola LG, Halbur PG. Polymicrobial respiratory disease in pigs. Anim Health Res Rev 2011; 12: 133–48.

169. Duquette SC, Fischer CD, Williams AC, et al. Immunomodulatory effects of tulathromycin on apoptosis, efferocytosis, and proinflammatory leukotriene B4 production in leukocytes from Actinobacillus pleuropneumoniae-or zymosan-challenged pigs. Am J Vet Res 2015; 76: 507–19.

170. Fullerton JN, Gilroy DW. Resolution of inflammation: a new therapeutic frontier. Nat Rev Drug Discov 2016; 15: 551–67.

171. Lamache DD de, Moges R, Siddiq A, et al. Immuno-modulating properties of Tulathromycin in porcine monocyte-derived macrophages infected with porcine reproductive and respiratory syndrome virus. PLoS One 2019; 14 :e0221560. doi: 10.1371/journal.pone.0221560

172. Auger E, Deslandes V, Ramjeet M, et al. Host-Pathogen Interactions of Actinobacillus pleuropneumoniae with Porcine Lung and Tracheal Epithelial Cells. Infect Immun 2009; 77: 1426–41.

173. Lévesque C, Provost C, Labrie J, et al. Actinobacillus pleuropneumoniae possesses an antiviral activity against porcine reproductive and respiratory syndrome virus. PLoS One 2014; 9: e98434. doi: 10.1371/journal.pone.0098434

174. Hernandez Reyes Y, Provost C, Traesel CK, Jacques M, Gagnon CA. Actinobacillus pleuropneumoniae culture supernatant antiviral effect against porcine reproductive and respiratory syndrome virus occurs prior to the viral genome replication and transcription through actin depolymerization. J Med Microbiol 2018; 67: 249–64.

175. Ferreira Barbosa JA, Labrie J, Beaudry F, Gagnon CA, Jacques M. Actinobacillus pleuropneumoniae induces SJPL cell cycle arrest in G2/M-phase and inhibits porcine reproductive and respiratory syndrome virus replication. Virol J 2015; 12: 188. doi: 10.1186/s12985-015-0404-3

176. Wasser SP. Current findings, future trends, and unsolved problems in studies of medicinal mushrooms. Appl Microbiol Biotechnol 2011; 89: 1323–32.

177. Yamamoto KA, Galhardi LCF, Rincão VP, et al. Antiherpetic activity of an Agaricus brasiliensis polysaccharide, its sulfated derivative and fractions. Int J Biol Macromol 2013; 52: 9–13.

178. Gao L, Zhang W, Sun Y, et al. Cryptoporus volvatus Extract inhibits porcine reproductive and respiratory syndrome virus (PRRSV) *in vitro* and *in vivo*. PLoS One 2013; 8: e63767. doi: 10.1371/journal.pone.0063767

179. Ma Z, Zhang W, Wang L, et al. A Novel Compound from the mushroom Cryptoporus volvatus inhibits porcine reproductive and respiratory syndrome virus (PRRSV) *in vitro*. PLoS One 2013; 8: e79333. doi: 10.1371/journal.pone.0079333

180. Binder EM, Tan LM, Chin LJ, Handl J, Richard J. Worldwide occurrence of mycotoxins in commodities, feeds and feed ingredients. Anim Feed Sci Technol 2007; 137: 265–82.

181. D'Mello JPF, Placinta CM, Macdonald AMC. Fusarium mycotoxins: a review of global implications for animal health, welfare and productivity. Anim Feed Sci Technol 1999; 80: 183–205.

182. Savard C, Pinilla V, Provost C, Segura M, Gagnon CA, Chorfi Y. *In vitro* effect of deoxynivalenol (DON) mycotoxin on porcine reproductive and respiratory syndrome virus replication. Food Chem Toxicol 2014; 65: 219–26.

183. Oršolić N. Bee venom in cancer therapy. Cancer Metastasis Rev 2012; 31: 173–94.

184. Nam S, Ko E, Park S-K, et al. Bee venom modulates murine Th1/Th2 lineage development. Int Immunopharmacol 2005; 5: 1406–14.

185. Perrin-Cocon L, Agaugué S, Coutant F, et al. Secretory phospholipase A2 induces dendritic cell maturation. Eur J Immunol 2004; 34: 2293–302.

186. Ramoner R, Putz T, Gander H, et al. Dendritic-cell activation by secretory phospholipase A2. Blood 2005; 105: 3583–7.

187. Lee J-A, Kim Y-M, Hyun P-M, et al. Honeybee (Apis mellifera) venom reinforces viral clearance during the early stage of infection with porcine reproductive and respiratory syndrome virus through the up-regulation of Th1-specific immune responses. Toxins 2015; 7: 1837–53.

188. Jadhav HB, Annapure US. Triglycerides of medium-chain fatty acids: a concise review. J Food Sci Technol 2023; 60: 2143–52.

189. Burdick M, Zhou M, Guan LL, Oba M. Effects of medium-chain fatty acid supplementation on performance and rumen fermentation of lactating Holstein dairy cows. Animal 2022; 16: 100491. doi: 10.1016/j.animal.2022.100491

190. Cochrane RA, Dritz SS, Woodworth JC, et al. Assessing the effects of medium-chain fatty acids and fat sources on PEDV infectivity. Transl Anim Sci 2020; 4: 1051–59. doi: 10.1093/tas/txz179

191. Gebhardt JT, Thomson KA, Woodworth JC, et al. Effect of dietary medium-chain fatty acids on nursery pig growth performance, fecal microbial composition, and mitigation properties against porcine epidemic diarrhea virus following storage. J Anim Sci 2020; 98: skz358. doi: 10.1093/jas/skz358

192. Tran HTT, Truong AD, Ly DV, et al. The potential anti-African swine fever virus effects of medium chain fatty acids on *in vitro* feed model: an evaluation study using epidemic ASFV strain circulating in Vietnam. Open Vet J 2021; 11: 346–55. doi: 10.5455/OVJ.2021.v11.i3.3.

193. Yang L, Wen J, Zhang Y, et al. The antiviral activity of caprylic monoglyceride against porcine reproductive and respiratory syndrome virus *In vitro* and *in vivo*. Molecules 2022; 27: 7263. doi: 10.3390/molecules27217263

194. Ganz T. Defensins: antimicrobial peptides of innate immunity. Nat Rev Immunol 2003; 3: 710–20.

195. Park CH, Valore EV, Waring AJ, Ganz T. Hepcidin, a urinary antimicrobial peptide synthesized in the liver. J Biol Chem 2001; 276: 7806–10.

196. Kokryakov VN, Harwig SS, Panyutich EA, et al. Protegrins: leukocyte antimicrobial peptides that combine features of corticostatic defensins and tachyplesins. FEBS Lett 1993; 327: 231–6.

197. Steinberg DA, Hurst MA, Fujii CA, et al. Protegrin-1: a broad-spectrum, rapidly microbicidal peptide with *in vivo* activity. Antimicrob Agents Chemother 1997; 41: 1738–42.

198. Rothan HA, Abdulrahman AY, Sasikumer PG, Othman S, Rahman NA, Yusof R. Protegrin-1 inhibits dengue NS2B-NS3 serine protease and viral replication in MK2 cells. J Biomed Biotechnol 2012; 2012: 251482. doi: 10.1155/2012/251482

199. Guo C, Cong P, He Z, et al. Inhibitory activity and molecular mechanism of protegrin-1 against porcine reproductive and respiratory syndrome virus *in vitro*. Antivir Ther 2015; 20: 573–82.

200. Frederiksen PD, Thiel S, Larsen CB, Jensenius JC. M-ficolin, an innate immune defence molecule, binds patterns of acetyl groups and activates complement. Scand J Immunol 2005; 62: 462–73.

201. Vigerust DJ, Shepherd VL. Virus glycosylation: role in virulence and immune interactions. Trends Microbiol 2007; 15: 211–8.

202. Balzarini J. Carbohydrate-Binding Agents: A potential future cornerstone for the chemotherapy of enveloped viruses? Antivir Chem Chemother 2007; 18: 1–11. doi: 10.1177/095632020701800101

203. Gadjeva M, Paludan SR, Thiel S, et al. Mannan-binding lectin modulates the response to HSV-2 infection. Clin Exp Immunol 2004; 138: 304–11.

204. Keirstead ND, Lee C, Yoo D, Brooks AS, Hayes MA. Porcine plasma ficolin binds and reduces infectivity of porcine reproductive and respiratory syndrome virus (PRRSV) *in vitro*. Antiviral Res 2008; 77:28–38.

205. Chiou PP, Chen MJ, Lin C-M, et al. Production of homozygous transgenic rainbow trout with enhanced disease resistance. Mar Biotechnol 2014; 16: 299–308.

206. Guo C, Huang Y, Cong P, Liu X, Chen Y, He Z. Cecropin P1 inhibits porcine reproductive and respiratory syndrome virus by blocking attachment. BMC Microbiol 2014; 14: 273. doi: 10.1186/s12866-014-0273-8

207. Zhang X, Guo C. Recent advances in inhibition of porcine reproductive and respiratory syndrome virus through targeting CD163. Front Microbiol 2022; 13: 1006464. doi: 10.3389/fmicb.2022.1006464

208. Liu X, Guo C, Huang Y, Zhang X, Chen Y. Inhibition of porcine reproductive and respiratory syndrome virus by Cecropin D *in vitro*. Infect Genet Evol 2015; 34: 7–16.

Od naravne lekarne do zdravja prašičev: Izkoriščanje naravnih spojin proti okužbi z virusom PRRSV

F. L. Orosco

Izvleček: Virus prašičjega reprodukcijskega in respiratornega sindroma (PRRSV) je pomemben virusni patogen, ki povzroča znatne gospodarske izgube v prašičereji po vsem svetu. Zaradi omejene učinkovitosti obstoječih terapevtskih pristopov in pojavov novih sevov PRRSV so nujno potrebne nove protivirusne strategije. Naravne spojine, pridobljene iz rastlin, živali, bakterij in gliv, so vse bolj poznana kot potencialna protivirusna sredstva. Ta izčrpen pregled se osredotoča na naravne spojine s protivirusnim delovanjem proti PRRSV ter raziskuje mehanizme njihovega delovanja, učinkovitost in morebitno uporabo. Te spojine imajo različne protivirusne mehanizme, kot so zaviranje pritrjevanja in vstopa virusa, zaviranje razmnoževanja in modulacija gostiteljevega imunskega odziva. Pregled izpostavlja tudi izzive in prihodnje usmeritve na tem področju. Raziskovalne vrzeli vključujejo potrebo po nadaljnjem pojasnjevanju natančnih mehanizmov delovanja, celoviti oceni varnostnih profilov in raziskovanju kombiniranih terapij za povečanje učinkovitosti. Potrebne so nadaljnje raziskave in translacijske študije, da bi izkoristili celoten potencial teh naravnih spojin in utrli pot učinkovitemu nadzoru in obvladovanju okužb z virusom PRRSV v prašičereji.

Ključne besede: protivirusna sredstva; naravne spojine; PRRSV; prašičereja

Slovenian Veterinary Research
DOI 10.26873/SVR-1711-2023
UDC 598.252.2:616.345:577:616-092
Pages: 29–35

Original Research Article

Localization of Aquaporin-1 in the Small and Large Intestines of Geese (*Anser anser*)

Key words

geese;
intestine;
aquaporin-1

Ebru Karadag Sari[1], Buket Bakir[2]*, Gizem Fidan Arslan[3], Sevda Elis Yildiz[4]

[1]Department of Histology and Embryology, Faculty of Veterinary Medicine, Kafkas University, 36100 Kars, [2]Department of Histology and Embryology, Faculty Of Veterinary Medicine, Namık Kemal University, 59100 Tekirdağ, [3]Department of Histology and Embryology, Health Science Institute, Kafkas University, 36100 Kars, [4]Department Of Midwifery, Faculty Of Health Sciences, Kafkas University, 36100 Kars, Turkey

***Corresponding author:** buketbakir@nku.edu.tr

Abstract: Aquaporins are selective water channels that serve transportation of water across cell membranes, which play a vital role in all cells. In this study, using the immunohistochemical method, the authors intended to investigate the localization of Aquaporin-1 in the small and large intestines of geese. In this study, small and large intestine tissue samples taken from healthy adult geese (*Anser anser*) (n = 10) were used as materials. After fixation for 24 hours at 10% formaldehyde, the tissue samples were passed through graded series of ethanol and xylol and embedded in paraffin. Mallory's modified triple-staining method was used to examine the general structure of the intestine. The Avidin-Biotin-Peroxidase Complex (ABC) method was applied to determine the immunoreactivity of Aquaporin-1. The apical parts of crypt epithelial cells showed strong Aquaporin-1 immunoreactivity in the duodenum and moderate Aquaporin1 immunoreactivity in the jejunum and ileum. Strong Aquaporin-1 immunoreactivity was determined in vascular endothelial cells in the duodenum, jejunum, and ileum, and weak immunoreactivity was found in smooth muscle cells. However, a weak Aquaporin-1 immunoreactivity was detected only in the smooth muscle cells of the cecum and rectum but not in vascular endothelial cells and crypt epithelial cells. The intestine tissue regulates salt transport and hydrostatic pressure differences, enabling the transportation of water. It was suggested that the duodenum and jejunum sections in particular are permeable to high levels of water for balancing the osmotic pressure of the intestinal content. Consequently, with this study, Aquaporin-1 immunoreactivity was detected in the crypt epithelial cells, smooth muscle cells, and vascular endothelium of the small intestines of geese.

Received: 23 February 2023
Accepted: 6 July 2023

Introduction

Water passes through the plasma membrane by simple diffusion. Channels consisting of specialized membrane proteins are required for the rapid and intense passage of water (1). Aquaporins (AQPs), a family of water channel proteins, are small hydrophobic and integral membrane channel proteins that facilitate the transportation and velocity of water and are responsible for water balance regulation by ensuring continuous and rapid permeability of water with low activation energy throughout the epithelial cells (2, 3). Water molecules that pass through AQP channels move very quickly. In one second, 109 water molecules pass through the AQP channel. The speed of water that transit through the AQP channel is even faster than the catalase enzyme, which is known metabolically as the fastest. This speed is a high speed for metabolic events (4).

Aquaporins have been reported to be hydrophobic proteins with six transmembrane domains whose molecular weight ranges from 28 kDa (unglycosylated form) to 40-50 kDa (glycosylated form), and they are mostly found as a homotetramer (5). Depending on their permeability, AQPs in mammals are divided into three groups 1): Water-selective Aquaporins (AQP0, AQP1, AQP2, AQP4, AQP5, AQP6, and AQP8), 2); Aquaglyceroproteins which mediate the passage

of glycerol, urea, and some neutral molecules besides water (AQP3, AQP7, AQP9, and AQP10), and unorthodox or super-aquaporins (AQP11 and AQP12) (6, 7).

AQP 1, 2, 4, and 5 show the widespread distribution in every tissue and organ where water is crucial (8). At least eleven varieties of Aquaporin are expressed in various tissues in the gastrointestinal tract. AQP1 is expressed in duodenum, ileum, large intestine, liver, pancreas and gallbladder, AQP2 in small intestine, AQP3 in small intestine, colon and liver, AQP4 in duodenum and colon, AQP5 in duodenum and pancreas, AQP7 in small intestine and colon, AQP8 in large intestine, liver, pancreas, and gallbladder, AQP9 in duodenum, ileum and liver, AQP10 in small intestine, AQP11 in small intestine, colon and liver and AQP12 in pancreas (9, 10).

Aquaporin-1 (AQPl) was first discovered by chance during studies of the human red cell Rh protein as a homologous protein to MIP (Major Intrinsic Protein of Bovine lens) and was labelled as CHIP28 (Channel Forming Intrinsic Protein of 28 kDa). After that CHIP was designated Aquaporin-1 (abbreviated AQPl) by the Human Genome Committee (11, 12).

AQP1 was determined to have important roles in physiological processes such as water homeostasis, neuro-homeostasis, digestion, body temperature regulation, and reproduction by contributing to fluid release and fluid absorption in the body (13). It has been suggested that AQP1 may be involved in angiogenesis, wound healing, organ regeneration, and tumor metastasis (14). A positive correlation has been established between endometrial adenocarcinoma progression and AQP1, microvascular density, as well as vascular endothelial growth factor (VEGF) (15).

Chicken ceca and rectum were determined to have AQP4 immunoreactivity (16). Also, jejunum, ileum, and colon have ck-AQP5 mRNA (17), and the lower intestinal tract of a sparrow has AQ1 distribution (18), but no study of AQ1 immunoreactivity in the small and large intestines of geese was encountered in the literature. In this study it was aimed to determine immunolocalization of Aquaporin-1, that is important in terms of physiological and pathological roles it assumes in the small and large intestines of geese which has economic importance.

Material and Methods

Animal Material

Tissue samples were harvested in compliance with an approved Kafkas University Animal Care and Use Committee Protocol (No. 2018/04, dated 26.04.2018 and coded KAÜHADYEK/2018-049) for this study. The small and large intestine tissue samples taken from 10 female geese (*Anser anser*) at the age of 8 months that local breeders slaughtered for consumption purposes were used as materials.

Histological Procedure

The small and large intestinal tissue samples were fixed for 24 hours in a 10% formaldehyde solution. Afterwards, they were dehydrated (ethanol), cleared (xylol), and embedded in paraffin. Paraffin blocks were cut into 5-µm thick sections on a rotary microtome (LIECA) and stained with Mallory's modified triple staining to examine the general structure of the tissues.

Immunohistochemical procedure

The Avidin-Biotin Peroxidase complex (ABC) technique was used to determine the localization of Aquaporin 1 (AQP 1) immunohistochemically in small and large intestine tissues. 4-µm cross-sections were fixed to lamellas covered with chrome alum gelatin and were subjected to deparaffinization and dehydration. They were then incubated for 20 minutes in the solution of hydrogen peroxide in methanol (3%) to prevent endogenous peroxide activity. Then they were kept in the microwave oven at 600 watts for 20 minutes within a sodium citrate buffer (pH 6.0) solution to release antigenic receptors. Sections incubated for 10 minutes with Blocking Solution A (Invitrogen-Histostatin Plus Bulk Kit) were kept at room temperature for 1 hour after dripping the Aquaporin 1 primary antibody [1/500] (abcam: ab9566) without a PBS wash. The sections were then incubated for 30 minutes with the biotinylated secondary antibody and 30 minutes in Streptavidin Peroxidase solution. To demonstrate the antibody reaction, the DAB (3.3 ' -Diaminobenzidine) chromogen solution was added to the cross-sections, and they were examined with a light microscope. The reaction was stopped with PBS by checking the condition of immunoreactivity. Distilled water-washed sections were subjected to Harris hematoxylin stain for reverse staining and were dehydrated and covered with entellan.

The evaluation was made by two independent observers using the semi-quantitative method by taking the degree of staining in the cross-sections as a criterion. Depending on the staining properties, the slides were scored within the range of 0–3 during their evaluation: no immunoreactivity 0(-), weak immunoreactivity 1(+), moderate immunoreactivity 2(++), and strong immunoreactivity 3(+++). To determine whether immunohistochemical staining is specific, the sections were subjected to an immunohistochemical staining procedure without adding a primary antibody (negative control), provided that all processes were identical. The preparations prepared for histological and immunohistochemical examinations were then photographed and assessed under the light microscope (Olympus Bx53 JAPAN).

Statistical analysis

The data were analyzed with the IBM Statistical Package for Social Sciences (SPSS) program. In analysis, minimum-maximum values, mean, and standard deviation were used and median was calculated to evaluate the data.

Table 1: Statistical analysis of Aquaporin-1 immunoreactivity in geese small and large intestine

	Cells	N	Min	Max	Mean±SD	Median
Duodenum	Crypt epithelial cells	8	2	3	2,56±0,42	2,50
	Vascular endothelial cells	8	2	3	2,56±0,42	2,50
	Smooth muscle cells	8	0	2	1,1875±0,65	1
Jejenum	Crypt epithelial cells	8	1	3	2,06±0,62	2
	Vascular endothelial cells	8	2	3	2,625±0,44	2,75
	Smooth muscle cells	8	0	2	1,0625±0,582	1
Ileum	Crypt epithelial cells	8	1	3	1,88±0,69	2
	Vascular endothelial cells	8	2	3	2,63±0,44	2,75
	smooth muscle cells	8	0,5	2	1,0625±0,49	1
Cecum	Crypt epithelial cells	8	0	1	0,25±0,38	0
	Vascular endothelial cells	8	0	1	0,19±0,37	0
	Smooth muscle cells	8	0	2	1,0625±0,67	1
Rectum (Colon)	Crypt epithelial cells	8	0	1	0,31±0,46	0
	Vascular endothelial cells	8	0	1	0,25±0,46	0
	Smooth muscle cells	8	0,5	2	1,0625±0,49	1

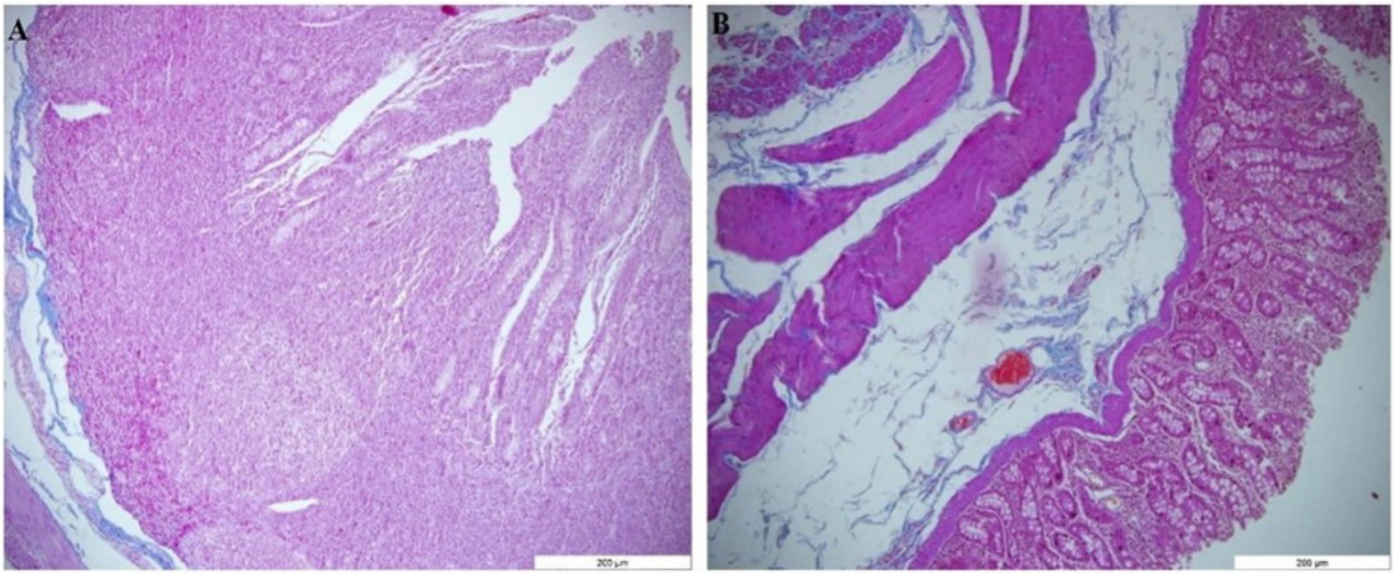

Figure 1: Goose intestine tissue. A; İleum, B; Cecum. Mallory's modified triple staining. A and B; Bar: 200 µm, original magnification, X10

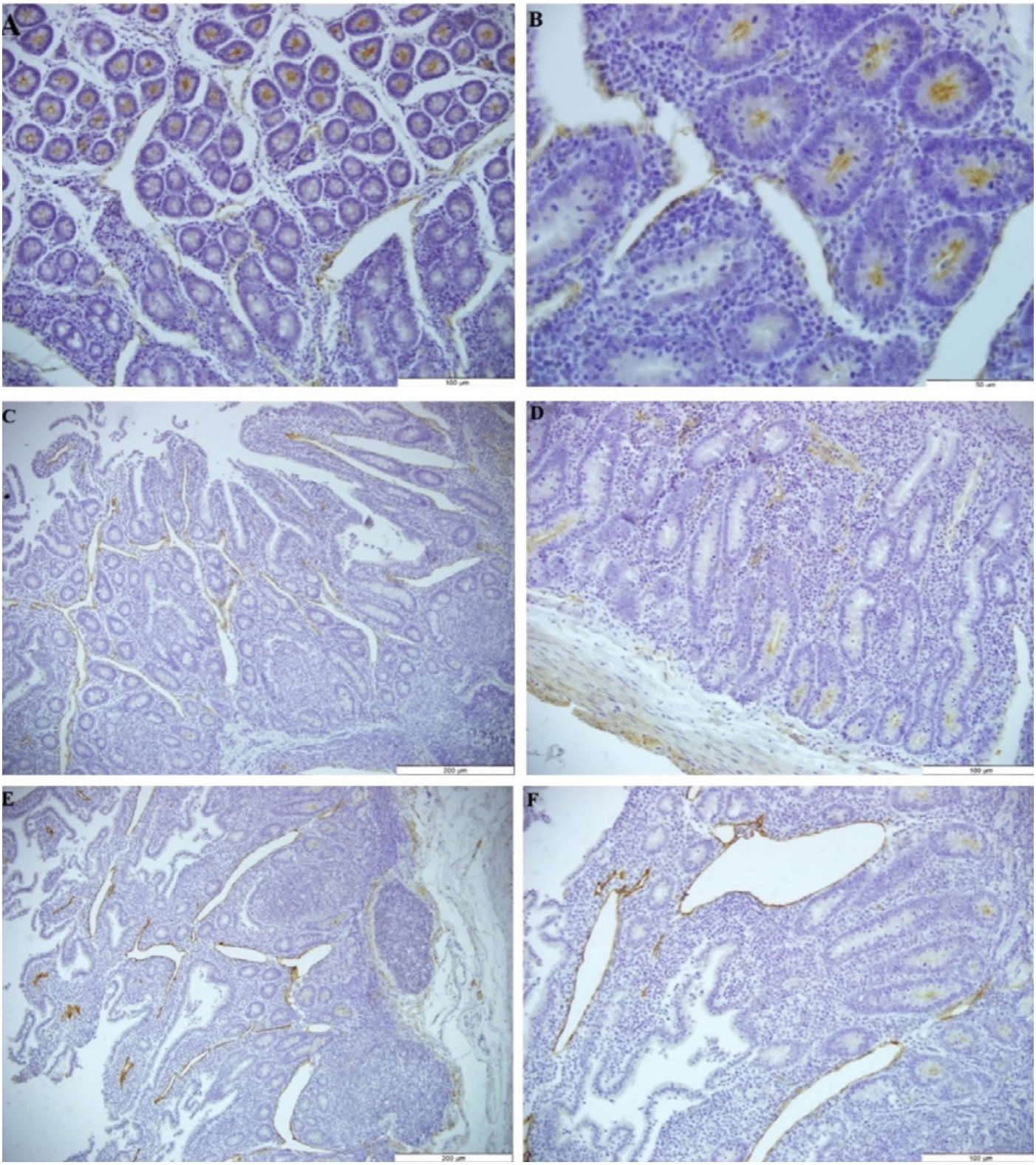

Figure 2: Goose small intestine tissue. AQ1 immunoreactivity. A, B; duodenum, C, D; jejenum E, F; ileum. The Avidin-Biotin-Peroxidase Complex (ABC) method. B; Bar: 50 µm, original magnification, X40, A, D, F; Bar: 100 µm, original magnification, X20, C, E; Bar: 200 µm, original magnification, X10

Results

The normal histological structure of the small and large intestines of geese is shown in Figure 1. The apical parts of crypt epithelial cells in the duodenum showed strong, and the apical parts of crypt epithelial cells in the jejunum and ileum showed moderate AQP1 immunoreactivity. In the duodenum, jejunum, and ileum, strong AQP1 immunoreactivity was determined in vascular endothelial cells and weak immunoreactivity in smooth muscle cells. Weak AQP1 immunoreactivity was detected in the smooth muscle cells of the

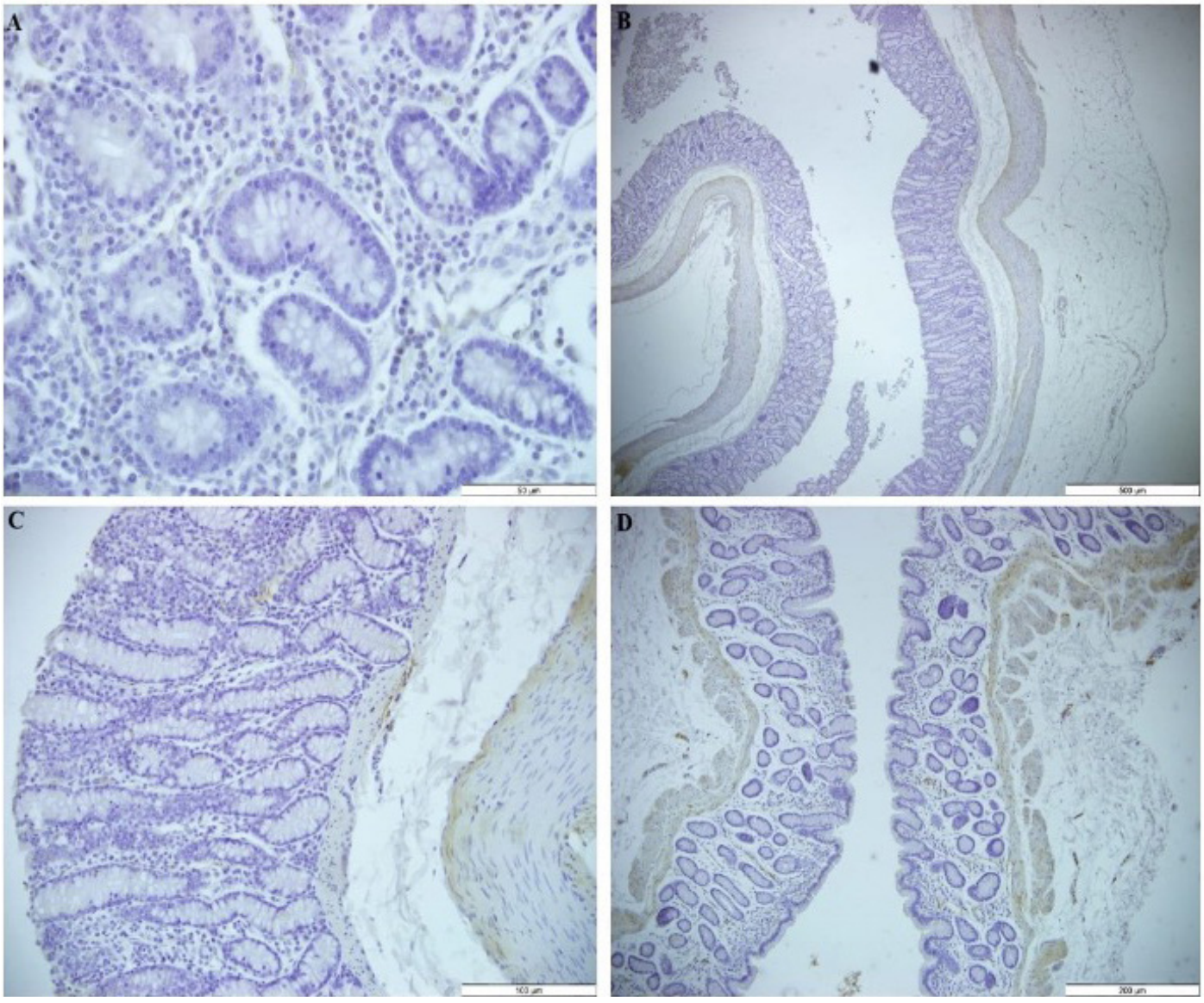

Figure 3: Goose large intestine tissue. AQ1 immunoreactivity. A; cecum, B, C, D; rectum (colon). The Avidin-Biotin-Peroxidase Complex (ABC) method. A; Bar: 50 µm, original magnification, X40, B; Bar: 500 µm, original magnification, X4, C; Bar: 100 µm, original magnification, X20, D; Bar: 200 µm, original magnification, X10

cecum and rectum but no immunoreactivity was observed in either the crypt epithelial cells or the vascular endothelial cells (Table 1 and Figures 3).

Discussion

In the transportation of water, the intestines are the second most important organ after the kidneys. Water transport occurs in the digestive tract because of hydrostatic pressure and osmotic pressure caused by the transport of salt. Much of the transported water is used to regulate saliva, gastric juice, bile, pancreatic fluid, and intestinal fluid, and to adjust water and ion balance (19, 20).

The feed material is ingested, moisturized, ground into small particles, acidified, and attacked by endogenous enzymes in the digestive tract of poultry similar to other animal species (21). In poultry, the intestine is an important organ where enzymatic digestion takes place, and nutrients are absorbed via numerous ion channels and transporters present on the apical intestinal epithelial border. Materials consisting of indigestible food and waste are mixed up with urine in the cloaca and are excreted from the body as feces (22). Intestine composed of duodenum, jejunum, ileum and ceca, rectum (colon), and cloaca. The wall structure of the poultry intestines consists of mucosa, submucosa, muscularis, and serosa layers, like the mammalian intestine (23).

AQP-1 gene sequences of chicken, human, and toad exhibit 94%, 88%, and 78% homology, respectively (18). Specific AQP1 labeling was seen in the endothelia of central lacteals in the villi of the porcine small intestine (24). In the calf of adult buffalo, AQP-1 was detected in the endothelium,

enterocytes, lymphoid tissue, and enteric neurons of both the small and large intestines (25). AQP1 was demonstrated on endothelial cells of lymphatic vessels in the submucosa and lamina propria and capillary endothelial cells in the smooth muscle layer throughout the rat gastrointestinal tract and villus intestinalis and crypt epithelium cells, vascular endothelium, erythrocytes and connective tissue within the small intestine and serosa layer, vascular endothelium and erythrocytes in the large intestines of the mice (26, 27).

Strong AQP4-immunoreactivity was demonstrated in a fiber network in the enteric plexus in chicken ceca and rectum (16). In poultry, ck-AQP5 mRNA was found in the crypt cells of the jejunum, ileum, and colon, but not in the cells that cover the villi (17). Goose testis and vas deferens capillaries were reported to have AQP-1 immunoreactivity in endothelial cells (28). In bird and mammal kidneys, AQP-1,2 and 4 were expressed (29). In this study it was determined that there was AQP1 immunoreactivity in crypt epithelial cells, vascular endothelial cells, and smooth muscle cells in geese duodenum, jejenum and ileum like rat (26), mice (27), and porcine (24) whereas only smooth muscle cells showed a reaction in cecum and rectum.

AQP1 distribution was determined on the apical membrane of the enterocytes, especially in the crypts, and on the cell membrane of erythrocytes of bottlenose dolphin's small intestine. Strong immunostaining was reported in the apical membrane of enterocytes in the mid and bottom regions of the crypt, also comparatively moderate immunostaining was demonstrated at the apical membrane and cytoplasm of enterocytes in the villi and upper region of the crypt (30). It was observed the apical parts of crypt epithelial cells in the duodenum showed strong AQP1 immunoreactivity, and the apical parts of crypt epithelial cells in the jejunum and ileum showed moderate AQP1 immunoreactivity. Also, strong AQP1 immunoreactivity was determined in vascular endothelial cells in the duodenum, jejunum, and ileum and a weak immunoreactivity in smooth muscle cells of geese intestine.

The presence of AQP-1 in the distal rectum of sparrows was reported in large intestines from the ceca to coprodeum with limited distribution. It was suggested that the AQP-1 was present within the cecae especially in the lamina propria and in the mucosa and the muscularis of the proximal rectum and in the epithelium, the lamina propria and muscularis of the distal rectum of house sparrows (18). In this study it was seen that a weak Aquaporin-1 immunoreactivity was detected only in the smooth muscle cells of the geese cecum and rectum. Furthermore, identification of AQP-1 in the mucosa of the large intestine suggested that AQP1 may play a role in water transportation, while localization of AQP-1 in the distal rectal epithelium drew more attention to the importance of retrograde peristalsis for water conservation (18).

In conclusion, indicating that Aquaporin 1 immunoreactivity was observed especially in the apical membranes of crypt enterocytes in geese small intestines as in dolphins (30) and that Aquaporin 1 was localized in endothelial cells of lymph vessels in lamina propria and in the submucosa from the esophagus to the colon of rats (26) suggests that Aquaporin 1 release may be similar in poultry and mammalian intestines.

Acknowledgements

This study was presented as an oral presentation at the 2nd International Congress on Advances in Veterinary Sciences & Technics (ICAVST-2017) in Barcelona.

Ethical approval. Ethics Committee approval was obtained from the Experimental Animal Ethics Committee of Kafkas University (No. 2018/04, dated 26.04.2018 and coded KAÜ-HADYEK/2018-049) for this research.

Conflict of interest. There are no conflicts of interest to be declared by the authors.

Author's Contribution. EKS conceptualized the study. methodology, E.K.S., B.B., G.F.A., and S.E.Y; software, E.K.S, G.F.A. and S.E.Y; validation, E.K.S., B.B., G.F.A., and S.E.Y; formal analysis, E.K.S., B.B., G.F.A., and S.E.Y; resources, E.K.S. and B.B. ; data curation, E.K.S., B.B., G.F.A., and S.E.Y; writing—original draft preparation, E.K.S., B.B., G.F.A., and S.E.Y; writing—review and editing, E.K.S., B.B., G.F.A., and S.E.Y; visualization, E.K.S., B.B., G.F.A., and S.E.Y; supervision, E.K.S., B.B. and S.E.Y; All authors have contributed to the final version of the manuscript. All authors approved the final manuscript.

Funding. The authors received no financial support for the research, authorship, and/or publication of this article.

References

1. Smith BL, Agre P. Eriythrocyte Mr 28,000 transmembrane protein exists as a multisubunit oligomer similar to channel proteins. J Biol Chem 1991; 266: 6407–15.
2. Huang HF, He RH, Sun CC, Zhang Y, Meng QX, Ma YY. Function of aquaporins in female and male reproductive systems. Hum Reprod Update 2006; 12: 785–95.
3. Brown D, Verbavatz JM, Valenti G, Sabolić I. Localization of the CHIP28 water channel in reabsorptive segments of the rat male reproductive tract. Eur J Cell Biol 1993; 61: 264–73.
4. Toker A. Aquaporins; hidrophilic transmembrane channels for water transport. Tıp Araştırma Dergisi 2006; 4: 39–44.
5. Yasui M, Hazama A, Kwon TH, Nielsen S, Guggino WB, Agre P. Rapid gating and anion permeability of an intracellular aquaporin. Nature 1999; 402: 184–7.

6. Murai-Hatano M, Kuwagata T, Sakurai J, et al. Effect of low root temperature on hydraulic conductivity of rice plants and the possible role of aquaporins. Plant Cell Physiol 2008; 49: 1294–305.

7. Zhu C, Chen Z, Jiang Z. Expression, distribution and role of aquaporin water channels in human and animal stomach and intestines. Int J Mol Sci 2016; 17: e1399. doi: 10.3390/ijms17091399

8. Agre P, King LS, Yasui M, et al. Aquoporin water channels-from atomic structure to clinical medicine. J Physiol 2002; 542: 3–16.

9. Ma T, Verkman AS. Aquaporin water channels in gastrointestinal physiology. J Physiol 1999; 517: 317–26.

10. Pelagalli A, Squillacioti C, Mirabella N, Meli R. Aquaporins in health and disease: an overview focusing on the gut of different species. Int J Mol Sci 2016; 17: e1213. doi: 10.3390/ijms17081213

11. Landon SK, Agre P. Pathophysiology of the aquaporin water channels. Ann Rev Physiol 1996; 58: 619–48.

12. Preston GM, Carroll TP, Guggino WB, Agre P. Appearance of water channels in Xenopus oocytes expressing red cell CHIP28 protein. Science 1992; 256: 385–7.

13. Sui H, Han BJ, Lee JK, Walian P, Jap BK. Structural basis of water-specific transport through the AQP1 water channel. Nature 2001; 414: 872–8.

14. Saadoun S, Papadopoulos MC, Hara-Chikuma M, et al. Impairment of angiogenesis and cell migration by targeted aquaporin-1 gene disruption. Nature 2005; 434: 786–92.

15. Pan H, Sun CC, Zhou CY, Huang HF. Expression of aquaporin-1 in normal, hyperplastic and carcinomatous endometria. Int J Gynaecol Obstet 2008; 101: 239–44.

16. Keiji Y, Kanae S, Yasushige O, Aste N, Saito N. Immunolocalization of aquaporin-4 in the brain, kidney, skeletal muscle, and gastro-intestinal tract of chicken. Cell Tissue Res 2011; 344: 51–61.

17. Ramírez-Lorca R, Muñoz-Cabello A, Toledo-Aral JJ, Ilundain AA, Echevarria M. Aquaporins in chicken: localization of ck-AQP5 along the small and large intestine. Comp Biochem Physiol A Mol Integr Physiol 2006; 143: 269–77.

18. Casotti G, Waldron T, Misquith G, Powers D, Slusher L. Expression and localization of an aquaporin-1 homologue in the avian kidney and lower intestinal tract. Comp Biochem Physiol A Mol Integr Physiol 2007; 147: 355–62.

19. Zhang EB. Intestinal water and electrolyte transport. In: Zhang, EB, Sitrin MD & Black DB, eds. In gastrointestinal, hepatobilliary, and nutritional physiology. Philadelphia: Lippincott-Raven, 1996: 91–118.

20. Spring, KR. Routes, and mechanism of fluid transport by epithelia. Annu Rev Physiol 1998; 60: 105–19.

21. Svihus B. Function of the digestive system. J Appl Poult Res 2014; 23: 306–14.

22. Nighot M, Nighot P. Pathophysiology of avian intestinal ion transport. Worlds Poult Sci J 2018; 74: 347–60.

23. Denbow DM. Gastrointestinal anatomy and physiology. In: Whittow GC. ed. Sturkie's Avian Physiology. 5th ed. Oxford: Elsevier 2000; 303–5.

24. Jin SY, Lie YL, Xu LN et al. Cloning, and characterization of porcine aquaporin 1 water channel expressed extensively in gastrointestinal system. World J Gastroenterol 2006; 12: 1092–7.

25. De Luca A, Vassalotti G, Pelagalli et al. Expression and localization of aquaporin-1 along the intestine of colostrum suckling buffalo calves. Anat Histol Embryol 2015; 44: 391–400.

26. Koyama Y, Yamamoto T, Tani K, et al. Expression and localization of aquaporins in rat gastrointestinal tract, Am J Physiol 1999; 276: C621–7.

27. Yediel Aras S, Bayrakcı G, Karadag Sari E. The effects of tribulus terrestris on aquaporin-1 (AQP1) immunolocalization in small and large intestines of mice. Turk Vet J 2022; 4:10–7.

28. Skowronski MT, Leska A, Robak A, Nielsen S. Immunolocalization of aquaporin-1, -5, and -7 in the avian testis and vas deferens. J Histochem Cytochem 2009; 57(10): 915–22.

29. Nishimura H. Urine concentration and avian aquaporin water channels. Pflugers Arch 2008; 456: 755–68.

30. Suzuki M. Expression and localization of aquaporin-1 on the apical membrane of enterocytes in the small intestine of bottlenose dolphins. J Comp Physiol B 2010; 180: 229–38.

Določanje mesta nahajanja akvaporina-1 v tankem in debelem črevesu gosi (*Anser anser*)

E. K. Sari, B. Bakir, G. F. Arslan, S. E. Yildiz

Izvleček: Akvaporini so selektivni vodni kanali za prenos vode skozi celične membrane in imajo pomembno vlogo v vseh celicah. V tej študiji smo z imunohistokemično metodo ugotavljali mesto nahajanja akvaporina-1 v tankem in debelem črevesju gosi. Uporabili smo vzorce (n = 10) tankega in debelega črevesa odraslih, zdravih gosi (Anser anser). Po 24 urni fiksaciji v 10% formaldehidu smo vzorce dehidrirali v zaporednih stopnjah etanola in ksilola ter jih vpeli v parafin. Za pregled splošne strukture črevesa smo uporabili Malloryjevo modificirano metodo trojnega barvanja. Za določanje imunoreaktivnosti akvaporina-1 je bila uporabljena metoda kompleksa avidin-biotin-peroksidaza (ABC). Močno imunoreaktivnost akvaporina-1 smo ugotovili na apikalnih delih epitelijskih celic kript dvanajstnika ter žilnih endotelijskih celicah v dvanajstniku, jejunumu in ileumu. Zmerna imunoreaktivnost akvaporina-1 je bila prisotna v jejunumu in ileumu. Imunoreaktivnost je bila šibka v celicah gladkih mišic, vendar le v celicah slepega črevesa in danke, ne pa tudi v žilnih endotelijskih celicah in epitelijskih celicah kripte. Črevesno tkivo omogoča prenos vode z uravnavanjem prenosa soli in razlik v hidrostatičnem tlaku. Predpostavljeno je, da sta zlasti odseka dvanajstnika in jejunuma prepustna za velike količine vode za namen uravnavanja osmotskega tlaka črevesne vsebine. Posledično je bila tudi v tej študiji ugotovljena imunoreaktivnost akvaporina-1 v epitelijskih celicah kript, gladkih mišičnih celicah in žilnem endoteliju tankega črevesa gosi.

Ključne besede: gosi; črevo; akvaporin-1

Slovenian Veterinary Research
DOI 10.26873/SVR-1726-2023
UDC 165.243:591.133.15:613.24:636.7.09:636.09-051
Pages: 37–47

Original Research Article

Evaluation of Some Element and Mineral Levels in Prescription and Non-Prescription Dog Diets

Key words

elements;
minerals;
dog;
food;
prescription

Mehmet Erman Or[1], Bengü Bilgiç[1]*, Duygu Tarhan[2,3], Fatma Ateş[4], Banu Dokuzeylül[1], Tevfik Gülyaşar[5]

[1]Department of Internal Medicine, Faculty of Veterinary Medicine, 34320, Istanbul, [2]Department of Biophysics, Cerrahpaşa Faculty of Medicine, Istanbul, 34098, University-Cerrahpasa, Istanbul, [3]Department of Biophysics, School of Medicine, Bahcesehir University, Istanbul, 34734, [4]Department of Biophysics, Medical School, Beykent University, Istanbul, 34520, [5]Department of Biophysics, Faculty of Medicine, Trakya University, Edirne, 22030, Turkey

***Corresponding author:** bengu.bilgic@iuc.edu.tr

Abstract: Various prescription diets prescribed by veterinarians for specific diseases in dogs have been developed and introduced to the market. Trace element and mineral levels, which are essential for healthy living conditions in animals, can differ in both prescription and non-prescription foods. In our study, it was aimed to determine the levels of some elements and minerals in various prescription and non-prescription dry foods used in dog nutrition and to evaluate their therapeutic importance.

In the study, a total of 100 different prescription dry food formulated for hepatic diseases (H, n=25), renal diseases (R, n=25), gastrointestinal diseases (GI, n=25) and, allergic diseases (HA, n=25) were used. Non-prescription dry foods from different flavors and brands in the market were considered as the control group (C, n=50). Copper (Cu), Iron (Fe), Manganese (Mn), Zinc (Zn), Selenium (Se), Calcium (Ca), and Phosphorus (P) levels of all dry foods were analyzed by Inductively Coupled Plasma-Optical Emission Spectrometer (ICP-OES, Thermo iCAP 6000 series) and the results were compared between groups. Statistical analysis was evaluated using SPSS 21.

Cu levels in GI and HA groups were higher than in the control group ($p<0.05$ and $p<0.01$, respectively). Fe levels were higher in the GI group and lower in the HA group than in the control group ($p<0.05$). Mn level was significantly higher in the H group compared to the control group ($p<0.001$). The Mn levels in GI and HA groups were higher than the control group ($p<0.01$). There was no statistical difference in Se and Zn levels between prescription and non-prescription dry foods. Ca and P levels in all groups were statistically lower than in the control group ($p<0.001$).

There are significant differences in element and mineral levels in prescription and non-prescription dry foods. These values may be out of the legal limits determined by EU Regulation. Considering the therapeutic purpose of these prescription formulas, some element and mineral amounts were determined as inappropriate.

Received: 21 March 2023
Accepted: 25 May 2023

Introduction

The growing interest in pets has led to an increase in the annual growth rate of the pet food industry. It was reported that 8.5 million tonnes of pet food products are sold annually in Europe (1). Commercial foods are widely preferred by pet owners because they meet the nutritional needs of pets practically and economically (2). In addition

to commercial foods used in healthy animals, various prescription diets formulated for many disease conditions have also been introduced to the market (3). Today, prescription foods are widely prescribed by veterinarians and many studies were on their clinical efficacy (4-10). Urinary diets effective on urinary system that contain lesser amounts of high-quality protein, low phosphorus and magnesium in order to decrease the concentration of urea, phosphorus and magnesium in the urine (4); hepatic diets include moderate fat, high carbohydrates, highly digestible, high biologic value protein that is low in aromatic amino acids and methionine and high in branched-chain amino acids and arginine (5); gastrointestinal diets with high digestibility and biological value protein; pancreatic diets with high digestibility, restricted protein and fat formulated to reduce pancreatic secretions (7); dermatological diets enriched with omega-6 EFA linoleic acid (8) hypoallergenic diets against food allergies containing lamb and rice [9] and diets developed against obesity (10) are among the prescription foods in veterinary medicine.

Trace and macro elements are essential for healthy dogs. While the deficiency of essential trace elements such as can lead to various dysfunctions and death (11,12), greater amounts of these elements such as selenium, copper and zinc may also cause various tissue and organ damage in dogs. Therefore the optimum amount of these elements in pet foods plays an important role in maintaining health conditions (13-18). In this study, it was aimed to evaluate and compare some element and mineral levels between various non-prescription dry foods used in healthy dog nutrition and prescription dry foods used in various diseases.

Material and Methods

Study design

The study was carried out at Istanbul University-Cerrahpaşa, Faculty of Veterinary Medicine, Department of Internal Medicine collaboration with Cerrahpaşa Faculty of Medicine, Department of Biophysics. Non-prescription dry food from different brands of various companies sold on the market and prescription dry food from different brands of various companies sold in veterinary clinics were collected. All food type was dry food for dog nutrition. For non-prescription foods, predominant flavours were chicken, fish and lamb manufactured by Italy and Turkey. Hepatic foods were chicken and fish flavoured manufactured by France and Italy. All renal foods were fish flavoured manufactured by Italy and Spain. Gastrointestinal foods had chicken, fish and duck protein source manufactured by Spain, Italy and France. All hypoallergenic foods were fish flavoured manufactured by Italy and Spain. In the study, a total of 100 prescription dry dog foods developed for hepatic diseases (n=25), kidney diseases (n=25), gastrointestinal system diseases (n=25) and allergic skin diseases (n=25) were used. As a control group (n=50) non-prescription dry foods from different flavors and brands were analyzed. Accordingly, five different study groups were determined as follows:

- Control (C, n=50): Non-prescription dry dog food samples from different flavors and brands used in healthy dogs,
- Hepatic (H, n=25): Dry dog food samples used in liver diseases,
- Renal (R, n=25): Dry dog food samples used in kidney diseases,
- Gastrointestinal (GI, n=25): Dry dog food samples used in gastrointestinal system diseases,
- Hypoallergenic (HA, n=25): Dry dog food samples used in allergic skin diseases.

Element and mineral analysis

Element and mineral analyzes were performed by Inductively Coupled Plasma-Optical Emission Spectrometer (ICP-OES, Thermo iCAP 6000 series). Copper (Cu), Iron (Fe), Manganese (Mn), Zinc (Zn), Selenium (Se), Calcium (Ca), Phosphorus (P) were analyzed from each dry food sample. In order to analyze the elements in ICP-OES, suitable wavelengths for each element were selected (Table 1).

Table 1: Wavelengths of each element in ICP-OES measurements

Element	Wavelengths (nm)
Cu	324.754
Fe	259.940
Mn	257.610
Zn	206.200
Se	196.090
Ca	317.933
P	177.495

In order to determine the Cu, Fe, Mn, Zn, Se, Ca, and P levels from the collected dry foods, 4 samples were prepared from each type of food and the average values of the elemental analysis results were calculated. The element levels obtained as a result of the measurements were expressed as mg/gr $_{(sample)}$ for Fe, Ca and P, and µg /gr $_{(sample)}$ for Cu, Mn, Zn, and Se. 1 mL nitric acid was added to the food samples, which were transferred into heat resistant graduated glass tubes, and left to melt in an oven at 200°C. Then, 1 mL of perchloric acid was added to the nitric acid food sample,

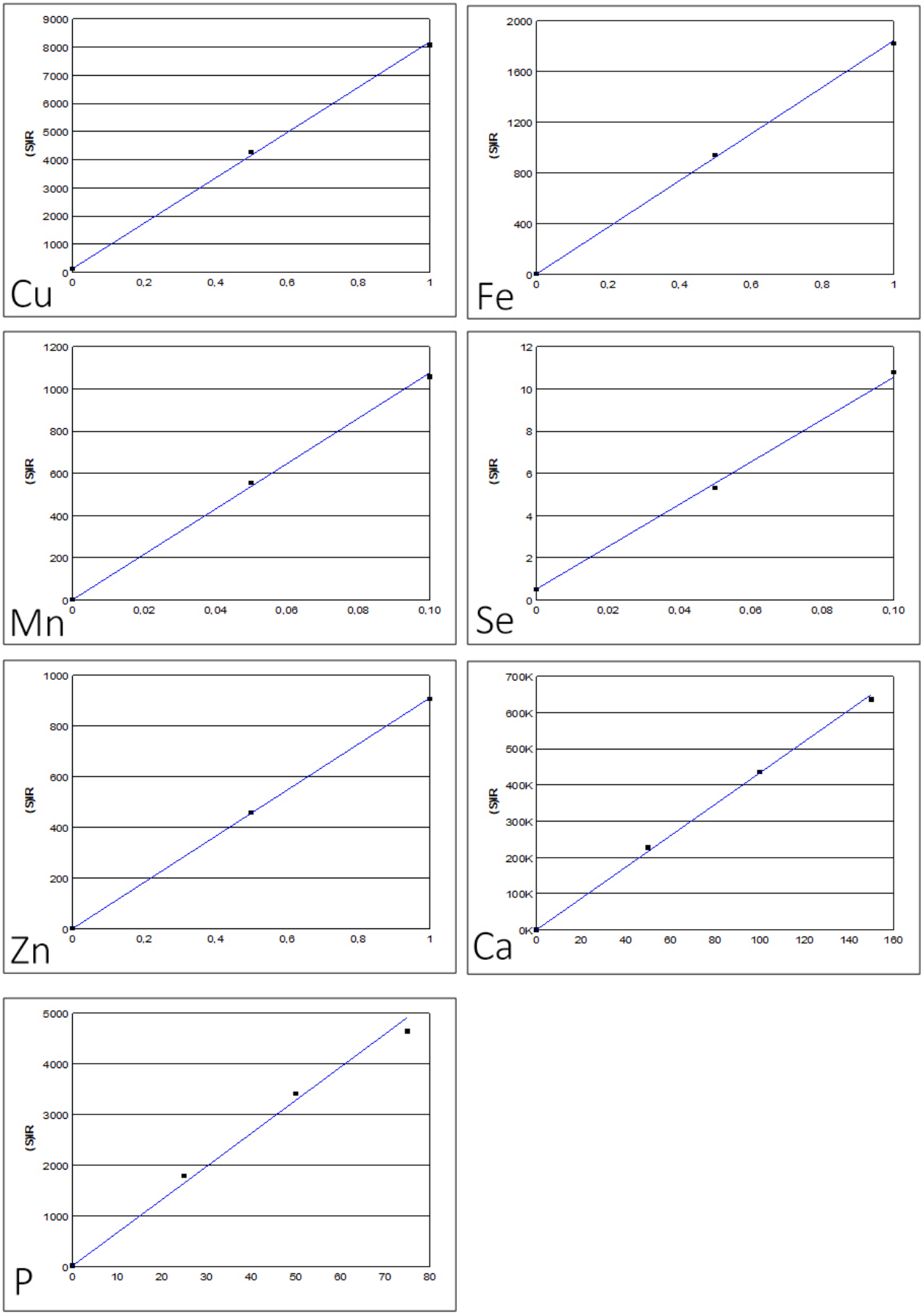

Figure 1: Calibration curves for Cu, Fe, Mn, Se, Zn, Ca and P, respectively

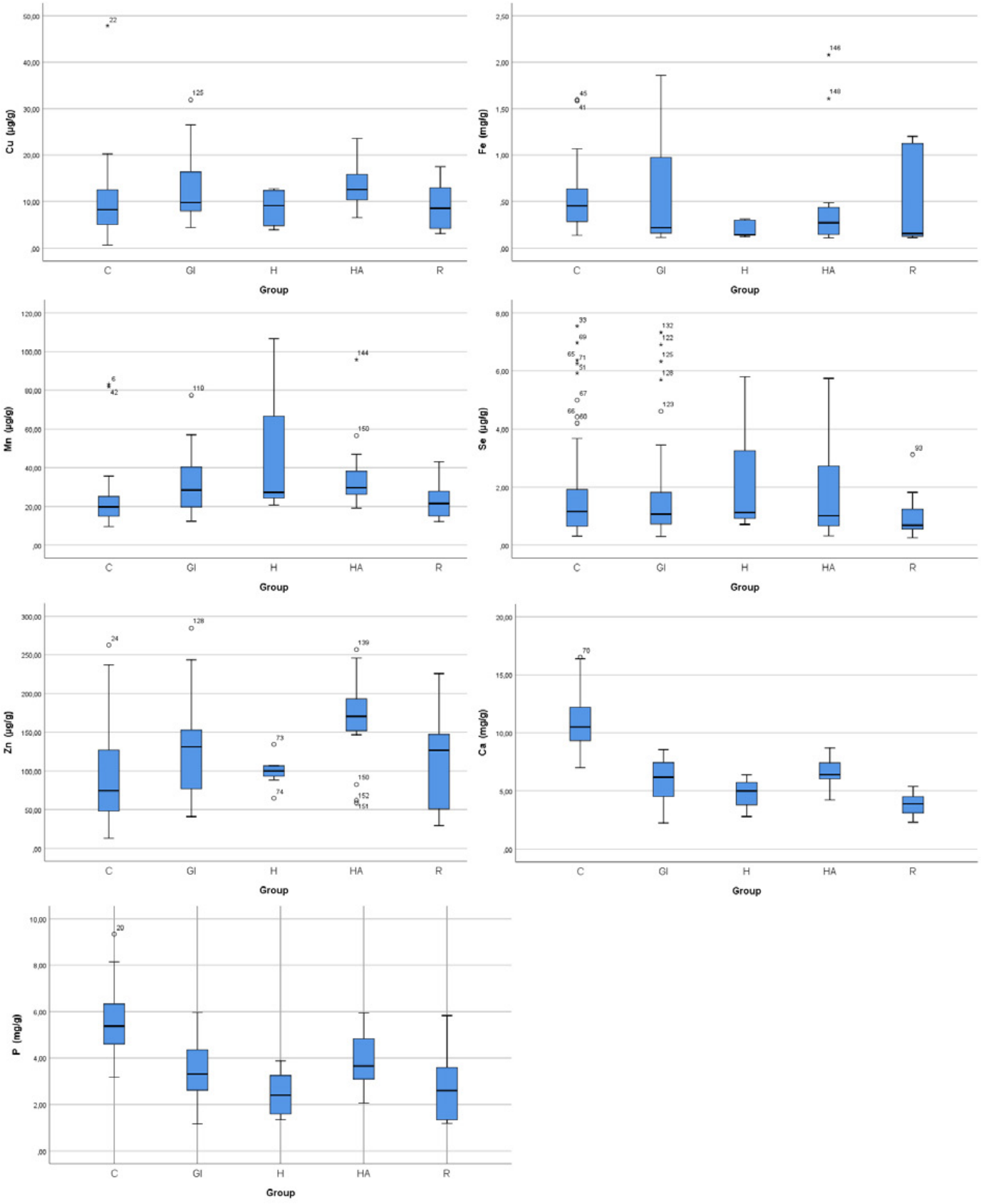

Figure 2: Box-plots for Cu, Fe, Mn, Se, Zn, Ca and P. C: Control, GI: Gastrointestinal, H: Hepatic, HA: Hypoallergenic, R: Renal

which was left to cool at room temperature and vortexed. The mixture, which was put in an oven at 200°C and a wet burning process, was vortexed and left to cool. Distilled water was added to the samples and the total volume was completed to 13 mL. It was vortexed again and analyzed in the ICP-OES device.

Working standard solutions (Chem-Lab NV) were co-prepared from standard stock solutions (1000 pg/dL) of each element. Calibration graphics for each element were drawn and evaluated using standard solutions and deionized water as a blank solution, and then measured (Figure 1). The biggest advantage of this method is that it allows to measure the main emission of many elements at the same time, as well as their emissions at 4-5 different wavelengths. Elemental concentrations in food samples prepared for measurement were determined using these standard curves. All samples were analyzed on the same day and with the same calibration in order to minimize the factors affected by temperature, humidity and device calibration.

Statistical analysis

SPSS 21 statistical program was for statistical analysis of the data obtained as a result of the measurements. All results were given as Mean±Standard Error. One-way Analysis of Variance (One-Way ANOVA), a parametric test, was used to compare groups with more than two homogeneous and normal distributions, and the Kruskal-Wallis test, a non-parametric test, was used to compare groups that did not have normal distribution. In interpretations, the limit of significance was accepted as $p<0.05$.

Results

Copper measurement

Comparisons between H group (8.678±1.430), R group (9.026 ± 1.266) and the control group (9.442±0.846) showed that there wasn't a statistically significant difference between the groups. However, there was a statistically significant increase in Cu levels in the GI (12.431±1.120) and HA groups (13.263±1.070) compared to the control group ($p<0.05$ and $p<0.01$, respectively). With the comparisons among each prescription foods, a statistically significant difference was observed between the H and HA groups and similarly between the R and HA groups in terms of Cu levels ($p<0.05$) (Table 2) (Figure 2). All values obtained were expressed as $\mu g/gr_{sample}$

Iron measurement

Although the Fe levels of the control group (0.495 ± 0.035) and R group (0.479 ± 0.216) decreased mathematically, there was no statistically significant difference. It was determined that the Fe level in the GI group (0.499 ± 0.106) was statistically higher than the control group, and the Fe level in the HA group (0.471 ± 0.160) was statistically lower than the control group ($p<0.05$). The Fe level in the H group (0.202 ± 0.042) was statistically lower ($p<0.01$) than the control group. When the prescription food groups were compared among themselves, no statistically significant difference was observed (Table 2) (Figure 2). All obtained values were expressed as mg/gr_{sample}.

Manganese measurement

Statistically significant increased Mn level was observed in the H group (45.46 ± 13.7) compared to control group (21.81 ± 1.43) ($p<0.001$). In the comparison of control group

Table 2: Element values measured in different food groups

Elements	Control (n=50)	H (n=25)	R (n=25)	GI (n=25)	HA (n=25)
Cu ($\mu g/gr_{(sample)}$)	9.442 ± 0.846	8.678 ± 1.430	9.026 ± 1.266	12.431 ± 1.120*	13.263 ± 1.070**^{a,b}
Fe ($mg/gr_{(sample)}$)	0.495 ± 0.035	0.202 ± 0.042**	0.479 ± 0.216	0.499 ± 0.106*	0.471 ± 0.160*
Mn ($\mu g/gr_{(sample)}$)	21.81 ± 1.43	45.46 ± 13.17***	22.50 ± 2.17^{a}	31.66 ± 2.42**^{,b}	35.00 ± 3.74**^{,bb}
Zn ($\mu g/gr_{(sample)}$)	89.44 ± 8.52	99.85 ± 6.89	112.06 ± 14.06	126.44 ± 9.87**	168.28 ± 11.89***^{,aa,bb,cc}
Se ($\mu g/gr_{(sample)}$)	2.006 ± 0.297	2.286 ± 0.737	1.008 ± 0.199^{a}	1.894 ± 0.337	1.842 ± 0.404
Ca ($mg/gr_{(sample)}$)	10.734 ± 0.262	4.779 ± 0.451***	3.840 ± 0.205***	5.941 ± 0.282***^{,bbb}	6.581 ± 0.271***^{,a,bbb}
P ($mg/gr_{(sample)}$)	5.534 ± 0.152	2.465 ± 0.334***	2.634 ± 0.337***	3.446 ± 0.212***	3.897 ± 0.249***^{,a,b}

*^{,a,b}: $p<0.05$; **^{,aa,bb}: $p<0.01$; ***^{,aaa,bbb,ccc}: $p<0.001$. M±S.E.:Mean ± Standard Error
H: Hepatic Diet, R: Renal Diet, GI: Gastrointestinal Diet, HA: Hypoallergenic Diet.
*: Between control group and prescription food groups.
a: Between H group and R, GI, HA groups. b: Between R group and GI, HA groups. c: Between GI group and HA group.

compare to GI (31.66 ± 2.42) and HA group (35.0 ± 3.74), Mn levels were similarly higher in the GI and HA groups than the control group (p<0.01). There was no statistical difference in Mn levels between control and R groups. When the H, R, GI and HA groups were compared among themselves according to Mn levels, a statistically significant difference was observed in the H and R groups (45.46 ± 13.17 and 22.50 ± 2.17, respectively) (p<0.05). In addition, statistically significant differences were observed when R group compared with GI and HA groups (p<0.05 and p<0.01, respectively) (Table 2) (Figure 2). All values obtained were expressed as μg/gr$_{sample}$.

Zinc measurement

Although there was a mathematical difference in H (99.85 ± 6.89) and R group (112.06 ± 14.06) compare to control group (89.44 ± 8.5), there was no statistically significant difference. However, Zn levels in the food samples of the HA (168.28 ± 11.89) and GI (126.44 ± 9.87) groups were statistically higher compared to the control group (p<0.001 and p<0.01, respectively). When the H, R, GI and HA groups were compared among themselves, there was a statistically significant difference between HA group and the H, R and GI groups (p<0.01) (Table 2) (Figure 2). All values obtained were expressed as μg/gr$_{sample}$.

Selenium measurement

There was no statistically significant difference in the H group (2.286 ± 0.737), R group (1.008 ± 0.199), GI group (1.894 ± 0.337), and HA group (1.842 ± 0.404) compared to the control group (2.006 ± 0.297). However, a statistically significant decrease was observed in the R group compared to the H group (p<0.05) (Table 2) (Figure 2). All values obtained are expressed were μg/gr$_{sample}$.

Calcium measurement

The Ca levels measured in the prescription dry food groups were 4.779 ± 0.451, 3.840 ± 0.205, 5.941 ± 0.282 and 6.581 ± 0.271 for the H, R, GI and HA, respectively. Ca levels in all groups were statistically lower than the control group (10,734 ± 0.262) (p<0.001). There were statistically significant differences between the H group and the HA (p<0.05) group; between the R group and the GI and HA groups (p<0.001) (Table 2) (Figure 2). All obtained values were expressed as mg/gr$_{sample}$.

Phosphorus measurement

The P levels measured in the prescription dry food groups were 2.465 ± 0.334, 2.634 ± 0.337, 3.446 ± 0.212 and 3.897 ± 0.249 for the H, R, GI and HA groups, respectively. The P level in all groups was lower than the control group (5.534 ± 0.152) (p<0.001). There was a significant difference between the H group and HA (p<0.05) and between the R group and the HA group (p<0.05) (Table 2) (Figure 2). All obtained values were expressed as mg/gr$_{sample}$.

Discussion

Copper Levels

Cu is an essential micronutrient for all living organisms. All pet foods originated from vegetable or animal based protein contain Cu. Cu uptake occurs mainly through the digestive system. Although Cu absorption is regulated by enterocytes, it is mainly taken into the organism through food. Experimental studies have shown that chronically high dietary Cu intake leads to Cu accumulations in the liver (19). It is known that hepatic Cu accumulations cause hepatocellular necrosis, chronic hepatitis, cirrhosis and inflammation in cats and genetically susceptible dog breeds (Bedlington terrier, West Highland White Terrier, Skye Terrier, Dalmatian) (20-22).

In the current recommendation of FEDIAF published in 2021, the minimum value for Cu in adult dog foods is 0.83 – 0.72 mg (95 kcal – 119 kcal per kg) per 100 gr dry matter, minimum 1.10 mg and maximum 2.80 mg (legal limit) in early and late growth periods in puppies. Cu values measured in both prescription and non-prescription foods in our study are consistent with the recommended amounts (Table 3). Cu levels in prescription foods used in various kidney and liver diseases and non-prescription foods used in healthy dogs were measured at similar amounts. Therefore, a food-related Cu deficiency unlikely occurs in dogs fed long-term with these foods. 48% (24/50) for non-prescription, 16% (4/25) for HA, 32% (8/25) for GI, 52% (13/25) for H and 56% (14/25) for R group revealed non-compliance with FEDIAF Guidelines in terms of minimum level. Only for non-prescription group, 2% (1/50) were greater than the maximum legal limit.

Cu acts as a cofactor for many antioxidant enzymes (23). In the case of gastroenteritis of various etiologies, decreases in plasma Cu levels may be observed due to Fe and Cu lost with diarrhea (23, 24). In our study, the Cu level in GI group was higher than non-prescription dog foods. This result confirms that the use of GI foods, especially in dogs affected by severe and hemorrhagic diarrhea, is more appropriate compare to non-prescription dog food in terms of compensating the potantial Cu deficiency.

Dry foods included in the HA group are a diet formulated with selected protein and carbohydrate sources to reduce sensitivity to nutrients in dogs. In our study, the Cu level in the HA group was significantly higher than the non-prescription formulas. Since the quality of the protein used for allergy elimination is substantial in hypoallergenic formulas, the high amount of Cu content may be insignificant considering its purpose of use. In fact, many studies in humans have reported that Cu may cause hypersensitivity in

people (25-27). Therefore, the higher Cu level in HA group compared to the non-prescription formulas may not be appropriate and may contribute to allergic reactions.

Iron Levels

Some of the Fe additive sources in commercial dog foods are in the form of Dicalcium phosphate (1.4% Fe) and Ferrous sulfate heptahydrate (21.8% Fe) (28). According to FEDIAF Nutritional Guidelines 2021, the minimum Fe level is determined as 3.60 mg (for 110 kcal/kg), 4.17 mg (for 95 kcal/kg) in 100 gr dry matter in adult dog foods. Legal upper limit is 68.18 mg/100 gr dry matter. Comparing the FEDIAF recommended limits and the results of our study, Mean Fe levels in all food groups was measured within the legal limits (Table 3). However 16% (8/50) for non-prescription, 8% (2/25) for HA, 20% (5/25) for GI, and 12% (3/25) for R group revealed non-compliance with FEDIAF Guidelines in terms of maximum level.

National Research Council (NRC) declared in 2006 that there is no suitable data for determining the safe upper limit for Fe. In addition, it is taken into account that some Fe sources cannot be able to used in some animals. For this reason, For this reason, it is stated that the use of Fe in food production is aimed for coloring rather than nutrition. As a result, although the exact amount of Fe required for dogs is not known, it is emphasized that producers should be aware that excessive iron intake out of the recommended values may be toxic (AAFCO 2014) (29).

Although there were no significant differences in mean Fe levels between formulas, the mean Fe value in prescription formulas used in allergic and liver diseases (HA and H) was lower than non-prescription formulas, and higher in formulas used in gastrointestinal diseases (GI). Fe, like Cu, is essential for normal cellular functions. Excessive intake of Cu and Fe leads to oxidative damage, resulting in hepatocyte loss and inflammation in the liver (30). Therefore, lower Fe levels may be expected in hepatic prescription diets compared to non-prescription diets. However, the relatively high level of Fe in GI foods, which may be preferred especially in cases of diarrhea or hemorrhagic diarrhea, may be important in compensating the possible Fe loss with hemorrhagic diarrhea.

In some studies in human medicine, the association of low Fe concentrations with allergic conditions such as atopic dermatitis and eczema in humans has been reported (31-33). Although this relationship is not clear enough in cats and dogs, according to the results of our study, it may be significant that the Fe level in HA group foods is lower than in non-prescription foods.

Manganese Levels

According to FEDIAF, Mn values are minimum 0.58 mg (110 kcal/kg) and 0.67 mg (95 kcal/kg); legal upper limit is 17 mg in 100 gr dry matter for adult dogs. In our study, the mean Mn values in all formulas were between the legal limits determined by FEDIAF (Table 3). None of the groups were revealed non-compliance with FEDIAF Guidelines in terms of minimum and maximum level.

Mn levels were significantly higher in H, GI, R and HA groups compared to non-prescription group. Mn concentration is controlled by the liver. In human medicine, an increase in serum Mn concentration in patients with liver failures, decreased portal perfusion, cirrhosis and congenital portosystemic shunts (PSS) therefore, accumulations in the

Table 3: Comparison of mean trace element and mineral values in 100 gr dry matter for H, R, GI, HA and non-prescription food groups with minimum and maximum values determined by FEDIAF

Trace elements	Minimum Recommended Level for adults (95 kcal - 110 kcal per kg)	Maximum Recommended Level (Legal limit)	Mean measured element levels in H, R, GI, HA and N-P groups respectively				
			H	R	GI	HA	Control
Cu (mg)	0.83 - 0.72	2.80	0.86	0.9	1.24	1.32	0.94
Fe (mg)	4.17 - 3.60	68.18	20.2	47.9	49.9	47.1	49.5
Mn (mg)	0.67 - 0.58	17.00	4.5	2.2	3.1	3.5	2.1
Zn (mg)	8.34 - 7.20	22.70	9.9	11.2	12.6	16.8	8.9
Se (µg)	22.00 - 18.00	56.80	228.6	100.8	189.4	184.2	200.6
Ca (gr)	0.58 - 0.50	2.50	0.47	0.38	0.59	0.65	1
P (gr)	0.46 - 0.40	1.60	0.24	0.26	0.34	0.38	0.55

H: Hepatic Diet, R: Renal Diet, GI: Gastrointestinal Diet, HA: Hypoallergenic Diet

associated tissues and organs was reported (34). It has been suggested that due to the inability to remove Mn from the liver, Mn level may be also high in dogs with congenital PSS (35). In our study, it was observed that the Mn level was the highest in the formulas used in the treatment of liver diseases compared to other prescription diet foods, and this elevation was significant at the $p<0.001$ level compared to the control group. As a result, we think that high Mn levels in hepatic formulas may pose a significant risk due to possible Mn accumulations in liver diseases.

About 5% of Mn is distributed from the plasma to the kidney. Therefore, exposure to excessive Mn levels can cause kidney dysfunction. Both in vivo and in vitro studies have shown that high levels of Mn exposure are associated with renal dysfunction (36). The Mn level measured in this study was inappropriately high in renal formulas compared to non-prescription formulas. Manganese superoxide dismutase has been defined in the IgE-reactive autoantigens and its allergic role has been reported in some studies (37,38). Therefore, lower Mn levels may be expected in the HA group compared to the other groups in the study.

Zinc Levels

According to a study conducted in 1991, the minimum value for Zn determined by the National Research Council was 39 µg/gr (39), whereas today the minimum Zn value in adult dog foods is 7.2 mg (110 kcal/kg) per 100 gr dry matter and 8.34 mg (for 95 kcal/kg); legal upper limit is 22.7 mg per 100 gr dry matter according to FEDIAF. In our study, Mean Zn was measured within the determined limits in all study groups (Table 3). 28% (14/50) for non-prescription, 12% (3/25) for HA, 24% (6/25) for GI, 12% (3/25) for H and 32% (8/25) for R group revealed non-compliance with FEDIAF Guidelines in terms of minimum level. 2% (1/50) for non-prescription, 16% (4/25) for HA, 4% (1/25) for GI, 8% (2/25) for R group revealed non-compliance with FEDIAF Guidelines in terms of maximum level.

The highest Zn level (168.28 µg /gr) was obtained in foods used in allergic skin diseases. It was found that the Zn values in the formulas used in gastrointestinal diseases and allergic diseases were significantly higher, at $p<0.01$ and $p<0.001$, respectively, compared to the control group. Zn deficiency may cause gastrointestinal diseases characterized by diarrhea and loss of appetite (40). Considering the important effects of Zn on the improvement of skin diseases and hair growth, the higher level of Zn in diets used in allergic skin diseases compared to the control group and other prescription formulas may contribute to the treatment of allergic skin diseases.

It is also reported that supplemental zinc in dogs stimulates hair growing (41). In a study conducted by Or et al. on 71 dogs (42), it was reported a correlation between low Zn levels and skin diseases. In addition, Zn provides membrane stabilization by preventing Cu accumulation and fibrosis formation in the liver. It also has free radical scavenging and antioxidant effects. Therefore, Zn supplements are recommended in liver diseases and conditions associated with hepatic Cu accumulation (35). In a study on Labrador Retriever dogs, it was reported that there was no data on the potential effect of dietary Cu and Zn on hepatic Cu and Zn levels (21). However, in our study, the lowest mean Zn level among the prescribed diet foods was obtained from the formulas used in liver diseases.

Selenium Levels

According to FEDIAF data, the legal limits of Se value in 100 gr of dry food in adult dog foods are minimum 18 µg for 110 kcal/kg and 22 µg for 95 kcal; maximum 56.80 µg/g per 100 gr dry matter. In our study, Se levels in all formulas were above the legal limits determined by FEDIAF (Table 3). 76% (38/50) for non-prescription, 84% (21/25) for HA, 80% (20/25) for GI, 100% (25/25) for H and 68% (17/25) for R group revealed non-compliance with FEDIAF Guidelines in terms of maximum level.

No data are available to accurately indicate the amount of Se requirement in adult dogs. According to the European Union legislation, the maximum legal limit for Se as a food additive is 0.5 µg/gr (43). Se bioavailability is affected by the Se form (selenite, selenate, selenocysteine, selenomethionine etc.), animal species, content of the food. Selenomethionine is known as the most bioavailable Se form. The optimal Se concentration may vary due to different Se forms and bioavailability. It has beneficial effects on healthy skin and joint, hair structure, immune resistance and antioxidant properties. Se deficiency in dogs leads to disorders associated with myopathies. It has been reported that Se deficiency causes myocardial necrosis in young people and myodegenerations in adults, and plays an important role in hair growth (44).

Although not statistically significant compared to the control group, the highest mean Se value among the groups was obtained from the foods used against liver diseases (2.286 µg /g). In our study, the average Se value obtained from foods for allergic skin diseases was measured as 1.842 µg /g. Considering its positive effects on skin and hair growth, high amount of Se in foods used in allergic skin diseases may be considered appropriate. However, in our results, although it was not statistically significant compared to others, a low Se level was obtained in diet used in dermatology. The mean amount of Se detected in foods recommended kidney diseases was lower than in hepatic foods ($p<0.05$). However, several human studies have shown a correlation between renal failure and low Se concentrations. Therefore, adequate dietary Se intake can be expected to have a positive effect on kidney damage (45-47).

Calcium Levels

Ca is an essential mineral plays both structural and functional roles in cats and dogs. These include bone and tooth formation, coagulation mechanism, and neural transmission (48). The Ca value in adult dogs is stated as minimum 5 gr for 110 kcal/kg and 5.8 gr for 95 kcal/kg; maximum upper limit is 2.5 gr in 100 gr dry matter according to FEDIAF. In our study, Ca levels in renal and hepatic diets were measured below the determined minimum values. In non-prescription foods mean Ca level was between the legal limits (Table 3). 16% (4/25) for HA, 32% (8/25) for GI, 48% (12/25) for H and 92% (23/25) for R group revealed non-compliance with FEDIAF Guidelines in terms of minimum level. Ca level was significantly lower in all prescription food groups compared to the control group. In dogs and cats with chronic renal failure, an increase in ionized Ca levels and consequently hypercalcemia usually occurs with disturbances in Ca homeostasis (49). Accordingly, Ca restriction is expected in renal diets.

Phosporus Levels

The P value in adult dogs is stated as minimum of 0.4 gr for 110 kcal/kg and 0.46 gr for 95 kcal/kg; maximum 1.6 gr as a legal limit according to FEDIAF. In our study, P levels in non-prescription market foods used in healthy dogs were between the lower and upper limits determined by FEDIAF. However in all prescription foods mean P levels were lower than minimum recommended level determined by FEDIAF (Table 3). 10% (5/50) for non-presciption, 56% (14/25) for HA, 64% (16/25) for GI, 100% (25/25) for H and 92% (23/25) for R group revealed non-compliance with FEDIAF Guidelines in terms of minimum level.

In small animals P is one of the most important indicators in chronic renal failure. Restriction of dietary P intake slows the progression of kidney damage. Therefore, it is recommended to significantly limit the P level in dry foods used in renal diseases. P values in all prescription formula groups are statistically lower than the control group. It is appropriate that the renal prescription formula contains lower P than the other prescription formulas. However, it should be taken into account that the use of long-term prescription diets may cause phosphorus deficiency and accordingly secondary diseases in dogs.

In a study comparing some element values of various pet foods in UK and FEDIAF guideline, it was reported a broad inconsistency in dog foods (61%) (50). In our study, the mean values showed consistent results with FEDIAF report except for Se, Ca and P. However similar with the previous study (50), when each dietary foods were evaluated individually, high number of incompatibility with FEDIAF was observed. Se was measured greater than the upper limits of FEDIAF in all food groups. P was lower than both determined minimum limits and non-prescription dry foods.

In a study investigating some trace element values in pet foods, Cu, Fe and Mn levels (min-max) were measured as 3.33-16.6, 23.9-71.1, and 3.28-24.4, respectively (µg/gr) (51). Cu values are consistent with our results. Mean Cu levels were measured minimum 8.67 µg/gr and maximum 13.26 µg/gr in all our food groups. Similarly, in this study, mean Mn levels (minimum 21.8 µg/gr and maximum 45.4 µg/gr) show compatibility with the study of Duran et al. However Fe was measured higher in all our study groups.

Conclusions

Some element and mineral values show significant differences between prescription and non-prescription market foods. Concentrations of these elements in formulas should be reconsidered, since Mn is measured higher in hepatic and renal formulas compared to the control group, and Zn is lower in hepatic formulas compared to the control group. We think that high Mn levels in hepatic renal formulas may pose a significant risk due to possible Mn accumulations in liver and kidney diseases. Se was measured greater than the upper limits of FEDIAF in all food groups. P was lower than both determined minimum limits and non-prescription dry foods. Our results were similar with the previous studies related to high Se values in pet foods. In our opinion, the upper and lower limits of trace element and mineral contents of pet foods should be reconsidered.

Acknowledgements

This work was supported by Scientific Research Projects Coordination Unit of Istanbul University-Cerrahpasa (BYP-2020-34779). A part of the study was presented as M. Erman Or's master thesis in Department of Biophysics, Faculty of Medicine, Trakya University.

Fundıng. The authors declare that no funds, grants, or other support were received during the preparation of this manuscript. Competıng ınterests. The authors have no relevant financial or non-financial interests to disclose.

Author contrıbutıons. All authors contributed to the study conception and design. Material preparation, data collection and analysis were performed by mehmet erman or, banu dokuzeylül, duygu tarhan and fatma ateş alkan. The first draft of the manuscript was written by mehmet erman or, duygu tarhan, bengü bilgiç, tevfik gülyaşar, fatma ateş alkan and banu dokuzeylül and all authors commented on previous versions of the manuscript. All authors read and approved the final manuscript.

Ethıcal statement. This is an observational study. Trakya University, Local Ethics Committee of Animal Expeiments has confirmed that no ethical approval is required (28.11.2016/ TUHADYEK-2016/47).

References

1. FEDIAF EuropeanPetFood. Annual Report 2023 [online]. Bruxelles: Fediaf, 2023. https://europeanpetfood.org/about/annual-report (18. 8. 2023)
2. Zicker SC. Evaluating pet foods: how confident are you when you recommend a commercial pet food? Top Companion Anim Med 2008; 23: 121–6.
3. Kelly RE. Feeding the modern dog: an examination of the history of the commercial dog food industry and popular perceptions of canine dietary patterns. Michigan: Michigan State University, 2012.
4. Seaman R, Bartges JW. Canine struvite urolithiasis. Compend Contin Educ Vet 2001; 23: 407–20.
5. Honeckman A. Current concepts in the treatment of canine chronic hepatitis. Clin Tech Small Anim Pract 2003; 18: 239–44.
6. Kato M, Miyaji K, Ohtani N, Ohta M. Effects of prescription diet on dealing with stressful situations and performance of anxiety-related behaviors in privately owned anxious dogs. J Vet Behav 2012; 7: 21–6.
7. Kerl ME, Johnson PA. Nutritional plan: matching diet to disease. Clin Tech Small Anim Pract 2004; 19: 9–21.
8. Olivry T, DeBoer DJ, Favrot C, et al. Treatment of canine atopic dermatitis: 2010 clinical practice guidelines from the International Task Force on Canine Atopic Dermatitis. Vet Dermatol 2010; 21: 233–48.
9. Roudebush P, Schick RO. Evalution of a commerical canned lamb and rice diet for the management of adverse reactions to food in dogs. Vet Dermatol 1994; 5: 63–7.
10. Yamka RM, Friesen KG, Frantz NS. Identification of canine markers related to obesity and the effects of weight loss on the markers of interest. Intern J Appl Res Vet Med 2006; 4: 282–92.
11. Kaya S. Biyoelementler. In: Burçak G, ed. Biyokimya Ders Kitabı. İstanbul: İstanbul Cerrahpaşa Tıp Üniversitesi, 2012.
12. Choong YY, Norli I, Abdullah AZ, Yhaya MF. Impacts of trace element supplementation on the performance of anaerobic digestion process: a critical review. Bioresour Technol 2016; 209: 369–79.
13. Grotto D, Carneiro MFH, De Castro MM, Garcia SC, Junior FB. Long-term excessive selenium supplementation induces hypertension in rats. Biol Trace Elem Res 2018; 182: 70–7.
14. Özçelik D, Toplan S, Özdemir S, Akyolcu MC. Effects of excessive copper intake on hematological and hemorheological parameters. Biol Trace Elem Res 2002; 89: 35–42.
15. Wang Y, Jiang L, Li Y, Luo X, He J. Excessive selenium supplementation induced oxidative stress and endoplasmic reticulum stress in chicken spleen. Biol Trace Elem Res 2016; 172: 481–7.
16. Gurnee CM, Drobatz KJ. Zinc intoxication in dogs: 19 cases (1991–2003). J Am Vet Med Assoc 2007; 230: 1174–9.
17. Seguin MA, Bunch SE. Iatrogenic copper deficiency associated with long-term copper chelation for treatment of copper storage disease in a Bedlington Terrier. J Am Vet Med Assoc 2001; 218: 1593–7.
18. Kather S, Grützner N, Kook PH, Dengler F, Heilmann RM. Review of cobalamin status and disorders of cobalamin metabolism in dogs. J Vet Intern Med 2020; 34: 13–28.
19. Thornburg LP. A perspective on copper and liver disease in the dog. J Vet Diagn Invest 2000; 12: 101–10.
20. Meertens NM, Bokhove CAM, Van Den Ingh TSGAM. Copper-associated chronic hepatitis and cirrhosis in a european shorthair cat. Vet Pathol 2005; 42: 97–100.
21. Fieten H, Hooijer-Nouwens BD, Biourge VC, et al. Association of dietary copper and zinc levels with hepatic copper and zinc concentration in Labrador Retrievers. J Vet Intern Med 2012; 26: 1274–80.
22. Haynes JS, Wade PR. Hepatopathy associated with excessive hepatic copper in a Siamese cat. Vet Pathol 1995; 32: 427–9.
23. Panda D, Patra RC, Nandi S, Swarup D. Oxidative stress indices in gastroenteritis in dogs with canine parvoviral infection. Res Vet Sci 2009; 86: 36–42.
24. Elsayed NM, Kubesy AA, Salem NY. Altered blood oxidative stress biomarkers in association with canine parvovirus enteritis. Comp Clin Pathol 2020; 29: 355–9.
25. Fage SW, Faurschou A, Thyssen JP. Copper hypersensitivity. Contact dermatitis 2014; 71: 191–201.
26. Hostynek JJ, Maibach HI. Copper Hypersensitivity: dermatologic aspects – an overview. Rev Environ Health 2003; 18: 153–83.
27. Vural H, Uzun K, Uz E, Koçyigit A, Akyol O. Concentrations of copper, zinc and various elements in serum of patients with bronchial asthma. J Trace Elem Med Biol 2000; 14: 88–91.
28. McCown JL, Specht AJ. Iron homeostasis and disorders in dogs and cats: a review. J Am Anim Hosp Assoc 2011; 47: 151–60.
29. AAFCO. AAFCO methods for substantiating nutritional adequacy of dog and cat foods [online]. Champaign: Association of American feed control officials, 2023.https://www.aafco.org/wp-content/uploads/2023/01/Model_Bills_and_Regulations_Agenda_Midyear_2015_Final_Attachment_A.__Proposed_revisions_to_AAFCO_Nutrient_Profiles_PFC_Final_070214.pdf
30. Whittemore JC, Newkirk KM, Reel DM, Reed A. Hepatic copper and iron accumulation and histologic findings in 104 feline liver biopsies. J Vet Diagn Invest 2012; 24: 656–61.
31. Shaheen SO, Newson RB, Henderson AJ, et al. Umbilical cord trace elements and minerals and risk of early childhood wheezing and eczema. Eur Respir J 2004; 24: 292–7.
32. David TJ, Wells FF, Sharpe TC, Gibbs AC, Devlin J. Serum levels of trace metals in children with atopic eczema. Br J Dermatol 1990; 122: 485–9.
33. Drury KE, Schaeffer M, Silverberg JI. Association between atopic disease and anemia in US children. JAMA Pediatr 2016; 170: 29–34.
34. Glow AG, Marques AIC, Yool DA, Duncan A, Mellanby RJ. Whole blood manganese concentrations in dogs with congenital portosystemic shunts. J Vet Intern Med 2010; 24: 90–6.
35. Norton RD, Lenox CE, Manino P, Vulgamott JC. Nutritional considerations for dogs and cats with liver disease. J Am Anim Hosp Assoc 2016; 52: 1–7.
36. Gandhi D, Rudrashetti AP, Rajasekaran S. The impact of environmental and occupational exposures of manganese on pulmonary, hepatic, and renal functions. J Appl Toxicol 2022; 42:103–29.
37. Valenta R, Mittermann I, Werfel T, Garn H, Renz H. Linking allergy to autoimmune disease. Trends Immunol 2009; 30: 109–16.
38. Watchmaker J, Collins R, Chaney K. Allergic contact dermatitis to manganese in metallic implant. Dermatitis 2015; 26: 149–50.
39. Booles D, Burger IH, Whyte AL, Anderson RS, Carlos GM, Robinson IP. Effects of two levels of zinc intake on growth and trace element status in labrador puppies. J Nutr 1991; 121(suppl. 11): S79–80.
40. Cummings JE, Kovacic JP. The ubiquitous role of zinc in health and disease. J Vet Emerg Crit Care 2009; 19: 215–40.
41. Lowe JA, Wiseman J, Cole DJA. Zinc source influences zinc retention in hair and hair growth in the dog. J Nutr 1994; 124(suppl. 12): S2575–6.

42. Or ME, Bakırel U, Tuncel H, et al. Deri hastalıklı köpeklerde serum cinko ve bakır Düzeyleri ile histopatolojik değişikliklerin ilişkisi. Istanbul Üniv Vet Fak Derg 2002; 28: 337–45.

43. Zentrichová V, Pechová A, Kovaříková S. Selenium and dogs: a systematic review. Animals 2011; 11: e418. doi:10.3390/ani11020418.

44. Sharada KC, Purushotha B, Radhakrish PM, Mantri AP, Vagdevi HM . Role of selenium in pets health and nutrition: a review. Asian J Anim. Sci 2011; 5: 64–70.

45. Zachara BA, Pawluk H, Korenkiewicz J, Skok Z. Selenium levels in kidney, liver and heart of newborns and infants. Early Hum. Dev 2001; 63: 103–11.

46. Aaseth J, Alexander J, Alehagen U, et al. The aging kidney-as influenced by heavy metal exposure and selenium supplementation. Biomolecules 2021; 11: e1078. doi:10.3390/biom11081078.

47. Xie C, Zeng M, Shi Z, Li S, Jiang K, Zhao Y. Association between selenium status and chronic kidney disease in middle-aged and older Chinese based on CHNS data. Nutrients 2022; 14: e2695. doi:10.3390/nu14132695.

48. Stockman J, Villaverde C, Corbee RJ. Calcium, phosphorus, and vitamin D in dogs and cats: beyond the bones. Vet Clin North Small Anim Pract 2021; 51: 623–34.

49. Parker VJ. Nutritional management for dogs and cats with chronic kidney disease. Vet Clin North Small Anim Pract 2021; 51: 685–710.

50. Davies M, Alborough R, Jones L, Davis C, Williams C, Gardner DS. Mineral analysis of complete dog and cat foods in the UK and compliance with European guidelines. Sci Rep 2017; 7: e17107. doi:10.1038/s41598-017-17159-7.

51. Duran A, Tuzen M, Soylak M. Trace element concentrations of some pet foods commercially available in Turkey. Food Chem Toxicol 2010; 48: 2833–7.

Vrednotenje vsebnosti nekaterih elementov in mineralov v predpisani in nepredpisani prehrani za pse

M. E. Or, B. Bilgiç, D. Tarhan, F. Ateş, B. Dokuzeylül, T. Gülyaşar

Izvleček: Na trgu so prisotne različne diete na recept, ki jih veterinarji predpisujejo za določene bolezni psov. Vsebnost elementov v sledovih in mineralov, ki so bistveni za zdravo življenje živali, se lahko razlikuje tako v hrani na recept kot v hrani brez recepta. V naši študiji smo želeli določiti vsebnost nekaterih elementov in mineralov v različnih predpisanih in nepredpisanih suhih vrstah hrane za pse, ter oceniti njihov terapevtski pomen.

V študiji je bilo uporabljenih 100 različnih vrst suhe hrane, formulirane za jetrne bolezni (H, n=25), ledvične bolezni (R, n=25), bolezni prebavil (GI, n=25) in alergijske bolezni (HA, n=25). Suha hrana brez recepta različnih okusov in blagovnih znamk na trgu je bila obravnavana kot kontrolna skupina (C, n=50). Vsebnost bakra (Cu), železa (Fe), mangana (Mn), cinka (Zn), selena (Se), kalcija (Ca) in fosforja (P) v vseh vrstah suhe hrane smo analizirali z optično emisijsko spektroskopijo z induktivno sklopljeno plazmo (ICP-OES, serija Thermo iCAP 6000) in rezultate primerjali med skupinami. Statistična analiza je bila narejena v programu SPSS 21.

Vsebnost Cu v skupinah GI in HA je bila višja kot v kontrolni skupini ($p<0,05$ oziroma $p<0,01$). Vsebnost Fe je bila višja v skupini GI in nižja v skupini HA kot v kontrolni skupini ($p<0,05$). Raven Mn je bila bistveno višja v skupini H v primerjavi s kontrolno skupino ($p<0,001$). Ravni Mn v skupinah GI in HA so bile višje kot v kontrolni skupini ($p<0,01$). Med suho hrano na recept in suho hrano brez recepta ni bilo statistične razlike v vsebnosti Se in Zn. Vsebnosti Ca in P so bile v vseh skupinah statistično značilno nižje kot v kontrolni skupini ($p<0,001$).

Vsebnost elementov in mineralov v suhi hrani na recept in suhi hrani brez recepta se je bistveno razlikovala. Te vrednosti so lahko izven zakonsko določenih mejnih vrednosti, ki jih določa uredba EU. Glede na terapevtski namen diete na recept smo nekatere količine elementov in mineralov določili kot neustrezne.

Ključne besede: elementi; minerali; pes; hrana; recept

Slovenian Veterinary Research
DOI 10.26873/SVR-1810-2024
UDC 636.1:675.015.26:601.4:577.212.3
Pages: 49–56

Original Research Article

Variation in the *ASIP* and *DUN* Genes Responsible for Coat Colour in Bosnian Mountain Horse

Key words

horse coat colour;
dun dilution;
DNA polymorphism;
allele frequency;
genotype frequency;
Bosnian mountain horse

Marko Cotman [1]*, Jelena Kotiščak [1], Matjaž Mesarič [2]

[1]Institute for Preclinical Sciences, University of Ljubljana, Veterinary Faculty, Gerbičeva 60, [2]Clinic for Reproduction and Large Animals, University of Ljubljana, Veterinary Faculty, Cesta v Mestni log 47, 1000 Ljubljana, Slovenia

***Corresponding author:** marko.cotman@vf.uni-lj.si

Abstract: Accurate determination of coat colours in Bosnian Mountain Horse (BMH) can be challenging as there are variations in coat colour shades and several dun dilution variants occur. In other studies found single nucleotide polymorphisms (SNPs) within two colour loci *T-box 3* (*TBX3*) and 11-bp indel polymorphism within *Agouti Signalling Protein* gene (*ASIP*), were genotyped in 313 BMH individuals. The obtained genotypes were then compared to the identified phenotypes by using the observed coat colour types from the International Association of Bosnian Mountain Horse Breeders (IABMHB) database. It was found that the dark bay and black were the most representative coat colours in BMH. The frequency of the dominant *Dun* (*D*) dilution allele in the study is higher (0.09) than the previously predicted frequency recorded in the available BMH register. Among the identified alleles, there was a discrepancy or inconsistency between the predicted coat colour based on genotypes and the observed coat colour in 73 horses (23%). The most frequent error concerned the misclassification of horses with genotypes *aa* and *Aa* at the *ASIP* gene, *non-dun1/non-dun1 (nd1/nd1)* and *non-dun2/non-dun1 (nd1/nd2)* at the *TBX3* gene, which can be associated with the occurrence of slight dilution phenotypes in these individuals. In contrast to the Konik and Hucul breeds, no homozygosity of the *D* allele was found in the BMH. The *D* allele can be easily overlooked or not recognised in different phenotypic groups, such as dark bay and black horses. Therefore, the hypothesis that Dun dilution effects itself is not as strongly epistatic in the BMH as described in other horse breeds. The results of the study confirm the importance of molecular testing in accurately determining the coat colour of horses. This would help to avoid errors in coat colour descriptions in official breeding records and provide valuable information for selective breeding programmes aimed at producing specific and desired coat colours.

Received: 14 July 2023
Accepted: 15 January 2024

Introduction

Coat colour as a trait was favoured in the domestication of horses. In recent years, rapid progress has been made in understanding the genetics of coat colour in horses (1). Tradition and practise are guided by certain principles and breeding programmes, which may be directed either towards the promotion of colour diversity or towards the pursuit of colour uniformity. In particular patterns associated with white are deliberately avoided because their occurrence is believed to be a sign of crossbreeding (2, 3). This deliberate avoidance can be attributed to concerns arising from potential negative influences, such as pleiotropism, which could compromise the safety and integrity of breeding initiatives (4). Long-standing selection for colour has resulted in the allele frequencies responsible for the different coat colours in horses changing under the influence of specific breeding practises, reproduction methods and breeding standards. Breed-specific segregation of alleles is related to the breeding history of breeds (5-7).

BMH is a breed with a long history, native to the region and adapted to semi-wild rearing conditions over a long period of time. BMH originate from the Alpine/Dinaric region, which is known for its difficult environmental conditions such as high altitude, rugged terrain, cold temperatures and lack of food, especially in winter (8). Similar to other indigenous small mountain horse breeds, the BHM has experienced a decline in its role as a working horse. This decline can be attributed to factors such as the migration of the population from rural areas to the cities, changes in the lifestyle of the Balkan inhabitants and the modernisation of agriculture. The number of purebred and registered animals includes 340 animals in the studbook (8). The majority of the BMH population consists of brown and black horses, while only a few individuals have white markings. In the breeding programme for the BMH, all colours except grey, pinto, chestnut and spotted, without white markings, are allowed (9, 10).

The analysis of official breeding documentation conducted by Mesarič et al. (2015) revealed that BMH registered in the IABMHB studbook are mainly dark bay, black, bay dun or blue dun. The presence of Dun colours in the BMH population is a clear indication of the influence of earlier horse types that contributed to the development of the native BMH. These horses often exhibit primitive markings such as horizontal leg stripes and distinctive eel stripes. The phenotypic similarity of Dun horses to the Tarpan and other related breeds such as the Hucul, Konik and BMH provide additional evidence of their common ancestry (8,11-13). The BMH mare lines Una, Medina, Lasta and Zorka in particular have retained a share of Dun horses. Historical records indicate that Dun horses accounted for about 3.2% of the BMH population in 1944 (9).

The *Dun* dilution gene, which affects the pigmentation of both red and black coat colour, is considered to represent the ancestral or wild colouration of horses (14). Dun horses have a dark dorsal stripe and many of them bear other "primitive markings" (leg stripes, shoulder shadow/stripes, face mask) (15). The presence of Dun horses can be seen on prehistoric cave paintings, such as at Chauvet Cave, suggesting a long-standing association between this colouration and equids (16). Several closely related Equus species, including the Przewalski's horse, the onager, the kiang, the African wild ass, an extinct subspecies of plains zebra known as the quagga, and an extinct subspecies of horse, the tarpan, have characteristics associated with the dun phenotype.

According to a study by Imsland et al. (2016), the Dun dilution effect was attributed to the presence of the *G* allele in SNP 18,227,267+1,066G > T at a 1.6 kb insert in the downstream region of the *TBX3* gene on ECA8. This insertion is known as the dominant *Dun* allele (*D*). On the other hand, the presence of the *T* allele is associated with the recessive allele *non-dun 1* (*nd1*) or the absence of a 1.6 kb fragment is associated with a recessive allele *non-dun 2* (*nd2*).

In countries where horse breeding plays an important role, breeders have found patterns and coat colours extremely interesting, as they can significantly increase the market value of horses. As a result, different colours and patterns have developed in many horse breeds. Accurate identification of the desired coat colour is of great importance to breeders as it helps in the selection of specific colours and facilitates future breeding plans. The development of a simple and efficient method to identify mutations responsible for dun dilution is of great interest to horse breeders as it allows for a better understanding and control of coat colour genetics in their breeding programmes (17).

The aim of this study was to characterize the variations in the base colour of the endangered BMH by revealing the genetic basis of coat colour. Furthermore, we want to investigate the influence of selection on coat colour and examine the relationship between genotype combinations of the *ASIP* and *DUN* genes and the variation in coat colour within the existing population.

Material and methods

A total of 313 genomic DNA samples from BMH individuals of both genders, representing different shades of coat colour, were used for this comprehensive study. These samples were obtained from the Laboratory of Molecular Biology and Genetics at the Faculty of Veterinary Medicine, University of Ljubljana, Slovenia. To compare, phenotypic data was taken from the IABMHB database, matching the coat colour descriptions in the official breeding documents. The validity of the method was confirmed by examining 28 dun and 78 non-dun horses. In addition, 10 samples of horses with known coat colour genotypes from the International Society for Animal Genetics (ISAG) Comparison Equine Test 2018/2019 were used as reference. First, a cohort of 80 individuals was randomly selected from the original sample group to calculate the frequencies of *TBX3* and *ASIP* genotypes. This selection was made to ensure a representative sample encompassing the aberrant traits observed in the closely related animals in a population of horses in this study. Due to the rare occurrence of chestnut coat colour in the BMH population, as chestnut horses are usually excluded from breeding, our focus was directed towards the two dominant alleles *TBX* and *ASIP*. These loci play an important role in determining the different coat colours observed in this breed. In addition, we carried out a comprehensive photographic documentation of all animals involved in the studies.

Genotyping of Dun / non-dun1 / non-dun2 alleles

Genomic DNA from hair roots was extracted according to the Chelex extraction protocol.

Genotype for the G > T SNP (*D* v. *nd1* alleles) on the *TBX3* gene was analysed using a dual-fluorescent multiprobe

assay. Analysis of the 1.6 kb indel of the *TBX3* gene (*D* v. *nd2* alleles) was developed using quantitative polymerase chain reaction (q-PCR). The oligonucleotide primers and probes for discrimination between *D* and *nd1* alleles were outsourced to a commercial service (Assay by Design Service, Applied Biosystems). These primers and probes were designed for the equine *TBX3* gene with the corresponding GenBank accession number KT 896509.1 and KT896508.1 (15). On the other hand, the oligonucleotide primers and probes for the detection of the *nd2* allele (1.6 kb deletion) were developed using Primer3 software v.4.1.0 (http://bioinfo.ut.ee/primer3/), targeting the regions upstream and downstream of the 1.6 kb deletion (18). The probes are labelled with different fluorescent dyes: VIC for *nd1*, FAM for *D* and Cy5 dye for *nd2*.

Genotyping of *TBX3* alleles was performed using two different reactions: an allele discrimination assay for *D/nd1* alleles and q-PCR for detection of the *nd2* allele (1.6 kb deletion). A standard PCR programme on a q-PCR reaction system (Quantstudio 5, Applied Biosystems) was used. The results were analysed using QuantStudioTM Design&Analysis software v1.5.2. (Applied Biosystems).

Sequencing of TBX3

To assess the reliability of the assay, direct sequencing of a 240 bp fragment of the *TBX3* gene was performed. The sequence of the *TBX3* gene was amplified by PCR. The sequence reaction of PCR product was performed on a thermal cycler (SimplyAmp, Applied Biosystems) according to the manufacturer's instructions (BigDye Terminator v1.1 cycle sequencing kit, Thermo Fisher Scientific). Sequencing was performed using SeqStudio (Applied Biosystems) and subsequently analysed (Chromas sequencing software, Technelysium, Brisbane, Australia).

Genotyping of the ASIP insertion-deletion

To determine the *ASIP* genotypes, the coat colour gene loci were genotyped for *ASIP* using polymerase chain reaction (PCR) according to procedures described by Rieder et al. (2001). The PCR products were analysed by capillary electrophoresis QIAxcel ScreenGel 1.5.0

Statistical analyses were performed in IBM SPSS Statistics 28.0.0.0. A group of 80 horses was selected to assess the correlation between *TBX3* and the *ASIP* genotypes. This correlation was assessed using the chi-square test and a p-value was determined. Comparisons of genotype frequency between groups were made using Fisher's exact test. Bonferroni's p-value correction was applied to account for multiple comparisons. Subsequently, the recorded coat colour of each horse in the database was compared to the predicted coat colour based on the genotypes for the *TBX3* and *ASIP* loci. All discrepancies between the recorded genotypes and coat colours were carefully noted. In addition, the percentage error rate for each phenotypic group (bay, dark bay, dun, and black) was calculated. This rate was determined by dividing the number of animals with misclassified coat colours by the total number of horses in the respective group.

Results

Genotyping of *TBX3* gene variants, including the 1.6 kb indel polymorphism and the *D/nd1*-related SNP, was carefully performed in a population of BMH. The result showed the

Table 1: The genotype frequencies of *TBX3* and *ASIP* in the Bosnian Mountain Horse population

	Genotype and allele frequencies												
	TBX3								***ASIP***				
Coat colour (classified by IABMHB)	***D/nd1***	***D/nd2***	***nd1/nd1***	***nd1/nd2***	***nd2/nd2***	***D***	***nd1***	***nd2***	***AA***	***Aa***	***aa***	***A***	***a***
Randomly sampled (n=80)	0.02	0.13	0.13	0.34	0.39	0.07	0.31	0.62	0.09	0.31	0.60	0.24	0.76
	All horses in this study (n=313)												
Bay (n=34)	0.03	0.00	0.09	0.18	0.71	0.02	0.19	0.80	0.29	0.71	0.00	0.64	0.36
Dark bay (n=138)	0.01	0.02	0.09	0.33	0.54	0.02	0.26	0.72	0.08	0.54	0.38	0.36	0.64
Black (n=115)	0.00	0.02	0.08	0.28	0.62	0.01	0.22	0.77	0.00	0.07	0.93	0.03	0.97
Dun (n=26)	0.08	0.73	0.04	0.15	0.00	0.41	0.15	0.46	0.04	0.15	0.81	0.12	0.88

IABMHB = International Association Of Bosnian Mountain Horse Breeders; *TBX3* = the T-box 3 gene; *ASIP* = the agouti signalling protein gene; *D* = dominant *Dun* allele (*TBX3*); *nd1* = recessive *non-dun 1* allele (*TBX3*); *nd2* = recessive *non-dun 2* allele (*TBX3*); *A* = dominant allele (*ASIP*); *a* = recessive allele (*ASIP*).

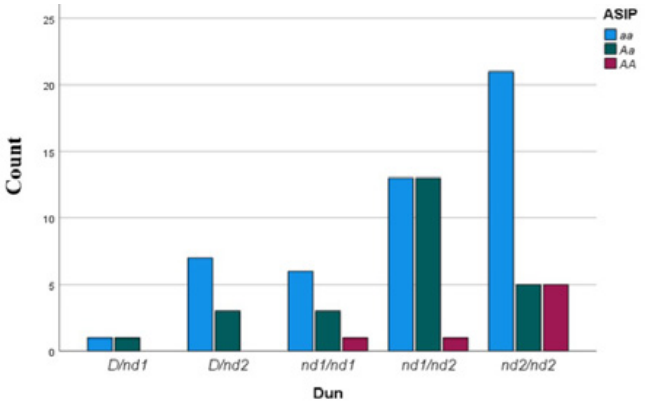

Figure 1: Comparison between *TBX3* and *ASIP* genotypes in a randomly selected population of the Bosnian Mountain Horse (BMH)

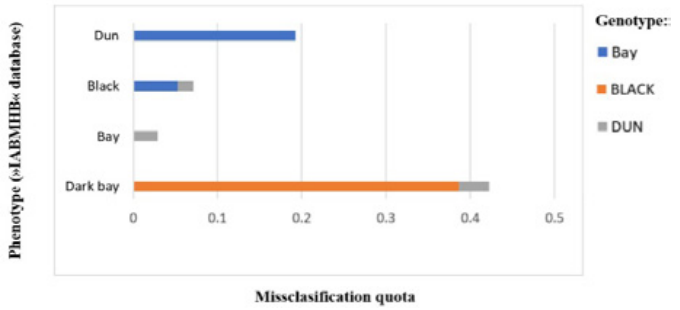

Figure 2: Misidentified coat colours within the phenotypic classifications in the BMH (IABMHB = International Association of Bosnian Mountain Horse Breeders)

presence of five of the six possible genotypes, with *nd2/nd2* having the highest frequency (0.39), while *D/nd1* had the lowest frequency (0.02) (Table 1).

Of note, the frequency of the *D* was determined to be 0.07, while the frequencies of *nd1* and *nd2* were 0.31 and 0.62, respectively. As for *ASIP* genotype frequencies, the distribution was as follows: *AA* - 0.09; *Aa* - 0.31 and *aa* - 0.60. Of the total data set of 313 genotyped horses, 29 animals (9.2%) were heterozygous for the *D* locus, while none of the horse's showed homozygosity. Interestingly, a higher frequency of the heterozygous *D/nd2* genotype was observed within the group of Dun horses, with a sixfold higher compared to the *D/nd1* genotype.

Genotyping of the 11 bp *ASIP* indel polymorphism, which is responsible for the bay base coat colour (Rieder et al. 2001), within the above-mentioned group of 80 randomly selected BMH individuals revealed that 40 % of the horses possessed the genotype *AA* or *Aa*, indicating that their genetic base colour is bay (Figure 1).

Comparison between *ASIP* and the *TBX3* gene yielded several interesting results regarding the *TBX3* genotype in a randomly selected group of BMH. When the combined genotypes of *TBX3* and *ASIP* were considered together, beneficial genotype combinations associated with different coat colours were identified (as shown in Figure 1).

Horses with dun-coloured coats had two genotype combinations: *D/nd1 - D/nd2*. Within this group, *ASIP* genotype combinations were observed: *aa* (1 and 7 horses) and *Aa* (1 and 3 horses), respectively. In contrast, three genotype combinations were observed in the non-coloured horses: *nd1/nd1*, *nd1/nd2* and *nd2/nd2*. These genotype combinations were associated with the three *ASIP* genotype combinations *aa* (6 and 13 horses), *Aa* (3 and 13 horses) and *AA* (1 and 1 horse, respectively). In particular, horses with the *nd2/nd2* genotype had the following *ASIP* genotype combinations: *aa* (21 horses), *Aa* (5 horses) and *AA* (5 horses) (Figure 1).

The population of BMH included individuals with different coat colours. The distribution of coat colours within the population was as follows: dark bay (138 horses, representing 44% of the population), black (115 horses, 36%), bay (34 horses, 11%) and dun (26 horses, 8%). When comparing the obtained genotypes with the recorded coat colour descriptions from the IABMHB database, remarkable inconsistencies were found, especially with regard to the dun dilution effect. About 2.9 % of the horses originally described as bay (including all shades) turned out to be genetically bay dun (Figure 2). Similarly, about 1.8 % of black horses were genetically identified as blue dun possessing at least one copy of the dominant *D* allele. However, within this relatively small sample, the majority of dun horses (85%) were correctly classified (Figure 2). It was also found that in 54 cases horses that were genetically black (with genotype *aa* in the *ASIP* gene and without the dominant allele *D*) were incorrectly classified as dark bay.

Discussion

In the breeding of BMH, coat colour is of great importance as a breeding objective. Breeding practises within the BMH population have led to a strong trend towards the use of dark stallions. As a result, approximately 81% of the BMH population consists of horses with black or dark bay coat colours. This preference for dark coat colour has influenced by the higher frequency of the recessive a allele at the Agouti locus. Similar high estimated frequencies for the recessive a allele at the Agouti locus have also been observed in several other horse breeds (19-23). The high frequency of the A/a genotype observed in the BMH horses for bay coat colour may reflect the breed's preference for a darker coat colour over lighter shades such as light bay, which are rare. In a recent association study, Corbin et al. (2020) confirmed the findings of a correlation between genotype *A/a* at the Agouti locus and genotype *E/E* at the Extension locus, especially in relation to the presence of dark shades of bay (24-27). The BMH breed is believed to have a similar origin as it is probably descended from the Tarpan, which was found in Europe and Asia until its extinction at the end of the 18th century (6, 9). We genotyped a large number of

Figure 3: Dun phenotype classification categories (IABMHB; first line: bay dun, dark blue dun; second line: dark bay, dark bay) and *TBX3* and *ASIP* genotypes (Fotos Matjaž Mesarič)

BMH for the *TBX3* gene Dun variant and found that it was not homozygous in any of the 313 horses. The low frequency of the *D* allele is a result of the long history of selection for the dark base coat colour in BMH. Through analysis of successive studbook volumes and previous studies using pedigree information, it has been documented that the incidence of BMH with coat colour diluted by the *Dun* gene has been consistently low (8, 9, 28, 29). Despite the ancestral nature of dun pigmentation, the overall frequency of the *D* allele in BMH has declined over time due to the preference for undiluted coat colours in the BMH studbook. However, our study has shown that the actual frequency of the dominant *D* allele in the *TBX3* gene is higher than predicted by Mesarič et al. (2015) based on the information recorded in the studbooks (0.09 and 0.03, respectively). One of the results of our study was the absence of the *AA* genotype at the agouti locus in individuals from the reference group with *D* allele at the dun locus, while an increased *AA* frequency was observed in the *nd2*/*nd2* genotype.

In the group of dark-coloured Dun horses, the frequency of individuals with a bay or light bay base coat is relatively low. During the emergence of BMH breeding, there was a strong preference for the use of the dark non-dun stallions, as darker horses were preferred by the Yugoslav army. The *D* allele has been maintained only among specific mare families, predominantly in the genotype *D/nd2*, which represents a darker shade of colour as in the Hucul and Polish primitive horse breed (11, 13). This trend in BMH breeding confirms the study by Cieslak et al. (2021), which indicates that the majority of the original dark Polish horses were *D/nd2* heterozygous and that mating dark individuals increased the probability of producing black offspring.

A comparison of *Dun/non-dun* allele frequencies between our study and previously published studies on Huculs (11,23) and Konik horses (13) shows clear differences. The population of BMH has a relatively high frequency of the *nd1* allele, reaching a value of 0.31, and a high frequency of the *nd2* allele (0.62). In comparison, the overall frequency of the *nd1* allele calculated in the study by Imsland et al. (2016) for 1.841 horses of different breeds was twice as low (0.18) as that determined in our study. This suggests that in the BMH breed, the *nd2* allele is subject to strong positive selection, while the *nd1* allele contributes to the presence of a diverse range of coat colours and primitive markings. Similar to Ezoe et al. (2019), who genotyped *TBX3* gene variants in four horse populations from Kazakhstan, Laos, Nepal and Vietnam, we also observed the presence of five possible genotypes, with the exception of the *D/D*. The *nd1*

allele was found in high frequency in Iberian horses (0.97 - PRE, 0.87 - Andalusian, 0.57 - Lusitano) as well as in the Arabian (0.68) (20).

Interestingly, the observed high frequency of the *nd1* allele in the BMH population might be similar to the genetic composition found in the ancestral population of wild horses that contributed to the process of domestication or might be influenced by Arabian horses brought to Bosnia with the Turkish invasion and later by the Austro-Hungarian Empire (8, 15). It should be noted, however, that the original allele distribution in the BMH breed was probably greatly affected by the bottleneck event during World War II and later during the Yugoslav Wars, as only a very limited number of founders survived (6).

Within the population of animals evaluated, we encountered several cases where genetically black or bay individuals were misclassified by the inspectors of the IABMHBA. Surprisingly, the number of discrepancies between molecular and phenotypic data exceeded our expectations and was comparable to previous records for Hucul breeds maintained in Poland (11). These discrepancies can be attributed to various genetic factors, such as the high frequency of *nd1*/*nd1* and *nd1*/*nd2* genotypes in the BMH breed. Therefore, we assume that carriers of the *nd1*/*nd1* and *nd1*/*nd2* genotypes have an 'intermediate' phenotype, showing traits that lie between fully diluted and non-diluted coat (Figure 3). The influence of *nd1*, along with individual factors such as age, season, *ASIP* and *MC1R* genotype, can be a challenge in accurately determining a horse's coat colour. An additional complication in visually distinguishing phenotypes may arise from an independent locus upstream of the *ASIP* gene, which has recently been identified as a factor that can subtly alter the pigmentation shade of dark colours (22). This can lead to the common nomenclatural problems in coat colour classification, as animals with such traits can be visually classified as 'non-dun' even though they show subtle signs of dilution in their coats. In our study, we found that some individuals with *nd1*/*nd1* or *nd1*/*nd2* genotypes were incorrectly assigned to the dun group.

Conclusions

We have observed and confirmed selection for dark basic coat colours in the BMH, as evidenced by the low frequency of the dominant *A* allele in the *ASIP* gene and the relatively higher frequency of the recessive *a* allele. In this study, we have shown that the *D* allele segregates at low frequency in the BMH population, while the *nd1* allele is present at high frequency. We confirm that due to the complex molecular background found within the coat colour genes in the BMH the correct assignation of particular coat colour can be challenging. Our study represents the first comprehensive investigation of the genetic background underlying coat colour in BMH and provides valuable insights into the phenotypic effects of Dun dilution. The results underline the importance of studying indigenous horse breeds as they contribute significantly to our understanding of the genetic basis of coat colour variation in horses.

Acknowledgements

The authors would like to thank the International Association of Bosnian Mountain Horse Breeders for their approval of the study, financial support and cooperation in carrying it out.

Bosnian mountain horse hair samples were collected as part of routine procedures during studbook registration of horses by the International Association of Bosnian Mountain Horse Breeders and the Institute for Breeding and Health Care of Horses at the Faculty of Veterinary Medicine in Ljubljana.

Author's contribution: Cotman Marko, DNA extraction and genotyping, writing, fundraising; Mesarič Matjaž, conceptualisation, sampling, data collection, data analysis, writing - original draft, Kotiščak Jelena, data analysis; all authors: reading, commenting and reviewing the final draft manuscript.

None of the authors has a conflict of interest.

Fundation. This work was financially supported by the Slovenian Research Agency program P4-0053 to M. Cotman.

References

1. Bellone RR, Avila F. Genetic testing in the horse. Vet Clin North Am Equine Pract 2020; 36: 211–34.
2. Hrasnica F. Prilog poznavanja boja dlake bijelih i tamnih znakova i njihova nasleđivanja kod konja. I dio. Zagreb: Poljoprivredna naučna smotra, 1946; 9: 165–82
3. Hrasnica F. Prilog poznavanja boja dlake bijelih i tamnih znakova i njihova nasleđivanja kod konja. II dio. Zagreb: Poljoprivredna naučna smotra, 1948; 10: 183–208
4. Bellone RR. Pleiotropic effects of pigmentation genes in horses. Anim Genet 2010; 41: 100–10.
5. Sponenberg DP, Bellone R. Equine colour genetics. 4th ed. Hoboken: Wiley Blackwell, 2017.
6. Mesarič, M. Barve konj: genetska osnova, opis in klasifikacija barv pri konjih. Podkum: Mednarodno združenje rejcev bosanskih planinskih konj, 2020.
7. Marín Navas, Delgado Bermejo JV, McLean AK, León Jurado JM, Torres ARBYR, Navas González FJ. One hundred years of coat colour influences on genetic diversity in the process of development of a composite horse breed. Vet Sci 2022; 9: 68. doi: 10.3390/vetsci9020068

8. Mesarič M, Dolinšek A, Dovč P. Bosanski planinski konj: najstarejša avtohtona pasma na Balkanu v izumiranju = Bosnian mountain horse: the oldest indigenous breed in the Balkans facing extinction. Rtiče: Planido - A. & A., 2015.

9. Hrasnica F. Beiträge zur Kenntnis der Streifhung beim bosnischen Gebirgspferde. Z.f. u Züchtungsbiolog. 1938; 41(3): 15–8.

10. Mesarič, M, Dolinšek, A, Žiga, E. Regeln und Anforderungen für reinrassige Bosnische Gebirgspferde im Internationalen Zuchtbuch der Bosnischen Gebirgspferde (IBMHSB). Rtiče: International association of Bosnian horse breeders, 2018.

11. Mackowski M, Wodas L, Brooks SA, Cieslak J. TBX3 and ASIP genotypes reveal discrepancies in officially recorded coat colours of Hutsul horses. Animal 2019; 13:1811–6. doi: 10.1017/S1751731118003506

12. Stefaniuk-Szmukier M, Ropka-Molik K, Piórkowska K et al. Variation in TBX3 gene region in Dun coat colour Polish Konik horses. J Equine Vet Sci. 2017; 49:60–2. doi: 10.1016/j.jevs.2016.10.003

13. Cieslak J, Brooks SA, Wodas L, et al. Genetic background of the Polish Primitive Horse (Konik) coat colour variation – new insight into Dun dilution phenotypic effect. J Hered 2021; 112: 436–42. doi: 10.1093/jhered/esab034

14. Ludwig A, Pruvost M, Reissmann M, et al. Coat colour variation at the beginning of horse domestication. Science 2009; 324(5926): 485. doi: 10.1126/science.1172750

15. Imsland F, McGowan K, Rubin CJ, et al. Regulatory mutations in TBX3 disrupt asymmetric hair pigmentation that underlies Dun camouflage colour in horses. Nat Genet 2016; 48: 152–8. doi: 10.1038/ng.3475

16. Pruvost M, Bellone R, Benecke N, et al. Genotypes of predomestic horses match phenotypes painted in Paleolithic works of cave art. Proc Natl Acad Sci 2011; 108: 18626–30.

17. Cotman, M, Mesarič, M. A simplified dual real-time PCR method for detection of dun coat colour allele in horse. In: Proceedings of Genetika 2022. Ljubljana: Genetic society of Slovenia, 2022: 28–30.

18. Koressaar T, Remm M. Enhancements and modifications of primer design program Primer3. Bioinformatics 2007; 23: 1289–91. doi: 10.1093/bioinformatics/btm091

19. Nakamura K, Tozaki T, Kakoi H, Owada S, Takasu M. Variation in the MC1R, ASIP, and MATP genes responsible for coat colour in Kiso horse as determined by SNaPshot™ genotyping. J Vet Med Sci 2019; 81: 100–2. doi: 10.1292/jvms.18-0458

20. Avila F, Hughes SS, Magdesian KG, Penedo MCT, Bellone RR. Breed distribution and allele frequencies of base coat colour, dilution and white patterning variants across 28 horse breeds. Genes (Basel). 2022; 13(9): 1641. doi: 10.3390/genes13091641

21. Reissmann M, Musa L, Zakizadeh S, Ludwig A. Distribution of coat-colour-associated alleles in the domestic horse population and Przewalski's horse. J Appl Genetics 2016; 57: 519–25. doi: 10.1007/s13353-016-0352-7

22. Corbin LJ, Pope J, Sanson J, et al. An independent locus upstream of ASIP controls variation in the shade of the bay coat colour in horses. Genes (Basel) 2020; 11: 606. doi: 10.3390/genes11060606

23. Stachurska A, Brodacki A, Grabowska J. Allele frequency in loci which control coat colours in Hutsul horse population. Czech J Anim Sci 2012; 57: 178–86. doi:10.17221/107/2018-CJAS

24. Rieder S, Taourit S, Mariat D, Langlois B , Guérin G. Mutations in the agouti (ASIP), the extension (MC1R), and the brown (TYRP1) loci and their association to coat colour phenotypes in horses (Equus caballus). Mamm Genome 2001; 12: 450–5.

25. Sakamoto T, Fawcett JA, Innan H. Evaluating the potential roles of the Gray and Extension loci in the coat coloration of Thoroughbred racing horses. J Equine Sci 2017; 28: 61–5. doi: 10.1294/jes.28.61

26. Druml T, Grilz-Seger G, Horna M, Brem G. Discriminant analysis of colour measurements reveals allele dosage effect of ASIP/MC1R in bay horses. Czech J Anim Sci 2018; 63: 347–55. doi: 10.17221/105/2017-CJAS

27. Grilz-Seger G, Mesarič M, Brem G, Cotman M. Characterisation of coat colour in the Slovenian Posavje horse. Slov Vet Res 2021; 58: 77–84. doi: https://doi.org/10.26873/SVR-1091-2020

28. Belić J. Prilog poznavanju eksterijera bosanskog tovarnog konja. Arh Min poj, Beograd, 1940, zvezek 18.

29. Bartolović T. Prilog poznavanja osnovnih tipova bosanskog brdskog konja. Radovi poljuprivrednog fakulteta Sarajevo, 1961: 10(12): 49–98.

30. Ezoe H. Genetic diversity of coat colour related genes in Asian native horses. Master thesis. Okayama University, Japan, 2019.

Variabilnost genov *ASIP* in *DUN*, odgovornih za barvo dlake pri bosanskem planinskem konju

M. Cotman, J. Kotiščak, M. Mesarič

Izvleček: Določanje barv dlake pri bosanskem planinskem konju (BPK) je lahko izziv, ker obstajajo razlike v barvnih odtenkih dlake in več oblik redčenja barve dlake (plavci). Pri 313 konjih pasme BPK smo genotipizirali polimorfizme posameznih nukleotidov (SNP) znotraj dveh lokusov za barvo dlake T-box 3 (*TBX3*) in polimorfizma 11-bp indel znotraj Agouti signalnega proteina (*ASIP*). Posamezne genotipe smo nato primerjali z vpisanimi fenotipi barv dlake iz baze podatkov MZRBPK (Mednarodno združenje rejcev bosanskega planinskega konja). Ugotovljeno je bilo, da sta bili temna rjava in črna najbolj reprezentativni barvi dlake pri BPK. Pogostnost prevladujočega alela za redčenje *Dun* (*D*) v študiji je višja (0,09) od predhodno zabeležene v razpoložljivem registru BPK. Med ugotovljenimi aleli je prišlo do neskladja ali nedoslednosti med predvideno barvo dlake na podlagi genotipov in opazovano barvo dlake pri 73 konjih (23%). Najpogostejša napaka se je nanašala na napačno razvrstitev konjev z genotipoma *aa* in *Aa* v genu *ASIP*, *non-dun1/non-dun1* (*nd1/nd1*) in *non-dun1/non-dun2* (*nd1/nd2*) pri genu *TBX3*, kar je lahko povezano s pojavom redčenja barve dlake pri teh fenotipih.V nasprotju s pasmami Konik in Hucul pri BPK ni bila ugotovljena homozigotnost alela *D*. Alel *D* je mogoče zlahka spregledati ali ga ne prepoznati v različnih fenotipskih skupinah, kot so temni rjavci in vranci. Zato hipoteza, da učinki redčenja Dun (plavci) pri BPK sami po sebi niso tako močno epistatični, kot je to opisano pri drugih pasmah konj. Rezultati študije potrjujejo pomen molekularnega testiranja pri natančnem določanju barve dlake konj. To bi pripomoglo k preprečevanju napak pri opisih barve dlak v uradnih rejskih evidencah in pomembna informacija pri selekciji na posebne in želene barve dlake pri konjih.

Ključne besede: barva dlake konj; dun redčenje barve dlake; polimorfizem DNK; frekvenca alelov; frekvenca genotipa; bosanski planinski konj

Slovenian Veterinary Research
DOI 10.26873/SVR-1694-2023
UDC 599.742.71:616.12-089:616-089.853:303.824
Pages: 57–71

Case Report

Clinical and Diagnostic Imaging Findings in a Bengal Tiger (*Panthera tigris tigris*) With Craniocervical Artery Dissection: A Case Report

Key words

Bergeyella zoohelcum;
ischemic stroke;
subarachnoid haemorrhage;
tiger;
transient ischemic attack

Peyman Mohammad Zadeh[1]*, Nilufar Shadan[2], Sajjad Mohammadi[3], Fatemeh Najafi[3], Aida Bashiri[4]

[1]Department of Pathobiology, Sanandaj Branch, Islamic Azad University, Sanandaj, Iran, [2]Islamic Azad University, Shahrekord Branch, Shahrekord, Iran, [3]Islamic Azad University, Sanandaj Branch, Sanandaj, Iran, [4]Razi University, Kermanshah, Iran

***Corresponding author:** peymanpathologist@iausdj.ac.ir

Abstract: This study aims to examine different aspects of Craniocervical Artery Dissections, which resulted in the animal's death following a sequence of pathological events. Following the physical damage to the female Siberian tiger neck due to the Agonistic behaviour of the male tiger, diagnostic tests such as complete medical examination, Time-of-Flight (TOF) MRA imaging and radiography, as well as sampling for clinical assessment, haematology, microbial culture, and antibiogram was performed, initial treatment was prescribed, and PCR was performed. Unfortunately, the Medical treatment measures were inadequate, and the animal died. Therefore, necropsy, histopathological examination, and immunohistochemistry staining were performed. The results of the microbiological study included the identification of *Bergeyella zoohelcum* for the first time in this animal species, as well as diagnostic findings; necropsy and histological examinations, including aneurysm, subarachnoid haemorrhage, and ischemic stroke, were provided as well as Horner's intramural hematoma and rupture of the carotid arteries and internal jugular vein, which has never been described before. Whole-body trauma computed tomography with an adapted scanning protocol for the craniocervical vessels is a safe, fast, and feasible method for detecting vascular injuries. It allows prompt further treatment if necessary. This method could be a part of a broad screening protocol for craniocervical vessels in documented injuries of the head and neck and trauma mechanisms influencing the craniocervical region as well.

Received: 28 January 2023
Accepted: 5 July 2023

Introduction

The Royal Bengal Tiger belongs to the Feliformia suborder of the Carnivora order consisting of "cat-like" carnivorans. He belongs to a subspecies of *Panthera tigris tigris* that is exclusive to The Middle East and India (1). The white tiger, also known as the bleached tiger, is a pigmentation variant (leucistic) variety of Royal Bengal Tigers, Amur tigers, and a Crossbreed hybrid of the two that are occasionally seen in the wild in Indian states (2,3). Tigers are globally listed as "Endangered" on the International Union for the Conservation of Nature (IUCN) Red List of Threatened Species (4). The Malayan and Sumatran sub-species are listed as "Critically Endangered." Intraspecific lethal encounters, Illegal hunting, habitat degradation, and fragmentation are all threats to this species, which is expected to have less than 3890 wild individuals by the end of 2023. (5). Thus, Examining different life-threatening factors and the pattern of causing injuries in each can directly benefit Wildlife survival biologists and wildlife veterinarians (6). Among these life-threatening factors, the pattern and type of injuries in fatal encounters due to conflict remain unknown. Tigers have lethal encounters with each other for access to Hunting resources, mates, and parental care. The most important reasons for interference between tigers in the wild include: Fighting over territory because they are solitary and maintaining individual territories. Next is Fighting over mates because tigers have a Polygyny mating system. As

a result, this characteristic leads to competition between males for access to females. Also, Infanticide and cannibalism are seen in felines, including tigers. Mortality caused by Hostile male tigers can affect Proportionate regional distribution, demography, and reproductive success. Finally, the last item is, Sibling rivalry; whenever a female tiger has two offspring at once, there is the potential for sibling rivalry. Tiger's Sibling rivalry is aggressive and can result in siblicide. Nevertheless, in zoos, the fundamental causes of conflicts between tigers include human errors, accidental access to nearby shelters, behavioural and neurological problems such as zoochosis, and aggressive and stereotypic behaviour due to captivity. The chance to experience positive social interactions and mating are vital for captive tigers. However, if this experience is not managed and happens accidentally, it often leads to unfortunate results, and in most cases, it will lead to death. The result is often clear regardless of the reason for these deadly conflicts. Severe pathological injuries often lead to damage to the vital organs of the neck, multiple cranial lacerations, fractures, traumatic amputations, persistent neurological deficits and fracture-dislocation of cervical vertebrae, abrasions, and crushes secondary to the dragging of the victim's body.

This case report outlines the multiple sources of injury and pathology that can result from such an attack. The discussion focuses on the injury pattern seen in large feline attacks. We present a rare fatal case of a tiger attack on another tiger during the night hours while the male entered the female cage. These two tigers had a five-year-long relationship with each other, and the discovery of his death astonished the zoo administration. This case describes the necropsy findings emphasizing the distribution of injuries and the histopathological findings. The details of the Histopathological injury pattern and radiological findings have been discussed.

Materials and methods

Case presentation

A brutal fight between two tigers took place due to sexual coercion following the access of a male Bengal tiger (*Panthera tigris tigris*) to the night enclosure of a white Siberian tiger (*Amur tiger*) at the Eram Zoo in Tehran, Iran. After entering, the male tiger violently tries to mate (After being informed that the zoo keepers saw them in a sexual position), but the female did not allow it due to oestrus problems. As a result, the male tiger violently bites the neck of the female tiger later, and after being informed, the zoo keepers separate the two tigers. Initial treatment immediately began with taking the necessary measures, including irrigation of the affected area using sterile saline to reduce bacterial load. After 10 hours, and due to the symptoms of pain and restlessness, the animal was anaesthetized using a combination of Ketamine Hydrochloride (Bremer Pharma GMBH, 34414 Warburg, Germany) and Medetomidine Hydrochloride (Laboratorios syva s.a.u, Avda. Parroco Pablo Diez, 49-5724010 Leon, Spain) (K: 2.3mg/kg+M:0.9 mg/kg IM; antagonized by 0.23mg/kg IM Atipamezole (Laboratorios syva s.a.u, Avda. Parroco Pablo Diez, 49-5724010 Leon, Spain).

Clinical examinations and diagnostic imaging

During anaesthesia, the gross examination was performed; A thorough examination of the animal initially began with signalling and a complete description of the animal, including species, breed, age, gender, reproductive status, and other distinguishing characteristics were noted. Further, history, including environment, diet, medical history, fertility history, vaccination status, and current status, were evaluated. Hydration status is further expressed as a percentage of body weight (0-15%), which can be somewhat subjective, and it is reported as "adequate," "marginal," or "inadequate," which was insufficiently observed in the case of this animal. Next, the vital signs were checked, which included (a body weight of 215.3 kg) and a temperature (of 40.6, which is the usual range in tigers 37.8-39.4). Then, the rectal area was checked for signs of diarrhoea, parasites, and other abnormalities. The heart/pulse rate (56 to 97 bpm) was (109 bpm). Evaluation of pulse rate, strength, and quality was done in the form of thread. The next item was Respiratory rate and character with a typical range (8.4 ± 3.6), which was 10.3 in this tiger. Then the perfusion indices were checked, which included Mucous membrane colour (MM) and Capillary refill time (CRT), which was prolonged CRT (> 2 seconds) (Table1). The next step was the head and neck evaluation (EENT/Oral) which both sides of the face and head were checked for symmetry. Assess eyes for size, position, discharge – lids, conjunctiva, sclera, pupil, cornea, lens note discharge, inflammation, redness, uneven/abnormal pupil size, corneal clouding, squinting. The nose was evaluated and nares for symmetry, conformation, and evidence of discharge. The oral cavity was examined - lips, mucous membranes, teeth, hard and soft palate, tongue, pharynx, and tonsils. Carriage and position of ears were evaluated, and thickness/malleability of pinnae and cleanliness of ear canals, submandibular lymph nodes, and salivary glands (normally palpable) were palpated. The following parameter was Trunk and Limbs (INTEG, M/S, PLN) evaluation. The body for symmetry, masses, and tenderness was Inspected. Each limb and joint was palpated, and abnormalities in angulation, deformities, swelling, bleeding, bony protrusions, obvious fractures or joint luxations, range of motion, atrophy, knuckling, and crepitus were examined. Skin and hair coat was examined for alopecia, masses, parasites, dryness, excessive oil, and matting. The palpate pelvic region was palpated for conformation and symmetry. The vertebral column was palpated to assess for deviations and pain. Peripheral lymph nodes (PLN) were palpated: submandibular, prescapular, axillary, inguinal, and popliteal. Thorax was observed and palpated for conformation, symmetry, and masses. In cardiac auscultation (CV) and respiratory auscultation (RESP), we first listened for noisy

Table 1: Clinical examination findings

Clinical examinations	Value	References	Index
Hydration status	Moderate(w~8%)	Euhydrated (standard), Mild (w~5%), Minimal loss of skin turgor, semidry mucous membranes, normal eye. Moderate(w~8%) Moderate loss of skin turgor, dry mucous membranes, weak rapid pulses, enophthalmos. Severe (.>10%) Considerable loss of skin turgor, severe enophthalmos, tachycardia, extremely dry mucous membranes, weak/thread pulses, hypotension, altered level of consciousness	%
Vital signs			
Body weight	115.3 kg	110-130	kg
Temperature	40.6	37.8-39.4	C°
Heart/pulse rate	109	56 to 97	bpm
Respiratory rate	10.3	8.4 ± 3.6	bpm
Perfusion indices(CRT)	2.8	≤ 2 seconds	SE

breathing at the mouth and nares without a stethoscope. We auscultated at least four chest areas, including right and left ventral and right and left dorsal lung fields. We heard 'Rales/crackles.' then we examined the Abdomen (ABD) and inspected for distention, deformity, displacement, symmetry, and bruising and auscultated the abdomen to detect intestinal hypermotility or hypomotility. Then we Palpated and visually assessed mammary glands for tumours, cysts, swelling, heat, or discharge and Inspected the vulva for size, inflammation, discharge (blood, pus), polyps, tumours, or structural defects. In the final stage, we determined the appropriate RAC Score for the animal. The area between the fourth and sixth intercostal spaces on both sides of the thorax was Palpated for the point of maximum intensity (PMI) of the heartbeat and any cardiac thrills. Heart rate (HR) and rhythm were evaluated, and Sinus arrhythmia and muffled heart sounds were heard. Examination of the body showed signs of superficial scratches on the left arm and palm and swelling and inflammation in the neck. Therefore, the neck area was immediately inspected by Time-of-Flight (TOF) MRA, imaging, and radiography (Figures 1 and 2).

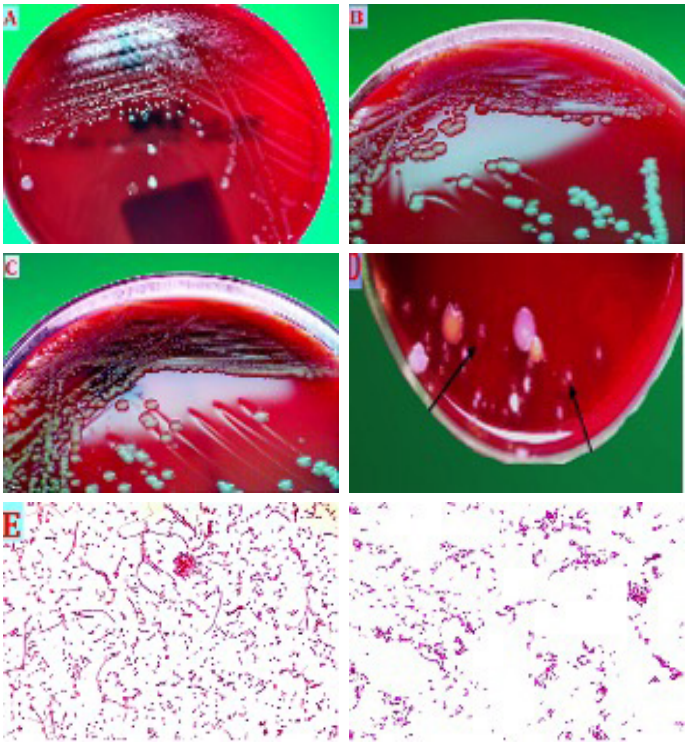

Figure 1: Morphological characterization of *Bergeyella (Weeksella) zoohelcum*. A, B: Bacterial colonies after culturing for 48 h on CBA (Columbia blood agar) (NCM0031A, Neogen ind., 620 Lesher Place Lansing, MI 48912 USA) C, D: colonies after culturing for 120 h on CBA. E: *Bergeyella (Weeksella) zoohelcum* staining properties. (gram staining, scale bar = 15 µm).F: *Bergeyella (Weeksella) zoohelcum* (acid stains quickly scale bar = 15 µm)

Sampling for clinical examination

At the same time of anaesthesia, chest and cervical X-rays, blood samples, and blood cultures were taken for clinical and microbiological evaluation (Figure 3). Empiric antimicrobial therapy was done using intravenous injection of Amoxirum Forte®300 mg (amoxicillin-sulbactam combination injectable antibiotic. Virbac, Pharmaceutical company, Carros, France), METACAM® (meloxicam, Boehringer Ingelheim. The pharmaceutical company, Ingelheim am Rhein, Germany)at the dosage (22 mg/kg), 0.2 mg/kg SC once then 0.1 mg/kg PO SID × 2d), and fluid therapy with Isotonic crystalloid solutions (lactated Ringer's solution plus dophalyte, Zoetis Pharmaceutical company, Parsippany-Troy Hills, New Jersey, United States)

Establishment of treatment protocol

After determining the results of haematology, microbiology, Time-of-Flight (TOF) MRA, imaging, and radiography and according to the antibiogram results, the initial treatment

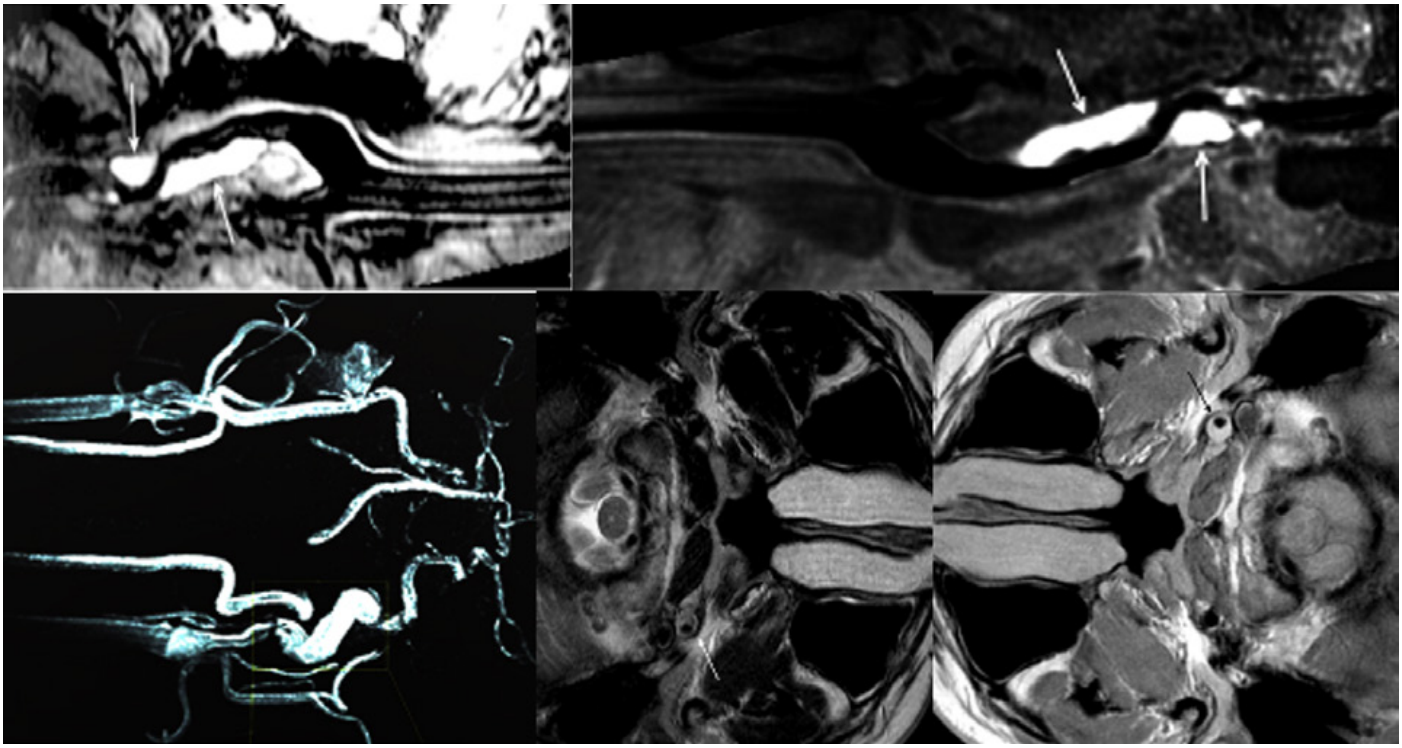

Figure 2: Unenhanced 2D TOF MRA of the craniocervical arteries: intra-cranial arteries 2D TOF (time-of-flight) demonstrates a patent left vertebral artery (major artery in the neck. It branches from the subclavian artery) (D). The MIP subvolume of the posterior circulation (consists of the two vertebral arteries, basilar artery, two posterior cerebral arteries, and their branches) (E) shows an irregular, stenotic mid-left vertebral artery initially felt to indicate a dissection. Axial reformatted source images show multiple small ring-shaped areas of signal severity corresponding to small cervical vessels (arrow, A). The interposition pattern created by these target patterns distorts the left vertebral artery that originates from the subclavian arteries, resulting in ill-defined or spiculated borders when compared with the right vertebral artery (Hitachi MRP 7000 MRI, Viable Med Services28470 Westinghouse Pl. Valencia, CA 91355)

process was confirmed. During the following days, the treatment was continued, and in order to facilitate the animal's breathing, after Wound Debridement, the tiger was intubated despite the concern about the exacerbated injury. Also, we use KENGREAL® (cangrelor) 30 mcg/kg IV bolus immediately followed by a four mcg/kg/min IV infusion to prevent blood coagulation. (The Medicines Company, Biotech company, Parsippany-Troy Hills, New Jersey, United States) for one week, then change to a dual therapy using Plavix® (clopidogrel) (18.75 mg PO q24h) (Bristol-Myers Squibb - Sanofi Pharmaceuticals, and XARELTO® (rivaroxaban) (2.5 mg PO q24h) (Janssen Pharmaceuticals, Inc., Beerse, Belgium) But Due to the severity of the injuries inflicted on the neck of the female tiger, the treatment was inconclusive. Twenty-eight days after causing the injury, the tiger died. After the death, a necropsy was performed, and all body organs were carefully inspected.

Genus identification of the isolate and genus-specific primers for the PCR identification

After receiving the initial microbiology results, to confirm the genus identification results of the isolate, PCR amplification of the 16S rRNA gene fragment by use of the primer set (forward primer 5'-AGA GTT TGA TCC TGG CTC AG-3' and reverse primer 5'-AAG GAG GTG ATC CAG CC-3') (Cat. Number: UN-PR001-005, Synbio Technologies,4250 US-1 Suite 3, Monmouth Junction, NJ 08852, United States) sequenced. Ribosomal RNA sequences were checked for the best match returned with the 16S-ribosomal rRNA gene database at NCBI.

Histopathology and immunohistochemistry techniques

In this study, depending on the conditions and needs, various diagnostic and immunohistochemical techniques were used as follows:

Verhoeff-Van Gieson (VVG) Staining Protocol

We used NovaUltra H&E Stain Kit (IHC-IW-3100) (Hölzel Diagnostika Handels GmbH, Germany) for this staining. First, we Deparaffinized and hydrated slides to distilled water. Then we Stained in Verhoeff's solution for 1 hour. The tissue should be completely black. After this step, we rinsed in tap water with 2-3 changes. Then we differentiated in 2% ferric chloride for 1-2 minutes. Moreover, Stop differentiation with several changes of tap water and check microscopically for black elastic fibre staining and grey background. It is better to slightly under-differentiate the tissue since the subsequent Van Gieson's counterstain can extract the elastic stain somewhat.

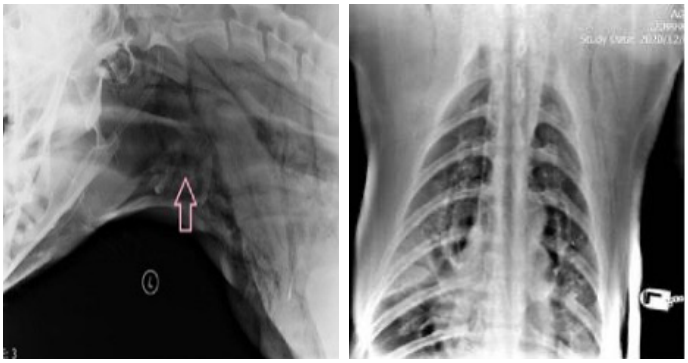

Figure 3: Neck and thorax radiography: Neck and thorax radiographic regions show significant amounts of gas density seen subcutaneously in the cervical region, which is extended up to the lateral aspect of the left thoracic wall—visibility of great vessels in the cranial mediastinum. The alveolar pattern, especially in the ventral aspects of lung lobes in the thoracic cavity, is noticeable. Lobar signs are also seen in the left middle lung lobe due to lobar consolidation. The presence of strip signs in the cervical region is probably secondary to gas densities within the oesophagus due to the anaesthesia process and respiratory distress. The diaphragm and rib cage are intact. No sign of pneumothorax is seen in the current radiographic examination (Veterinary X-ray system Maxivet 300 HF FF, COMES ELECTRO SRL, Via dell' Industria, 54 - 21044 Cavaria con Premezzo (VA) Italy).

Then we Washed slides in tap water. And then, we Treated it with 5% sodium thiosulfate for 1 minute and Discarded the solution. After this step, we washed in running tap water for 5 minutes. Moreover, we Counterstain in Van Gieson's solution for 3-5 minutes. Then we dehydrated quickly through 95% alcohol, two changes of 100% alcohol. Then we clear in 2 changes of xylene for 3 minutes each. And finally Coverslip with a resinous mounting medium

Immunohistochemistry Iba1 Antibody Staining Protocol

Iba1 (Allograft inflammatory factor 1 or ionized calcium-binding adapter molecule 1) is a 17-kDa EF-hand protein specifically expressed in macrophages and microglia and is upregulated during the activation of these cells.

Antigen retrieval (AR) method

Formic acid treatment: Free-floating tissue sections were incubated in 98% formic acid (EMD) inside closed 5 mL Eppendorf plastic tubes for 5 min at room temperature In a chemical fume hood, followed by removal for chemical waste disposal. The sections were immediately rinsed with room temperature ultrapure Type I water for 5 min, followed by two additional 5 min incubations in ultrapure Type I water.

Immunostaining

After antigen retrieval methods, free-floating Brain tissue sections were transferred to plastic mesh 70 µm cell strainers inserts (352350, BD Falcon, Franklin Lakes, New Jersey 07417, USA) and placed into six-well Cellstar plastic cell culture dishes (657-160, Greiner Bio-One North America, 4238 Capital Dr #7681, Monroe, NC 28110, United States) without lids for immunostaining. For immunostaining, slide-mounted sections were laid flat into a Prohisto slide staining container (Staining chamber StainTray™ Black lid, Sigma-Aldrich, St. Louis, Missouri, United States). All rinses and incubations were performed by placing the six-well plates of free-floating tissue onto a 55S Single Platform Shaker set at ten rocking motions per minute (Reliable Scientific, Inc., 1160 Thousand, Misty Oaks Ln, Hernando, MS 38632, United States). All free-floating or slide-mounted tissue sections were briefly washed in PBS for 5 min and then incubated with 0.3% H2O2 in PBS for 5 min at room temperature to inhibit endogenous peroxidase activity. A quick wash with PBS followed that for 5 min. For anti-Iba1 staining, free-floating tissue sections or slide-mounted tissue sections were blocked in PBS solution (PBS with 0.5% bovine serum albumin, BSA, 5% goat serum, and 0.1% Triton X-100) for one h, and then incubated in primary antibody in PBS solution (1:1000 anti-Iba1, rabbit polyclonal, 019-19741, Wako Pure Chemical Industries, Ltd, Wako Chemicals USA, Inc., Shibayagi Co., Ltd.,) overnight at four °C. After primary antibody incubation, the free-floating tissue or slide-mounted tissue sections were rinsed four times, 10 min each (with the PBS solution), then incubated with biotinylated anti-rabbit secondary antibody (1:2000, Vector Laboratories, Newark, California) for two h at room temperature. The secondary antibody was removed, and the free-floating tissue or slide-mounted tissue sections were rinsed four times with PBS solution and then incubated with PBS-Avidin-Biotin solution (2 µL each of solutions A and B per mL of PBS, Vectastain ABC kit, Vector Laboratories, Newark, California) for two h at room temperature. The free-floating tissue or slide-mounted tissue sections were rinsed four times with PBS only, then incubated for 5 min with a Vector VIP chromogen solution according to the manufacturer's instructions (Vector VIP peroxidase substrate kit, Violet SK-4600, Vector Laboratories, Newark, California) to develop the immunostains.

Immunohistochemical staining for glial fibrillary acidic protein (GFAP)

Glial fibrillary acidic protein (GFAP) is an astrocytic biomarker for the diagnosis, monitoring, and outcome prediction of acute brain ischemic stroke. GFAP is the major protein component of intermediate glial filaments, which increases within astrocytes in response to acute brain ischemic stroke. The slides were stained with a polyclonal rabbit GFAP antibody (GFAP Antibody (PA1-9565), Thermo Fisher Scientific, Waltham, Massachusetts, United States), dilution 1:4000, performed with a fully automated immunostainer (Oncore™ ProAutomated Slide Stainer from BIOCARE MEDICAL, 60 Berry Dr Pacheco, California 94553, United States) using DAB as the standard chromogen. After staining and preparing the slides under the microscope, characteristics such as nucleus morphology, nucleolus location, and cell borders were used to differentiate neurons from non-neuronal cells as established morphological criteria.

After the neurons' immunopositivity for GFAP was noted, the slides were stained analogously per immunolabelling and counterstained with hematoxylin.

Luxol Fast Blue–PAS staining

This method stains myelinated axons on formalin-fixed, paraffin-embedded brain tissue sections.

The myelin, including phospholipids, will be stained blue to green, and the neurons will be stained violet. To perform this procedure, we first Deparaffinize and hydrate sections to 95% ethyl alcohol, then we leave the sections in luxury fast blue solution overnight in a 58 C oven. Then we Rinse off excess stain with 95% ethyl alcohol and Rinse in distilled water. After this step, we differentiate the slides in the lithium carbonate solution for 45 seconds, then continue differentiation in the 70% ethyl alcohol for 40 seconds and rinse in distilled water. Then we Check the slides microscopically to see if the grey matter is straightforward and the white matter is sharply defined. Then we place the slides in distilled water and counterstain in the cresyl violet solution for 40-50 seconds. Then we rinse in distilled water and differentiate the slides in 95% ethyl alcohol for 4 minutes and 100% alcohol for 2x5 min, and xylene for 2x5 min. Finally, we mount with a resinous medium.

Results

Microbiology and blood biochemistry results

Bacteriological examination showed that catalase, urea, oxidase, and indol tests were positive, and Deoxyribonuclease (DNase) and Pyrrolidonyl Arylamidase (PYR) tests were negative. Initially, the isolate was misidentified as Bergeyella porcorum ATCC type strain 1350-03 by The MicroSEQ Rapid Microbial Identification System with Applied Biosystems™ components—only 83.2% identity (Thermo Fisher Scientific, Waltham, Massachusetts, United States). However, after the PCR, the results indicated the *Bergeyella zoohelcum*, ATCC 43767 type strain, with 97.9% identity. In contrast, the next best match was the Riemerella columbipharyngis, ATCC 8151 strain, with only 90.8% identity. Although, According to the principle of the extended phenotype, the identity algorithm of The Clinical & Laboratory Standards Institute guideline Anti-PD-1 Mouse Monoclonal Antibody (APC) (10377-MM18-A), about glucose non-fermenting Gram-negative bacilli, the 98.9% identity of this *Bergeyella zoohelcum* strain was lower than the requirement of ≥99.0% identity (With >0.7% allopatric speciation); In general, both based on the biological data obtained and based on the results of gene bank similarity measurement for 16S rRNA gene sequencing data supported the identification of *B. zoohelcum*. Weak growth of *Bergeyella zoohelcum*, ATCC 43767 was observed on CBA (Columbia blood agar) (NCM0031A, Neogen and., 620 Lesher Place Lansing, MI 48912 USA) after 48 h of incubation at 37°C. The stained strain was gram-negative, oxidase, and indole-positive (Figure 1).

This study is the first officially recorded finding of this bacterium in this animal species. Aerobic cultures from the wound surface tissue grew Pasteurella multocida, *Bergeyella* (*Weeksella*) *zoohelcum*, and two other gram-negative bacilli. These were subsequently identified as most as CDC group EF-4b and common species by the Tehran University Laboratory for Bacteriology, Veterinary Laboratory Centre for Disease Control in Tehran, Iran, based on cellular fatty acid composition data and biochemical reactions. Also, blood biochemistry findings are given in Table 2.

Results of the diagnostic imaging

According to the radiological observations, the Initial diagnosis was "open wound and subcutaneous emphysema" that was probably associated with an infective process in the cervical region and *pneumomediastinum*. Moreover, because we could not rule out the possibility of tracheal perforation in plain radiographs, the neck area was inspected by Time-of-Flight (TOF) MRA, imaging, and radiography (Figures 2 and 3).

Necropsy findings

The applied necropsy techniques enabled us to demonstrate the compound mechanism that inflicted them, combining penetration of tissues by the canines, crushing, and distension. Analyzing these wounds might reveal the motivation behind the injuries and the wild cat species involved in the attack. A tiger injury is sometimes compared with a scalpel injury, as multiple penetrating, scalpel-like ulcers characterize the patterned injuries due to a tiger bite. As a result, special attention is paid to determining the cause of death from bites by animal teeth under unknown trauma circumstances.

Gross Necropsy Findings in the Head and Nec

Traces of claws and tiger canine teeth indicate that the victim female tiger of the attack was knocked down from the ventral surface, along with profound and multifocal fatal wounds to the cervical region. The neck area was crushed due to the pressure caused by the force of the fangs (transfixing ulcer) and was violently expanded. In this area and on the skin, there were six deep and blunt wounds and traces of fangs. The cervical area indicated massive damage, including tearing the oesophagus, trachea, and muscles, and inflammation of vertebrae C1 and C4 with internal channels resulting directly from penetration by the tiger's fangs. The expansion of the muscles happened because of the vigorous movements of the male tiger's head while trying to suffocate the female tiger, which led to the rupture of vertebral arteries.

Table 2: Haematological and biochemical results. (41)

Parameters	Result	Reference	Parameters	Result	Reference
Glucose (mg/dL)	127	88-183	AST (IU/L)	370	14.4–84.0
Triglyceride (mg/dL)	110	25-165	ALT (IU/L)	46	21.2–109.0
Cholesterol (mg/dL)	176	77 - 253	ALP (IU/L)	13	13 - 71
Albumin (g/dL)	3.83	2.1–4.6	GGT (IU/L)	3.5	1-10
Total protein (g/dL)	6.5	3.7–8.7	CK (IU/L)	5903	69 - 893
Globulin (g/dL)	5.3	2.8 - 4.8	Amylase (IU/L)	585	100-1200
A/G	0.7	0.8–1.00	Lipase (IU/L)	11	10-450
Urea (mg/dL)	187.3	5.50–27.70	Total bilirubin (mg/dL)	4.9	0.4–3.2
BUN (mg/dL)	87.52	6.5–48.2	Direct bilirubin (mg/dL)	3.69	0.09-1.9
Creatinine (mg/dL)	7.2	1.6–4.6	Calcium (mg/dL)	13.1	7.53-14.7
Phosphorus (mg/dL)	28.6	2.2 - 5.5	Uric acid (mg/dL)	1.2	0.32-1.8
HCT (%)	57.2	34 - 48*	PLT (%)	0.09	0.07-1
RBC ($\times 10^6$/µL)	7.51	7.5 - 11.7	MPV (fL)	11.4	10-12
HGB (g/dL)	13.5	11.5 - 15.9	NCC^ ($\times 10^3$/µL)	9.1	8-10
MCV (fL)	52.3	36 - 46	Segs ($\times 10^3$/µL)	4.43	4-5
MCH (pg)	19	12.5 - 16.4	Bands ($\times 10^3$/µL)	3.91	0.0 - 4.0
MCHC (g/dL)	36.3	32.2 - 36.8*	Lymphs ($\times 10^3$/µL)	0.27	1.05 - 8
PLT ($\times 10^3$/µL)	168	169 - 480	Monos ($\times 10^3$/µL)	0.18	0.1 - 0.3
RDW-CV (%)	14.8	12-16	Eos ($\times 10^3$/µL)	0	0.2 - 1.1
RDW-SD (fL)	31.4	30-34	Baso ($\times 10^3$/µL)	0	0-4
D-dimer	1673	< 250 ng/ml	blood FDP	35	10 (µg/ml)

A/G = albumin/globulin ratio, ALP= Alkaline phosphatase, ALT= Alanine transaminase, AST= Aspartate transaminase, Bands= Band Cells, Bso= Basophils, BUN= Blood Urea Nitrogen, CGT = Gamma-Glutamyltransferase, CK = Creatine Kinase, Eos = Eosinophils, Fl = femtoliter, g/dL= Grams Per Deciliter, HCT= Hematocrit, HGB= Hemoglobin, IU/L= International Units Per Liter, Lymphs = Lymphocytes, MCH = Mean corpuscular haemoglobin, MCHC =Mean Corpuscular Hemoglobin Concentration MCV = Mean Corpuscular Volume, mg/dL= Milligrams per decilitre, Monos= Monocytes, MPV=Mean platelet volume, NCC= Nucleated cell counts, pg = pictogram, PLT = platelets, RBC = Red Blood Cell, RDW-SD = Red Cell Distribution Width Standard deviation, RDW-CV= Red Cell Distribution Width Coefficient of variation, Segs= Neutrophils, µL=microliter FDP= Fibrin Degradation Products. D-dimer(a fibrin degradation product, a small protein fragment in the blood after a blood clot is degraded by fibrinolysis).

Moreover, an intramural rupture of the carotid arteries during the tiger's battle has never been described. Therefore, a detailed necropsy was performed to evaluate the amount of bone damage and the injury to the spinal canal. The applied necropsy techniques enabled us to demonstrate the compound mechanism that inflicted them, combining penetration of tissues by the canines, crushing, and distension. Analyzing these wounds might reveal the motivation behind the injuries and the wild cat species involved in the attack.

A tiger injury is sometimes compared with a scalpel injury, as multiple penetrating, scalpel-like ulcers characterize the patterned injuries due to a tiger bite. As a result, special attention is paid to determining the cause of death from bites by animal teeth under unknown trauma circumstances.

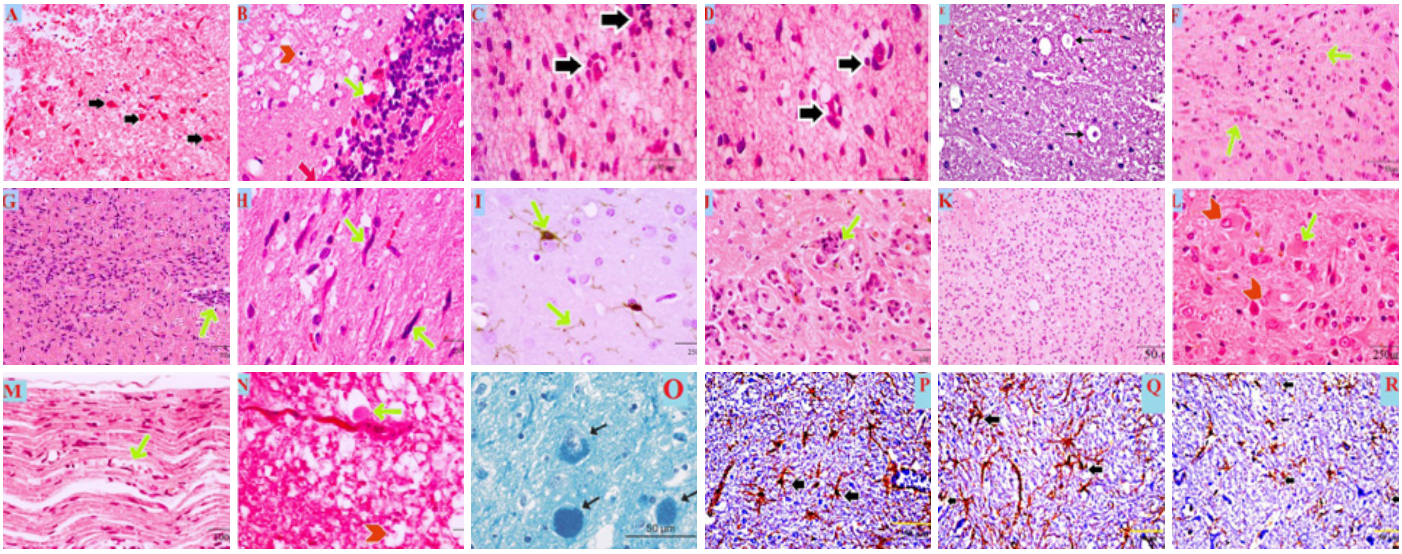

Figure 4: Cerebral Parenchyma Histopathological changes in transient ischemic attack A: red neurons (Yellow Arrows). (Hematoxylin and Eosin Staining, Scale Bar=μm). B: red neurons (Yellow Arrows), normal neuron (Pink Arrow), and pyknotic nucleus along with vacuolation of the neuropil(Red Head Arrow).C&D: perineuronal satellitosis, increase in the number of cells encircling a neuron(Yellow Arrows). (B, C, D: Hematoxylin and Eosin Staining, Scale Bar=100μm). E: Swollen and degenerated axons without myelin sheath are seen. (Yellow Arrows),F: A bubble-like biological feature(Axonal spheroid) is seen in the degenerated axon(Yellow Arrows). G: Various irregular, elongated nuclei of microglial cells formed as a Microgliosis near the inflammatory mononuclear perivascular cuffing (Yellow Arrow). (E, F, G: Hematoxylin and Eosin Staining, Scale Bar=50μm). H: irregular nuclear of microglial cells (Yellow Arrows). (H: Hematoxylin and Eosin Staining, Scale Bar=250μm). I: Immunohistochemical staining using Iba-1 antibody to visualize microglial cells(Yellow Arrows). J: Reactive gliosis and Hyperplastic capillaries (Yellow Arrow). (I,J:Iba1 Antibody Staining, Scale Bar: I=250μm,J=100 μm) K: Increase in nucleated cells Consisting of reactive astrocytes, macrophages, and mixed gliotic response. L: Reactive gemistocytes astrocytosis. Eccentric nucleus, prominent eosinophilic cytoplasm of reactive astrocytes (Red Head Arrows), and the less frequent micro-binucleate (Yellow Arrow). M: Wallerian degeneration(axonal fragmentation) (Axonal spheroid). N: A large swollen axon (pre-degenerative changes) and a degenerate macrophage in the necrotic axon space. (K, L, M, N: Hematoxylin and Eosin Staining, Scale Bar: K=50μm, L= 250μm, M=100 μm, N= 250μm).O: cerebrum: Intracytoplasmic Luxol fast blue positive pigments are seen in the neurons. (Black Arrows)(Luxol fast blue staining, Scale Bar=50μm). P: Short cytoplasmic processes of the astrocytes(Black Arrows). Q: Brown cytoplasmic granules in the neuroplastic astrocytes(Black Arrows). R: Degenerating and dead Astrocytes are seen. (Black Arrows). (P, Q, R: glial fibrillary acidic protein (GFAP) Staining, Scale Bar=50μm).

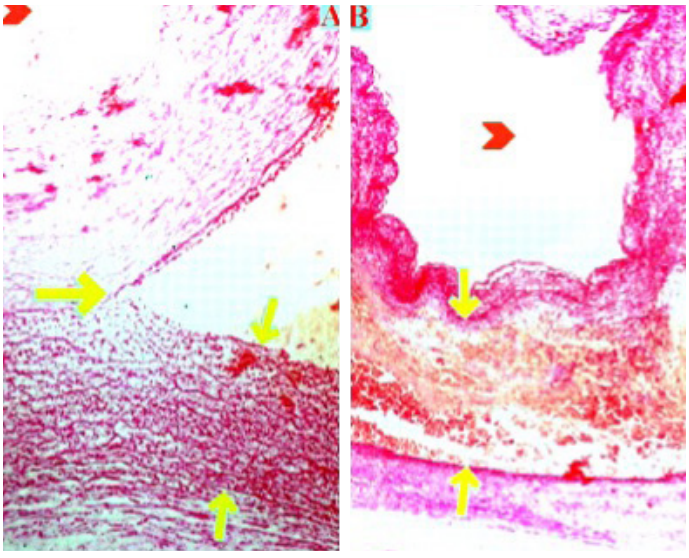

Figure 5: Intramural hematoma of the mid-left vertebral artery(major artery in the neck branches from the subclavian artery) (A) the arterial wall zipper-like separation, mucoid degeneration, and false lumen of the tunica media (Yellow arrows). (B) A cross-section of the dissected artery shows intermedial and subintimal hematoma (Yellow arrows). Red Head Arrow (lumen); Elastica van Gieson staining NovaUltra H&E Stain Kit (IHC-IW-3100)(Hölzel Diagnostika Handels GmbH, Germany), scale bar = 0.25 mm

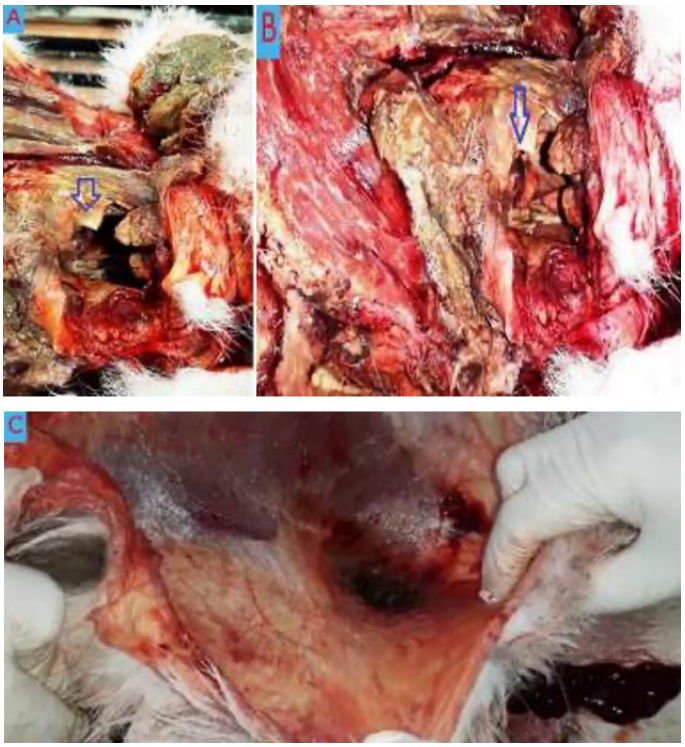

Figure 6: A and B: Complete rupture of the trachea. C: Skin blunt trauma

Brain

Red neurons appear in the earliest phase of infarction, consisting of increasing cytoplasm eosinophilia with the nucleus shrunken and basophilic. Then the cytoplasm becomes uniformly structureless, and the nucleus shows homogeneous degeneration. In the late stage, the neurons are disintegrated, resulting in eosinophilic debris dispersed throughout the neuropil and scattered eccentrically from the remainder of the dead neurons. Later, all these remains were phagocytized by foamy macrophages (ghost neurons). Finally, eosinophilic ischemic neurons spread and disseminated among the normal-looking neurons and were surrounded by an increased number of oligodendrocytes (steatosis). Around dying neurons, the microglial cells retract their processes and assume an amoeboid morphology, becoming activated (Figure 4).

Cervical Part

In the cervical region necropsy, complete rupture of the trachea was observed from two places (connection to the larynx) and 3 cm below it, as well as lateral and vertical rupture of the oesophagus with a length of 5 cm and rupture of the left subclavian artery, left vertebral artery, left common carotid artery. The rupture of these arteries led to extensive extravasation at the back of the throat and larynx (Figure 5).

Extensive adhesions and focal necrosis were also observed in the pectoralis area and on the *pectoantebrachialis*, *sternomastoid*, and *pectoantebrachialis* muscles that continued until the beginning of the *xiphihumeralis* area, which was filled with exudative and mucoproliferative secretions and a prominent inflammatory infiltrate into the subcutaneous space. Examination of the internal organs of the lungs revealed extensive pneumonia in both lungs, the development of interstitial bronchopneumonia and marbled of the lungs, and the effect of the ribs on the lungs due to pressure in the thoracic region. Lung tissue was full of foamy discharge due to weather and severe respiratory distress (Figure 6).

Pathological injuries, longitudinal tears, thinning, and loss of elastic fibres are well-defined using Verhoeff-Van Gieson elastic staining. This staining is a simple method that is used for visualizing elastic fibres.

Postmortem examination of the Thoracic Cavity

Trachea

Squamous metaplasia in the trachea epithelium with intense chronic inflammation visible in the submucosa, including cicatrization. The underlying cartilage indicated sequestration along with ossific metaplasia. By far, the most pathological changes included diffuse paracellular or hyperplastic fibrosis with intense hyperplastic scar formation or hyaline cicatrization found in the outer part of the perichondrium overlying adventitia. In the membranous portion, severe scar formation and hyperplastic fibrosis were predominant. Metaplastic pulmonary ossification was exclusively severe in the outer and lateral parts of the tracheal ring, particularly in the vicinity of the adventitia and outer perichondrium (a layer of dense irregular connective tissue). These changes were much more pronounced than the relatively minor changes observed in the mucosa and submucosa (Figure 7).

Lung

The pathophysiology of this injury was blunt chest trauma and pulmonary contusion, including pulmonary oedema, inflammation, enlarged basement membrane thickness,

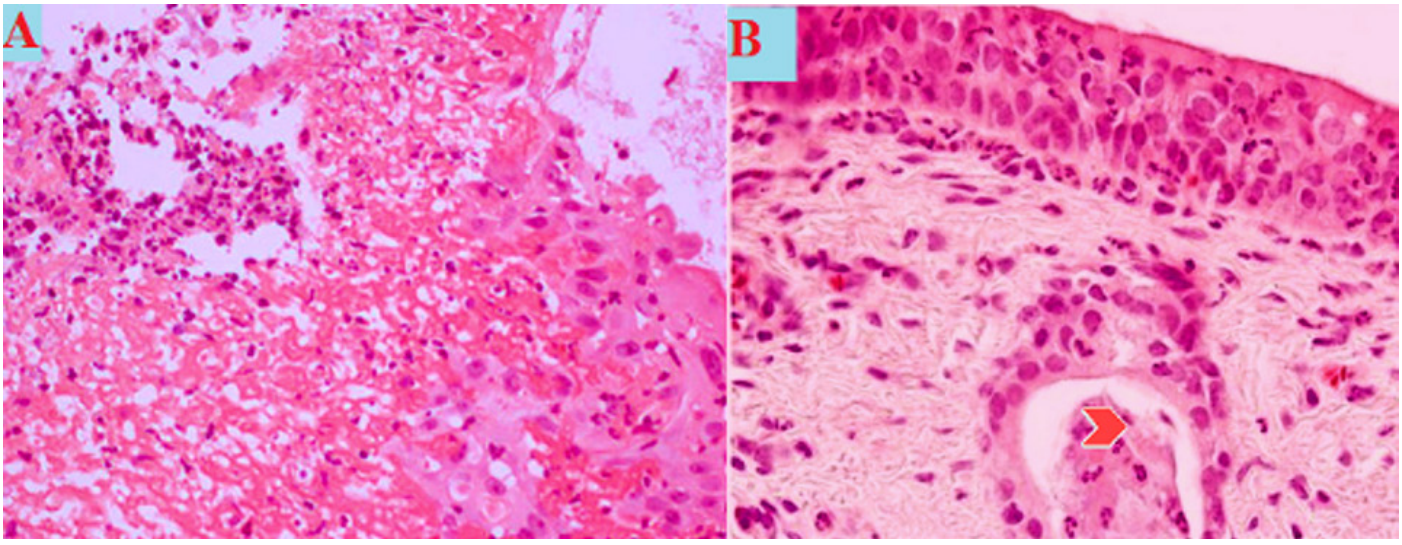

Figure 7: Occasional chronic inflammation along with squamous metaplasia A: Massive ulceration of the tracheal mucosa and abundant neutrophils admixed with pale extracellular eosinophilic material (oedema) within the submucosa and lamina propria (100×. H& E). B: A few lymphocytes are present within the lamina propria and submucosa and accumulation of cellular debris and neutrophils in the submucosal gland (Red Head Arrow), (H&E stain, 400×)

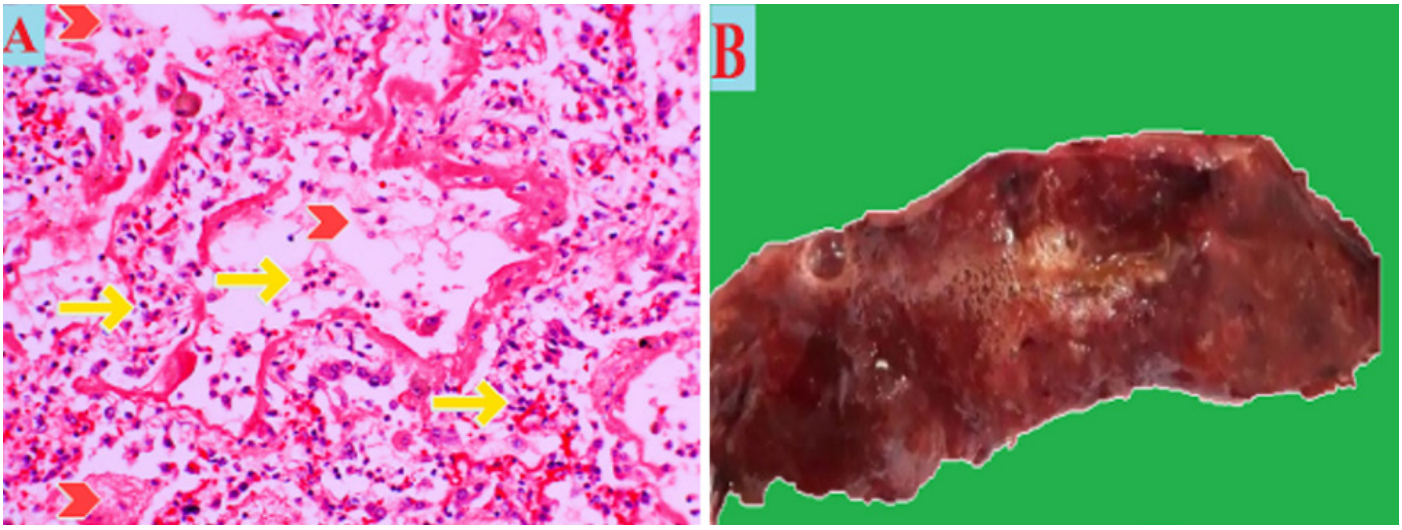

Figure 8: Diffuse alveolar damage. (A) The pulmonary alveolus is lined by hyaline membranes(Red Head Arrows). Immature fibroblasts and macrophages are present in different parts of the lung tissue, such as inside the alveoli and the interstitial space (Yellow Arrows). H&E stain, 100× (B): Aspiration Pneumonia due to the widespread inflow of fluid into the lungs, a substantial volume of fluid in the lung tissue that flows rapidly with low pressure. Putrefactive Disorganization and discolouration pneumonia caused ill-defined brownish-yellow (amber) areas of softening in the lung and necrotic slimy contents in the centres with malodor(stench)

increased diffuse alveolar damage, perfusion mismatching, cellular infiltration, increased intrapulmonary shunting, and a loss of compliance, injury to type 2 pneumocytes and endothelial cells. An area of oedema commonly surrounds the pulmonary contusion. Fluid accumulation in alveoli interferes with gas exchange and causes alveoli to be filled with proteins and collapse. Extensive pneumonia in both lungs and the development of interstitial bronchopneumonia and marbling of the lungs. Pulmonary contusion results in haemorrhage and exudate leakage into lung tissue, which becomes rigid and loses its average elasticity. The thin membrane between the alveolar sac and the capillaries is torn, and damage to the capillaries causes both blood and exudate to leak into the alveoli and the interstitial space of the lung parenchyma. Pulmonary contusion is characterized by micro-haemorrhages or microbleeds when the alveolar sac is traumatically separated from airway structures and capillaries (Figure 8).

Heart

Cardiac damage caused by ischemic coronary insufficiency may lead to fatal injuries and sometimes life-long heart problems. In most cases, mild and reversible damage, such as Takotsubo cardiomyopathy and neurogenic stress cardiomyopathy (Figure 9). A slight increase in cardiac enzymes characterizes takotsubo cardiomyopathy (Figure 10). Moreover, it is a sign of myocardial damage.

Other necropsy findings

The throat and larynx were completely erect and hemorrhagic. In the oesophagus, petechiae and foamy discharge, as well as symptoms of diverticulum and mega-oesophagus due to external pressure due to fluids, were evident. Gastric tissue contains small amounts of bloody secretions due to ingesting exudative fluids and blood from the bleeding throat and trachea. The liver has an average but inflamed consistency, and the kidneys have weak compensatory hypertrophy symptoms. Furthermore, in the cross-section, its radial lines were lost. Symptoms of interstitial nephritis and glomerulonephritis were seen. The spleen showed complete signs of lymphocyte depletion with atrophy.

Discussion

In human medicine, craniocervical artery dissection is one of the most common causes of stroke and severe brain damage in young and middle-aged adults (7). However, this injury has not been reported in animals, and this is the first recorded report of this condition in animals and wild carnivores.

This lesion initially started with the tear of the vessel's intima layer and was followed by the formation of an intramural hematoma (8). Most of these wastes occur spontaneously or after minor vessel trauma. Emergent assessment is required in these cases; recommended diagnostic tests are head and neck computerized tomography angiography with computerized brain tomography and head and neck magnetic resonance imaging (MRI) (9). In this study, we used the Time-of-Flight (TOF) MRA technique. The main advantage of the TOF-MRA technique is the direct visualization that uses the images in their original visible format of The Blood vessel walls and their interactions confirming the Intramural hematoma (IMH). Therefore, TOF- MRA is the method of choice for preliminary diagnosis and follow-up of craniocervical artery dissection. One of the most important complications of this study was determining the exact cause of TIA and stroke. Several factors have been introduced as triggers for stroke. Factors such as a family

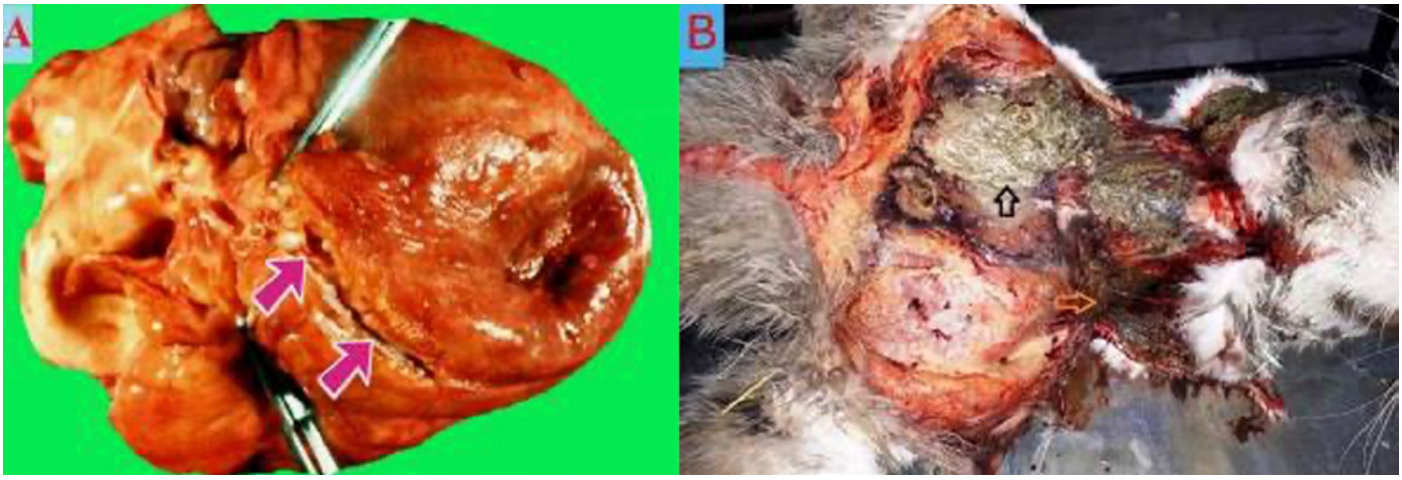

Figure 9: The myocardium was hypertrophic and flaccid. A: On cardiac examination, the myocardium was hypertrophic and flaccid. Also, postmortem thrombotic foci in cardiac septa and rough surfaces and ruffles on the Epicard layer indicate severe cardiac overload and output. B: Extensive adhesions. Additionally, focal necrosis was observed in the pectoralis area and on the pectoantebrachialis, sternomastoid, and pectoantebrachialis muscles that continued until the beginning of the xiphihumeralis area, which was filled with exudative and mucoproliferative secretions and a significant inflammatory infiltrate into the subcutaneous space

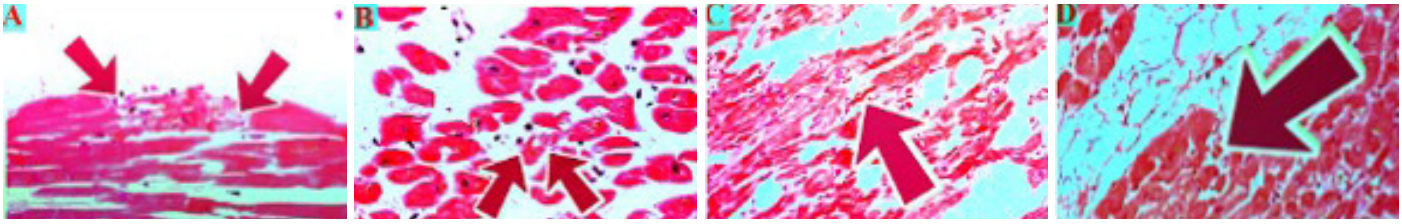

Figure 10: Tako-tsubo(ampulla) cardiomyopathy. A: Myocardial damage in the epicardium (outer layer). Apical posterior, external layer. H&E stain, x 400. B: Injured cardiac myocytes are removed by infiltrated macrophages and left ventricular apical, middle layer—Hematoxylin and eosin (H&E) stain, x 400

history of stroke or TIA, higher risk of TIA in males than females, high blood pressure, dyslipidemia, diabetes mellitus, Genetics, race, and imbalance in lipid profile, are other risk factors of TIA (10). However, in general, the predictive indices of cerebrovascular ischemia are still incomplete, which suggests that there may be risk factors that are not yet commonly recognized. Infections that occur acutely and suddenly in the body may be a risk factor for cerebrovascular ischemia, which has been underestimated. Bacterial organisms are the main cause of Brain stroke, among other infectious agents. Until the antibiotic era, rheumatic heart disease was a predisposing risk factor for infective endocarditis. (11). A positive correlation has been observed between the mortality rate of cardiovascular diseases and the epidemics of respiratory infections (12). In these cases, attention should be paid to important biochemical tests such as CRP with high sensitivity, number of leukocytes, blood sugar, and lipid profile. For example, the number of leukocytes is related to myocardial infarction and ischemic stroke risk. There is also clinical evidence of infections such as gastroenteritis, Respiratory tract infections (RTIs), and Urinary tract infection (UTI)., which are biochemically caused by leukocytosis and elevated levels of high-sensitivity C-reactive protein. Hence, these tests appear to be recognized early diagnostic tools with predictive value. They are good. Moreover, by paying close attention to them, early treatment of febrile illness and introducing or adjusting the dose of antiplatelet agents and antibiotics. can be determined to reduce the actual incidence of stroke. Considering the diagnosis of *Bergeyella zoohelcum* infection in this study, the existence of this infection can be considered an important risk factor. This case adds to the complexity of the final diagnosis of the chain of events leading to death in this study. The correlation between globulin and serum albumin with the Dissection of the Craniocervical Artery has been emphasized. Albumin and globulin are the most important components of feline blood serum proteins and play a major role in the body's systemic inflammatory processes. The data relating to serum albumin shows a valid indicator for evaluating the nutritional status as well as the status and degree of inflammation in the Craniocervical Artery Dissection. Also, an increase in serum globulin indicates the inflammatory response of the body and a response to the accumulation of various types of pro-inflammatory cytokines. On the other hand, hypoalbuminemia is associated with impaired survival rates in cases of Craniocervical Artery Dissection. Low globulin levels are a sign of liver and kidney insufficiency or malnutrition. Also, during kidney disorders such as nephrotic syndrome, this problem occurs due to the loss of proteins through renal filtration. On the other hand, An elevated globulin level (5.3) is independently associated with extravasation in intra-arterial thrombolysis and Vascular injuries such as rupture and inflammation. As it is clear from the results of

haematology studies, the ratio of albumin to globulin in this tiger is low and is around 0.72. A low albumin-to-globulin ratio has a high positive predictive value for Acute inflammatory processes. As a result, investigating these parameters justifies an acute inflammatory process following Craniocervical Artery Dissection. There are still uncertainties about the changes in these proteins and how they affect the occurrence or exacerbation of craniocervical pathological effects and Further research is needed in this field. As proven in previous studies, the CRP, blood urea nitrogen (BUN), and creatinine levels would be markedly elevated in craniocervical artery dissection and infarction of the Brain supplying arteries. It has also been proven that High blood urea nitrogen (BUN) is associated with an elevated mortality risk in various diseases, such as heart failure, pneumonia, and Dissection of different arteries. In this study, the amount of blood urea nitrogen (87.52), creatinine (7.2), and urea (187.3) were elevated, which confirms the occurrence of craniocervical artery dissection and the importance of these parameters in predicting the occurrence and evaluation of craniocervical artery dissection.Recent clinical studies have revealed that Craniocervical Artery Dissection is mediated by inflammation in the tunica adventitia and media of the vertebral artery, leading to degradation of the extracellular matrix, including elastin, collagen, enzymes, glycoproteins and hydroxyapatite and tearing in the medial tunica layer (13). According to histopathological analyses, macrophages and lymphocytes are recruited to the tunica media, and matrix metalloproteinase is involved in the degradation of elastin, collagen, non-collagen, and proteoglycan (14). Serum inflammatory markers, including CRP, serum amyloid A, cytokines, alpha-1-acid glycoprotein, plasma viscosity, ceruloplasmin, hepcidin, and haptoglobin, are often elevated in these animals. Interestingly, one observational study showed that the serum CRP level re-elevation is a useful marker of Craniocervical Artery Dissection (15). The authors speculated that local thrombogenesis triggers inflammatory cytokines, including interleukin-1(IL-1), IL-6, IL-12, IL-18, TNF-α, IFNγ, and GM-CSF that are released from immune cells like helper T cells, macrophages, and certain other cell types that promote inflammation, leading to increased production of CRP (16). Recent clinical studies have revealed that Craniocervical Artery Dissection is often accompanied by high levels of blood Fibrin Degradation Products (FDP) and D-dimer, indicating the presence of Basilar artery thrombosis and Intra-Arterial Thrombolysis and aiding in reaching The Accurate Diagnosis (17). Clinical guidelines for Craniocervical Artery Dissection state that a D-dimer level <250 ng/mL exhibits negative predictive value (NPV) for Craniocervical Artery Dissection in Felines presenting with traumatic injuries of the neck and chest area. In contrast, a D-dimer level >1400ng/mL exhibits a positive predictive value (PPV) (18). Indeed, in the present case, the D-dimer level was greater than 1,600 ng/mL (16,700 ng/mL), compatible with the typical paraclinical findings of Craniocervical Artery Dissection. In this study, the measurement of D-dimer level had diagnostic value because this parameter was measured within 11 hours after Craniocervical Artery Dissection. The observed hyperphosphatemia (28.6) was due to acute renal failure. A high serum CK value (5903) indicated muscle damage due to acute muscle injury within conflict. which had resulted in widespread acute rhabdomyolysis. A high level of AST (370) indicated inefficiency and acute liver and heart tissue damage due to the injury caused by the conflict and the effect on other organs. A high level of Direct bilirubin (3.69) was a sign of liver insufficiency, and a high level of total bilirubin (4.9) was also a sign of liver failure and widespread destruction of red blood cells due to injury and haemorrhage. higher amount of hematocrit (57.2), MCV (52.3), and MCH (19) indicated Dehydration due to haemorrhage, Lung and heart insufficiency, and anaemia.

Of course, the initial findings of this study and the course of the disease were such that, at first, it was more likely to be an acute traumatic injury instead of a longer degenerative lesion. However, when the disease took a chronic course and lasted for twenty-eight days, the occurrence of a chronic degenerative lesion was confirmed. As mentioned in the related texts, the cause of ischemic stroke is usually due to the complete loss of blood supply to the brain tissue, shown in this case. Moreover, since transient ischemic attacks usually do not cause ischemic stroke, the possibility of other factors being involved in causing stroke in this valuable species is raised, which, as mentioned at the beginning of the discussion, is one of the powerful and essential factors of bacterial infection.

In the acute setting, Craniocervical artery dissection may lead to a transient ischemic attack, Subarachnoid Hemorrhage, local compressive symptoms such as cervical radiculopathies, and cranial neuropathies (19). Therefore, intravenous thrombolytic therapy and, in select cases, mechanical thrombectomy are the Acute treatment of ischemic stroke in Craniocervical artery dissection (20). however, Anticoagulation should typically be avoided in intracranial craniocervical artery dissection (21). However, in the case of extracranial craniocervical artery dissection, despite no reliable and documented consensus on the strategy to prevent stroke, expert opinion favours Anticoagulation or dual antiplatelet therapy for at least six months (22).In a similar case of a young chimpanzee in Tehran's Eram Zoo, the author completely cured this problem with antiplatelet therapy for eight months. Therefore, young carnivores need Anticoagulation and antiplatelet therapy (23,24). Therefore, few side effects have been reported considering that dual antithrombotic treatment with clopidogrel and rivaroxaban is generally well tolerated in cats (25). Moreover, dual therapy may effectively prevent thrombosis in a high-risk population of cats with heart disease (26). Therefore, in this study, we decided to use these two drugs, and until the last day, when the animal died, at least the side effects caused by these drugs or blood coagulation problems were not observed.

Recurrent ischemic dissections are never reported in wild captive animals, but in human medicine are rare and occur in the first few months after diagnosis (27). There is a knowledge gap regarding the type of antithrombotic regimen, stenting, and duration of antithrombotic therapy for stroke prevention in craniocervical artery dissection (28). Therefore, because Recurrent ischemic dissections may occur if the tiger survives, from the very beginning of the diagnosis and for the first week, it was decided to use KENGREAL®. That is a direct P2Y12 platelet receptor inhibitor that blocks ADP-induced platelet activation and aggregation. Cangrelor binds selectively and reversibly to the P2Y12 receptor, preventing further signalling and platelet activation. Generally, A well-designed trial including advanced imaging and genetic biomarkers is required to compare various antithrombotic approaches, and stenting in craniocervical artery dissection is required (29).

For the first time, this study depicted the histopathological features of this condition in animals, including a scarce and endangered animal (white tiger). Moreover, in this sense, it has presented exciting findings.

Examining the results of this study shows a significant overlap in the histopathological findings of this condition in humans. The findings of this study in some tissues, such as the Brain and heart, are exciting and thought-provoking. Following the sequence of these events at the cellular level provides much help for the correct understanding of the lesion process from the time of emergence to death.

Another interesting finding of this study was accidentally obtained during sampling of damaged tissues. Moreover, It had no specific relation to the main finding of this study, i.e., Craniocervical Arterial Dissection was Isolation of *Bergeyella zoohelcum*, which is an aerobic, Gram-negative bacterium isolated from mammals' upper respiratory tract (30). *B. zoohelcum* has been reported to cause septicemia, tenosynovitis, and abscess, which relates to carnivores' bites (31). *Bergeyella zoohelcum* is susceptible to beta-lactams. It includes fluoroquinolones, ceftazidime, ceftriaxone, and penicillin and is variable in susceptibility to clindamycin, meropenem, and trimethoprim-sulfamethoxazole (32). Multiple reports have been associated with the wound, interstitial pneumonia, tenosynovitis, meningoencephalitis, abscesses, and cellulitis of the limbs, and only five cases of *B. zoohelcum* bacteremia have been reported before (33). Sharma reported detecting *B. zoohelcum* in Oral mucosal secretions of therapy toy dogs in close contact with the Elderly residing in a Retirement home (34). B*ergeyella zoohelcum* isolates were recovered from the lungs and tonsils of five deer, an 8-year-old female grey fox who developed bacteremia, nausea, fever, and diarrhoea after ingestion of donkey's meat (35). the source of B. zoolhelcum in animal infection is contact or exposure to foxes, wolfs, leopards, or contaminated food. In zoos, older dogs or cats may develop invasive diseases with *B. zoolhelcum* (36). Therefore, no antibiotic choice is recommended for *B. zoohelcum* infections (37). However, animals can be treated with agents that have been demonstrated effective against strains isolated from other animals (38). Meropenem, amoxicillin-clavulanic acid, ampicillin-sulbactam, ceftazidime, and marbofloxacin have successfully treated animals (39). In wild animal medicine, Betamax long act and etomoxir are appropriate for treating bite-related infections. It is a reasonable choice for co-infection with other pathogens, including *Pasteurella multocida* and anaerobes (40). However, the use of extended-spectrum antimicrobials for treating *B. zoohelcum* infection in the era of rising antimicrobial resistance deserves careful consideration (35).

Conclusions

This study showed that Craniocervical Arterial Dissection through multiple injuries leads to Transient ischemic attack in the Brain. Also, in this study, the bacterium *Bergeyella zoohelcum* was isolated for the first time, which is the first report of the isolation of this bacterium in a tiger. Our experience in this study showed that Craniocervical Arterial Dissection could cause many pathological injuries in different organs, the results of which are included in this study, also based on our experience, a quick and accurate accident diagnosis prevent many subsequent unfortunate events and can provide the basis for appropriate and optimal treatment in connection with the Dissection of the craniocervical artery. In the meantime, whole-body trauma computed tomography with an adapted scanning protocol for the craniocervical vessels is a safe, fast, and feasible method for detecting vascular injuries. It allows prompt further treatment if necessary. CTA could be a part of a broad screening protocol for craniocervical vessels in the documented head and neck injuries and trauma mechanisms influencing the craniocervical region.

Acknowledgements

The authors thank the Eram Zoo, Tehran, Iran, for their collaboration and support during all experimental research procedures.

References

1. Shi C, Xu J, Roberts NJ, Liu D, Jiang G. Individual automatic detection and identification of big cats by combining different body parts. Integr Zool 2023; 18: 157–68.
2. Xu X, Dong GX, Hu XS, et al. The genetic basis of white tigers. Curr Biol 2013; 23: 1031–5.
3. Xu X, Luo SJ. How the white tiger lost its colour but kept its stripes. Sci China Life Sci 2014; 57: 1041–3.
4. Marsh SME, Hoffmann M, Burgess ND, et al. Prevalence of sustainable and unsustainable use of wild species inferred from the IUCN Red List of Threatened Species. Conserv Biol. 2022; 36: e13844. doi: 10.1111/cobi.13844.

5. Bachmann ME, Kulik L, Gatiso T, et al. Analysis of differences and commonalities in wildlife hunting across the Africa-Europe South-North gradient. PLoS Biol 2022; 20: e3001707. doi: 10.1371/journal.pbio.3001707

6. Robinson HS, Goodrich JM, Miquelle DG, Miller CS, Seryodkin IV. Mortality of Amur tigers: the more things change, the more they stay the same. Integr Zool 2015; 10: 344–53.

7. Nash M, Rafay MF. Craniocervical arterial dissection in children: pathophysiology and management. Pediatr Neurol 2019; 95: 9–18.

8. Liu Y, Li S, Wu Y, et al. The added value of vessel wall MRI in the detection of intraluminal thrombus in patients suspected of craniocervical artery dissection. Aging Dis 2021; 1; 12: 2140–50.

9. Hakimi R, Sivakumar S. Imaging of carotid dissection. Curr Pain Headache Rep 2019;23: e2. doi: 10.1007/s11916-019-0741-9

10. Poledník I, Sulzenko J, Widimsky P. Risk of a coronary event in patients after ischemic stroke or transient ischemic attack. Anatol J Cardiol 2021; 25: 152–5.

11. Murala S, Nagarajan E, Bollu PC. Infectious causes of stroke. J Stroke Cerebrovasc Dis 2022; 31: e106274. doi: 10.1016/j.jstrokecerebrovasdis.2021.106274.

12. Patabendige A, Singh A, Jenkins S, Sen J, Chen R. Astrocyte Activation in neurovascular damage and repair following schaemic stroke. Int J Mol Sci 2021; 22: e4280. doi: 10.3390/ijms22084280.

13. Clark M, Unnam S, Ghosh S. A carotid and vertebral artery dissection review. Br J Hosp Med 2022; 83:1–11.

14. Xia H, Wu Y, Zhao J, et al. The aberrant cross-talk of epithelium-macrophages via METTL3-regulated extracellular vesicle miR-93 in smoking-induced emphysema. Cell Biol Toxicol. 2022; 38: 167–83.

15. Broekx S, Houben R, Stockx L, et al. The external carotid artery as a rare feeder of a spinal dural arteriovenous fistula causing cervical myelopathy: a literature review. Brain Spine 2021: 28; 1: e100299. doi: 10.1016/j.bas.2021.100299.

16. Morales-Primo AU, Becker I, Zamora-Chimal J. Neutrophil extracellular trap-associated molecules: a review on their immunohistological and inflammatory roles. Int Rev Immunol 2022; 41:253–74. DOI: 10.1080/08830185.2021.1921174.

17. Yao J, Bai T, Yang B, Sun L. The diagnostic value of D-dimer in acute aortic dissection: a meta-analysis. J Cardiothorac Surg 2021; 16: e343. doi: 10.1186/s13019-021-01726-1.

18. Koch V, Biener M, Müller-Hennessen M, et al. Diagnostic performance of D-dimer predicting venous thromboembolism and acute aortic dissection. Eur Heart J Acute Cardiovasc Care 2021; 10: 559–66. doi: 10.1177/2048872620907322.

19. Garner M, Yilmaz U, Behnke S. Spontane Dissektionen der hirnversorgenden Arterien. Radiologe 2021;61: 729–35.

20. Janská K, Bodnár R, Janský P, Vosko M. Intravenous thrombolytic therapy for acute nonarteritic central retinal artery occlusion. A review. Cesk Slov Oftalmol 2022; 78: 101–9.

21. Mendelson SJ, Prabhakaran S. Diagnosis and management of transient ischemic attack and acute ischemic stroke: a review. JAMA 2021 ; 325: 1088–98.

22. Bhatia K, Jain V, Aggarwal D, et al. Dual antiplatelet therapy versus aspirin in patients with stroke or transient ischemic attack: meta-analysis of randomized controlled trials. Stroke 2021; 52: e217–e23. doi: 10.1161/STROKEAHA.120.033033.

23. Hogan DF. Feline cardiogenic arterial thromboembolism: prevention and herapy. Vet Clin North Am Small Anim Pract 2017; 47: 1065–82.

24. Rosati LM, Vezzetti A, Redd KT, et al. Early anticoagulation or antiplatelet therapy is critical in craniocervical artery dissection: results from the COMPASS registry. Cerebrovasc Dis 2020; 49: 369–74.

25. Lo ST, Walker AL, Georges CJ, Li RH, Stern JA. Dual therapy with clopidogrel and rivaroxaban in cats with thromboembolic disease. J Feline Med Surg. 2022; 24: 277–83.

26. Birkbeck R, Humm K, Cortellini S. A review of hyperfibrinolysis in cats and dogs. J Small Anim Pract 2019; 60: 641–55.

27. Saw J, Humphries K, Aymong E, et al. Spontaneous coronary artery dissection: clinical outcomes and risk of recurrence. J Am Coll Cardiol 2017; 70: 1148–58.

28. Xu D, Wu Y, Li J, et al. Retrospective comparative analysis of clinical and imaging features of craniocervical artery dissection: spontaneous CAD vs. minor traumatic CAD. Front Neurol 2022; 13: e836997. doi: 10.3389/fneur.2022.836997.

29. Vezzetti A, Rosati LM, Lowe FJ, et al. Stenting as a treatment for craniocervical artery dissection: improved paramount adverse cardiovascular event-free survival. Catheter Cardiovasc Interv 2022; 99: 134–9.

30. Chen Y, Liao K, Ai L, et al. Bacteremia caused by *Bergeyella zoohelcum* in an infective endocarditis patient: case report and review of the literature. BMC Infect Dis 2017; 17: e271. doi: 10.1186/s12879-017-2391-z.

31. Muramatsu Y, Haraya N, Horie K, et al. *Bergeyella zoohelcum* isolated from oral cavities of therapy dogs. Zoonoses Public Health. 2019; 66: 936–42.

32. Lorenzo de Arriba M, Lopez-Serrano S, Galofre-Mila N, Aragon V. Characterisation of Bergeyella spp. isolated from the nasal cavities of piglets. Vet J 2018; 234: 1–6.

33. Yi J, Humphries R, Doerr L, Jerris RC, Westblade LF. *Bergeyella zoohelcum* associated with abscess and cellulitis after a dog bite. Pediatr Infect Dis J 2016; 35: 214–6.

34. Sharma S, Salazar H, Sharma S, Nasser MF, Dahdouh M. *Bergeyella zoohelcum* bacteremia from therapy dog kisses. Cureus 2019; 11: e4494. doi:10.7759/cureus.4494.

35. Zamora L, Domínguez L, Fernández-Garayzábal JF, Vela AI. Bergeyella porcorum sp. nov., isolated from pigs. Syst Appl Microbiol 2016; 39: 160–3.

36. Tomida J, Fujiwara N, Naka T, et al. Spodiobacter cordis gen. nov. sp. nov., a member of the family Flavobacteriaceae isolated from patients with infective endocarditis. Microbiol Immunol 2019; 63: 111–8.

37. Goldstein EJC, Citron DM, Tyrrell KL, Leoncio ES. In vitro activity of Pexiganan and 10 comparator antimicrobials against 234 isolates, including 93 Pasteurella Species and 50 anaerobic bacterial isolates recovered from animal bite wounds. Antimicrob Agents Chemother 2017; 61: e00246-17. doi: 10.1128/AAC.00246-17.

38. Harsent R, Macleod J, Rowlands RS, Smith PM, Rushmere N, Blaxland J. The identification of multidrug-resistant microorganisms, including *Bergeyella zoohelcum*, acquired from the skin/prosthetic interface of amputees and their susceptibility to Medihoney™ and garlic extract (Allicin). Microorganisms 2022 ; 10: e299. doi: 10.3390/microorganisms10020299.

39. Krumbeck JA, Reiter AM, Pohl JC, et al. Characterization of oral microbiota in cats: novel insights on the potential role of fungi in feline chronic gingivostomatitis. Pathogens 2021; 10: e904. doi: 10.3390/pathogens10070904.

40. Fajardo C, Martín C, Costa G, et al. Assessing the role of polyethene microplastics as a vector for organic pollutants in soil: ecotoxicological and molecular approaches. Chemosphere 2022; 288: e132460. doi: 10.1016/j.chemosphere.2021.132460.

41. Proverbio D, Perego R, Baggiani L, Ravasio G, Giambellini D, Spada E. Hematological and biochemical reference values in healthy captive tigers (Panthera tigris). Animals (Basel) 2021; 11: e3440. doi: 10.3390/ani11123440.

Klinične in diagnostične slikovne ugotovitve pri bengalskem tigru (*Panthera tigris tigris*) z disekcijo kraniocervikalne arterije: Poročilo o primeru

P. M. Zadeh, N. Shadan, S. Mohammadi, F. Najafi, A. Bashiri

Izvleček: Namen te študije je bil preučiti različne vidike disekcij kraniocervikalnih arterij, ki so po zaporedju patoloških dogodkov povzročile smrt živali. Po fizičnih poškodbah vratu samice sibirskega tigra, ki so bile posledica agonističnega vedenje samca tigra, smo opravili diagnostične teste, ki so vključevali popolni zdravniški pregled, slikanje MRA s časom leta (TOF) in radiografijo. Vzeli smo tudi vzorce za klinično oceno, hematologijo, mikrobiološko kulturo in antibiogram. Predpisali smo začetno zdravljenje in izvedli PCR. Na žalost so bili ukrepi zdravljenja neustrezni in žival je poginila. Zato smo opravili nekropsijo, histopatološki pregled in imunohistokemično barvanje. Rezultati mikrobiološke preiskave so vključevali prvo identifikacijo bakterije Bergeyella zoohelcum pri tej vrsti živali. Diagnostične ugotovitve na podlagi nekropsije in histoloških preiskav so vključevale anevrizmo, subarahnoidalno krvavitev, ishemično kap ter Hornerjev intramuralni hematom, rupturo karotidnih arterij in notranje jugularne vene, kar še ni bilo opisano. Računalniška tomografija celotnega telesa s prilagojenim protokolom slikanja kraniocervikalnih žil je varna, hitra in izvedljiva metoda za odkrivanje poškodb žil. Ta metoda bi lahko bila del širšega presejalnega protokola za kraniocervikalne žile pri dokumentiranih poškodbah glave in vratu ter mehanizmih poškodb, ki vplivajo tudi na kraniocervikalno področje.

Ključne besede: *Bergeyella zoohelcum*; ishemična kap; subarahnoidalna krvavitev; tiger; prehodni ishemični napad

Table of Content

Slov Vet Res 2024; 61 (1): 1–72